U.S.NRC

United States Nuclear Regulatory Commission

Protecting People and the Environment

NUREG/CR-6996
PNNL-18372

Nondestructive and Destructive Examination Studies on Removed-from-Service Control Rod Drive Mechanism Penetrations

Office of Nuclear Regulatory Research

AVAILABILITY OF REFERENCE MATERIALS IN NRC PUBLICATIONS

NRC Reference Material

As of November 1999, you may electronically access NUREG-series publications and other NRC records at NRC's Public Electronic Reading Room at http://www.nrc.gov/reading-rm.html. Publicly released records include, to name a few, NUREG-series publications; *Federal Register* notices; applicant, licensee, and vendor documents and correspondence; NRC correspondence and internal memoranda; bulletins and information notices; inspection and investigative reports; licensee event reports; and Commission papers and their attachments.

NRC publications in the NUREG series, NRC regulations, and *Title 10, Energy*, in the Code of *Federal Regulations* may also be purchased from one of these two sources.

1. The Superintendent of Documents
   U.S. Government Printing Office
   Mail Stop SSOP
   Washington, DC 20402–0001
   Internet: bookstore.gpo.gov
   Telephone: 202-512-1800
   Fax: 202-512-2250
2. The National Technical Information Service
   Springfield, VA 22161–0002
   www.ntis.gov
   1–800–553–6847 or, locally, 703–605–6000

A single copy of each NRC draft report for comment is available free, to the extent of supply, upon written request as follows:

Address: Office of Administration
Reproduction and Mail Services Branch
U.S. Nuclear Regulatory Commission
Washington, DC 20555-0001
E-mail: DISTRIBUTION@nrc.gov
Facsimile: 301–415–2289

Some publications in the NUREG series that are posted at NRC's Web site address http://www.nrc.gov/reading-rm/doc-collections/nuregs are updated periodically and may differ from the last printed version. Although references to material found on a Web site bear the date the material was accessed, the material available on the date cited may subsequently be removed from the site.

Non-NRC Reference Material

Documents available from public and special technical libraries include all open literature items, such as books, journal articles, and transactions, *Federal Register* notices, Federal and State legislation, and congressional reports. Such documents as theses, dissertations, foreign reports and translations, and non-NRC conference proceedings may be purchased from their sponsoring organization.

Copies of industry codes and standards used in a substantive manner in the NRC regulatory process are maintained at—

The NRC Technical Library
Two White Flint North
11545 Rockville Pike
Rockville, MD 20852–2738

These standards are available in the library for reference use by the public. Codes and standards are usually copyrighted and may be purchased from the originating organization or, if they are American National Standards, from—

American National Standards Institute
11 West 42nd Street
New York, NY 10036–8002
www.ansi.org
212–642–4900

Legally binding regulatory requirements are stated only in laws; NRC regulations; licenses, including technical specifications; or orders, not in NUREG-series publications. The views expressed in contractor-prepared publications in this series are not necessarily those of the NRC.

The NUREG series comprises (1) technical and administrative reports and books prepared by the staff (NUREG–XXXX) or agency contractors (NUREG/CR–XXXX), (2) proceedings of conferences (NUREG/CP–XXXX), (3) reports resulting from international agreements (NUREG/IA–XXXX), (4) brochures (NUREG/BR–XXXX), and (5) compilations of legal decisions and orders of the Commission and Atomic and Safety Licensing Boards and of Directors' decisions under Section 2.206 of NRC's regulations (NUREG–0750).

U.S.NRC
United States Nuclear Regulatory Commission
Protecting People and the Environment

NUREG/CR-6996
PNNL-18372

Nondestructive and Destructive Examination Studies on Removed-from-Service Control Rod Drive Mechanism Penetrations

Manuscript Completed: April 2009
Date Published: July 2009

Prepared by
S.E. Cumblidge, S.R. Doctor, G.J. Schuster, R.V. Harris,
S.L. Crawford, R.J. Seffens, M.B. Toloczko, S.M. Bruemmer

Pacific Northwest National Laboratory
P.O. Box 999
Richland, WA 99352

W.E. Norris, NRC Project Manager

NRC Job Code Y6867

Office of Nuclear Regulatory Research

Abstract

The U.S. Nuclear Regulatory Commission (NRC) and the Electric Power Research Institute (EPRI) conducted a collaborative research effort to address issues related to cracking of nickel-base alloys and degradation of reactor pressure vessel heads. Control rod drive mechanism (CRDM) nozzles and J-groove weldments were removed from the decommissioned North Anna Unit 2 reactor pressure vessel (RPV) head and shipped to Pacific Northwest National Laboratory (PNNL) in Richland, Washington, and Westinghouse Electric Company LLC in Pittsburgh, Pennsylvania, for study. The primary objectives of the research were to evaluate the effectiveness and reliability of nondestructive examination (NDE) methods as related to the in-service inspection of CRDM nozzles and J-groove weldments and to enhance the knowledge base of primary water stress corrosion cracking (PWSCC) through destructive characterization of the CRDM assemblies.

The North Anna 2 nozzles have been the subject of three series of nondestructive examinations. The first series consisted of the in-service examinations that determined that the RPV head required replacement. The second series of examinations was performed at PNNL by four inspection teams. The examinations were administered by EPRI as part of the cooperative agreement with the NRC. Finally, an extensive series of examinations was performed on several nozzles at PNNL and Westinghouse under laboratory conditions.

Ultimately, the laboratory studies focused on two CRDMs—Nozzle 31, which had cracks, as evidenced by through-wall leakage and the in-service inspection data, and Nozzle 54, which had circumferential defect indications in the penetration tube outer diameter, as evidenced by the in-service examinations.

The NDE procedures used to examine the CRDM assemblies followed standard industry techniques for conducting in-service inspections of CRDM nozzles and the crown of the J-groove welds and buttering. These techniques included eddy current testing (ET), time-of-flight diffraction ultrasound, and penetrant testing. In addition, laboratory-based NDE methods were employed at PNNL to conduct inspections of the CRDM assembly with particular emphasis on inspecting the J-groove weld and buttering. These techniques included volumetric ultrasonic inspection of the J-groove weld metal and visual testing via replication of the J-groove weld. The results from these NDE studies were used to guide the development of the destructive characterization plan.

The comparison of the examination results from the three series of nondestructive examinations performed (i.e., in-service, inspection team, and laboratory) indicate that the testing results are generally consistent. Many of the indications detected during the in-service examinations were detected also during the examinations performed by the inspection teams and in the laboratory. Many of these indications were confirmed through the destructive evaluation (DE) of the CRDMs. However, DE also showed that some significant indications were either not detected or mischaracterized. For example, several flaws were found by DE in the buttering region of Nozzle 54 that were not detected during the in-service examination. Volumetric inspection of the J-groove weld of nozzle 31 found many fabrication flaws but was not able to detect the through-weld crack, as the crack was axially oriented and presented almost no surface area to the ultrasonic beam. Eddy current testing was somewhat more reliable based on a comparison of results. However, eddy current testing also exhibited inconsistencies. In one area of a CDRM assembly, numerous surface-breaking indications were detected by ET were not confirmed in the laboratory.

Some differences between the results of the different inspection methods were expected. The reliability of NDE can vary with surface condition and the complexity of the geometry of a component. CRDM assemblies are very complex in this regard. However, there were two interesting findings from the comparisons of the results of NDE and DE. The first finding was that a significant number of the NDE indications were actually determined to be fabrication-related. The second finding was a realization that the meandering and branched nature of PWSCC can greatly affect detection and characterization. PWSCC cracks are generally tight at the surface. These findings provide a basis for explaining why it can be more difficult to detect cracks than leaks through in-service inspections.

The industry has been working to improve inspection methods and the quality of inspections. The NRC has amended Title 10 of the *Code of Federal Regulations*, Part 50, paragraph 50.55a(g)(6)(ii)(D), to require that all licensees of pressurized water reactors (PWRs) augment their inservice inspection programs by implementing the recently developed American Society of Mechanical Engineers (ASME) Code Case N-729-1, "Alternative Examination Requirements for PWR Reactor Vessel Upper Heads with Nozzles Having Pressure-Retaining Partial-Penetration Welds, Section XI, Division 1."

The goal of in-service inspection of nuclear reactor piping and pressure vessels is to reliably detect service-related defects in a timely manner and, thereby, maintain the structural integrity of the inspected components. Thus, relative to this goal, the results of the research reported here indicate that NDE can be improved to be a more effective tool for detecting and characterizing indications in CRDM assemblies.

Foreword

Between November 2000 and March 2001, leaks were discovered from Alloy 600 control rod drive mechanism (CRDM) nozzles and associated Alloy 182 J-groove attachment welds at Oconee 1, Oconee 3, and Arkansas Nuclear One. Destructive examination of several CRDMs showed that the leaks were the result of primary water stress corrosion cracking (PWSCC). By mid-2002, over 30 leaking CRDM nozzles had been reported in the United States. In response, the Nuclear Regulatory Commission (NRC) issued the following information notices and bulletin:

- Information Notice 2001-05, "Through-Wall Circumferential Cracking of Reactor Pressure Vessel Head Control Rod Drive Mechanism Penetration Nozzles at Oconee Nuclear Station, Unit 3," April 30, 2001 [Agency Document and Management System (ADAMS) Accession No. ML011160588]

- Bulletin 2001-01, "Circumferential Cracking of Reactor Pressure Vessel Head Penetration Nozzles," August 3, 2001 [ADAMS Accession No. ML012080284]

- Bulletin 2002-01, "Reactor Pressure Vessel Head Degradation and Reactor Coolant Pressure Boundary Integrity," March 18, 2002 [Agency Document ADAMS Accession No. ML020770497]

- Information Notice 2002-11, "Recent Experience with Degradation of Reactor Pressure Vessel Head," March 12, 2002 [ADAMS Accession No. ML020700556]

The purpose of the information notices was to alert the industry to the occurrences of degradation of CRDM nozzles and weldments, and the purpose of the bulletins was to request information related to the structural integrity of the affected components and the inspections and repairs that had been undertaken.

In late 2002, widespread cracking in CRDM nozzles and associated Alloy 182 and 82 J-groove attachment welds was discovered at North Anna Unit 2. Accordingly, the utility decided to replace the reactor pressure vessel head. The NRC and the Electric Power Research Institute (EPRI) developed a joint program to study some of the defective North Anna Unit 2 CRDMs.

This report describes the nondestructive and destructive examinations that were performed and assesses the effectiveness and reliability of the nondestructive examinations (NDE). There were several interesting observations. The destructive evaluations (DE) revealed that a significant number of the indications detected during NDE were fabrication-related. The DE also showed that the meandering, branched, and tight cracks can be difficult to detect which is why NDE sometimes either did not detect or mischaracterized some significant indications.

The results of this research led, in part, to the industry development of American Society of Mechanical Engineers (ASME) Code Case N-729-1, "Alternative Examination Requirements for PWR Reactor Vessel Upper Heads with Nozzles Having Pressure-Retaining Partial-Penetration Welds, Section XI, Division 1." The code case was developed to improve the inspection of CRDMs and associated weldments. On September 8, 2008, the NRC published a final rule in the *Federal Register* [73 FR 52730] amending Title 10 of the *Code of Federal Regulations*, Part 50, paragraph 50.55a(g)(6)(ii)(D), to require that all licensees of pressurized water reactors (PWRs) augment their inservice inspection programs by implementing Code Case N-729-1.

Contents

Figures

Tables

Executive Summary

Studies conducted at the Pacific Northwest National Laboratory (PNNL) in Richland, Washington, and Westinghouse Electric Company LLC in Pittsburgh, Pennsylvania, focused on assessing the effectiveness and reliability of nondestructive examination (NDE) techniques for inspecting control rod drive mechanism (CRDM) nozzles and J-groove weldments. In addition, the studies were conducted to enhance the knowledge base of primary water stress corrosion cracking (PWSCC) through destructive characterization of the CRDM assemblies. The studies were initiated by the U.S. Nuclear Regulatory Commission (NRC) and the Electric Power Research Institute (EPRI) to address issues related to cracking of nickel-base alloys and degradation of reactor pressure vessel heads. The nozzles selected for study had been examined during normal in-service inspections and a series of round-robin tests at PNNL. A subset of these nozzles was then used in a series of laboratory-quality nondestructive and destructive examinations at PNNL and Westinghouse.

Based on the results of the in-service inspections (ISIs), the round-robin tests focused on four CRDM assemblies. After those results were analyzed, three of the four CRDM assemblies were further inspected under laboratory conditions. The studies were predicated on addressing the following basic questions: (1) What did each NDE technique detect? (2) What did each NDE technique miss? (3) How accurately did each NDE technique characterize the detected flaws? (4) Why did the NDE techniques perform or not perform? (5) What was the type and extent of the degradation present in the CRDMs?

After further consideration, a decision was made to focus on two of the CRDM assemblies that contained suspected PWSCC, based on ISI data and through-wall leakage. An overview of the results for the Westinghouse destructive examination also is provided.

Nondestructive Testing of CRDM Nozzle 59

The penetration tube of Nozzle 59 was examined by the ISI teams during a round-robin examination at PNNL administered by EPRI, and under laboratory conditions at PNNL using eddy current testing (ET), time-of-flight diffraction (TOFD), and visual testing (VT) via Microset replicant. The annulus was examined for signs of wastage using deep penetrating eddy current and ultrasonic examinations. The examinations of the penetration tube yielded some areas of interest but no confirmed cracking. The penetration tube was considered a lower priority than the J-groove weld of Nozzle 31.

The J-groove weld and buttering were inspected volumetrically using ultrasound, and the surface was examined using visual testing via replicant. No large crack-like indications were found in the J-groove weld using direct or replicant VT. Immersion ultrasonic testing (UT) identified indications that appeared to be embedded welding defects. The Microset replica and VT did reveal several small crack-like indications, but no indication was longer than 1 cm (0.39 in.). Although there were a series of UT signals coincident with the locations of the small cracks at 90–135 degrees found via VT, the UT data in this area more closely resembled a string of fabrication flaws.

Nondestructive Testing of CRDM Nozzle 54

The penetration tube of Nozzle 54 was examined by the ISI teams and during the round-robin tests. The penetration tube was examined both ultrasonically and using eddy current, and the annulus was examined for leakage using deep penetrating eddy current and ultrasonic testing. The J-groove weld was examined using ET by the ISI team but not by the round-robin teams.

The bare metal examination of the nozzle showed no discernable leakage. The ISI examinations did find some ultrasonic indications located at the interface between the nozzle outer diameter (OD) with the J-groove weld and eddy current indications in several places at the outer portion of the crown of the J-groove weld. No leak path was found using the ultrasonic leak path examination technique.

The round-robin testing of Nozzle 54 found many more indications in the penetration tube, and deep penetrating eddy current techniques found evidence of wastage in the annulus above the weld. Two eddy current indications were found in the penetration tube inner diameter (ID) above the weld, which could lead to leakage if these indications were cracks and penetrated through the tubing and into the annulus.

Destructive Testing of CRDM Nozzle 54

After the round-robin testing was completed, Nozzle 54 was shipped to Westinghouse for laboratory-quality nondestructive testing and destructive evaluation of the NDE results. A high-resolution replicant was applied to the J-groove weld surface of Nozzle 54 and the interior of the penetration tube of Nozzle 54. Nozzle 54 was then sectioned into 12 pieces to allow for microscopic examination of the weld surfaces and an examination of the cut faces to determine the properties of the weld below the surface. Selected cut faces were milled to allow for highly sensitive ET, PT, and other examinations of the cut surfaces.

Cracking was confirmed in the outer portions of the J-groove weld of Nozzle 54. Scanning electron microscopy examinations of the surfaces and the cut faces show cracking at several locations around the outer regions of the J-groove weld in or near the buttering and penetrating into the buttering at some of the cut faces. The visual examination of the replica showed a string of defects from 270 to 60 degrees and individual defects at 70, 85, and 95 degrees. Some of the cracks were further sectioned and examined via microscopy and fractography. Although some cracks were confirmed as PWSCC, none was more than a few millimeters deep, and all were contained in the buttering. No confirmation of deep cracking or leakage was found during the destructive evaluation of this CRDM.

Nondestructive Testing of CRDM Nozzle 31

Nozzle 31 was considered to be leaking based on the presence of boric acid on the pressure vessel head. The NDE examinations on the penetration tube of Nozzle 31 found the penetration tube to be free of significant surface-breaking defects. The penetration tube in Nozzle 31 contained no strong ET indications; only weak (<1 V) scratch-like indications were detectable. The only TOFD indications that were found were determined to be embedded in the tube and not surface-breaking, as no break in the lateral wave was seen.

The J-groove weld of Nozzle 31 was found to be cracked by bare metal VT, ET, and PT. The cracking was not detectable using the volumetric UT inspection, but UT inspection did reveal what appeared to be areas with fabrication flaws. Sixteen crack-like indications were found by ET in four distinct areas. Seven small crack-like indications were found clustered around 60 degrees; five were found clustered around 150 degrees; three were found clustered around 210 degrees; and one was found at 255 degrees. The ET indications at 200 and 225 degrees were confirmed using PT and bare metal VT.

A crack-like indication was found using both PT and ET at 215 degrees. This indication is unusual for two reasons—the indication is circumferential (transverse to axis of tube), not axial like the other crack-like indications, and the ET response is relatively weak at 1.8 V with a 15-dB gain setting. Because of this indication, all ET responses larger than 1.8 V were considered crack-like for this analysis.

Destructive Testing of CRDM Nozzle 31

Cutting Nozzle 31 revealed the through-weld crack to start at 155 degrees on the wetted surface at the weld–buttering interface and end at 135 degrees above the triple point. The cutting of this section also revealed two nearby cracks that had penetrated 8 mm (0.31 in.) into the material.

The metallographic characterization of the serial sections effectively mapped the cracks from their initiation in Alloy 182 weld metal on the pressurized water reactor (PWR) primary water surface to their end, either when intersecting with low-alloy steel, entering the Alloy 600 CRDM tube, or exiting at the interference-fit gap above the J-groove weld. Cracking in Alloy 182 weld metal is interdendritic or intergranular and clearly has propagated because of stress corrosion cracking (SCC). No evidence for hot cracking in the weld was observed. Initiation appears to result from SCC near the fusion line between the butter passes and the J-groove weld. Surface damage and defects in the near-surface region may have promoted crack nucleation.

The main crack is observed at a length of ~8 mm (0.31 in.) on the PWR primary water surface and expands to a lateral length of ~25 mm (1 in.) across the Alloy 182 weld metal within 8 mm (0.31 in.) below the surface. At this depth, the crack has already reached the low-alloy steel plate material on one side and remains in the Alloy 182 J-groove weld on the other. The main crack path length from the PWR primary water surface initiation site to the gap exit surface is estimated at ~25 mm (1 in.). Based on laboratory tests in simulated PWR primary water, typical crack-growth rates can range from $\sim 3 \times 10^{-8}$ to $\sim 3 \times 10^{-7}$ mm/s for as-welded Alloy 182 at 290 to 320°C. This results in an estimated time of ~2.5 to 25 years for the crack to propagate through-wall after initiation. Because crack initiation normally accounts for some important fraction of life and through-wall cracking occurred at some time before its full 20-year life, the SCC crack-growth rate experienced in service was probably closer to the high end for measured propagation rates in the laboratory.

Conclusions

Based on the results of the NDE and the subsequent comparison of the results with the destructive evaluations, the following conclusions may be drawn:

- Visual testing via replicant using high-resolution photography of the replicant was ineffective at finding PWSCC, as the cracks were very tight and short, and the surface conditions were not conducive to an accurate visual test.

- Visual testing via direct high-resolution photography of the weld surface was for the most part ineffective at finding PWSCC, as the geometry prevented a complete inspection, the surface conditions were poor, and the cracks were both very short and very tight.
- Volumetric inspection of the J-groove weld using zero-degree ultrasound at frequencies ranging from 5 MHz to 500 kHz found fabrication flaws but was not able to detect the through-weld cracks, which is not surprising given the well-known difficulties in examining components with complicated geometries and varying microstructures with ultrasonic techniques.
- Penetrant testing had mixed results in detecting PWSCC as some cracks were too tight to allow the penetrant dye into the crack in sufficient amounts to produce a visible indication.
- Eddy current testing was the most useful technique for finding PWSCC on the J-groove weld and showed much higher sensitivity than any of the other NDE techniques. The PNNL and ISI ET results for Nozzle 31 were very consistent. Although ET provided the most consistent results, several flaws found in the buttering region of Nozzle 54 were not found by the ISI ET testing.
- It would be very useful for a volumetric technique, such as TOFD, to be developed and deployed on the J-groove weld to verify ET results, as currently only ET provides good sensitivity for inspecting the J-groove weld metal and ET is incapable of depth-sizing flaws.
- A detailed characterization of ET noise levels and ET responses to fabrication flaws in J-groove welds would be helpful in discriminating between the possibly small and low-voltage, service-induced PWSCC and innocuous indications.

Acknowledgments

The work described in this report was sponsored by the U.S. Nuclear Regulatory Commission under NRC Job Code Numbers Y6867, Y6534, and N6329. Wallace Norris, Ms. Carol E. Moyer, and Dr. Iouri Prokofiev were the NRC program monitors. Thanks also go to Dr. William Cullen for his support and ideas.

This work was performed in cooperation with the Electric Power Research Institute. The CRDMs were cut from the pressure vessel head by EPRI, important decontamination equipment was paid for by EPRI, and the CRDMs are to be disposed of by EPRI as well. Thanks go to Dr. Al Aluwhalia and Robert Barnes from EPRI for their work in making this project a success. Thanks go also to Jack Lareau from Westinghouse for providing information on in-service inspection of the nozzles.

Abbreviations, Acronyms, and Initialisms

BSE	backscatter-electron
CCW	counterclockwise
COD	crack opening dimension
CRDM	control rod drive mechanism
DE	destructive evaluation
dpm	decays per minute
EDM	electrical discharge machined
EPRI	Electric Power Research Institute
ET	eddy current testing
ID	inner diameter
IDSCC	interdendritic stress corrosion cracking
ISI	in-service inspection
MDA	minimum detectable activity
NDE	nondestructive examination
NRC	Nuclear Regulatory Commission
OD	outer diameter
PNNL	Pacific Northwest National Laboratory
PT	penetrant testing
PV	pressure vessel
PWR	pressurized water reactor
PWSCC	primary water stress corrosion cracking
RPL	Radiochemical Processing Laboratory
RPV	reactor pressure vessel
RVH	reactor vessel head
SAFT	synthetic aperture focusing technique
SCC	stress-corrosion cracking
SEM	scanning electron microscopy
TOF	time of flight
TOFD	time-of-flight diffraction
UT	ultrasonic testing
VT	visual testing

1 Introduction

Significant degradation has been found in welded assemblies that contain nickel-based alloys (Buisine et al. 1993; Embring and Pers-Anderson 1994; Faidy et al. 1994; Champigny et al. 2002; Lang 2003). On April 1, 1997, the U.S. Nuclear Regulatory Commission (NRC) issued Generic Letter (GL) 97-01, "Degradation of Control Rod Drive Mechanism Nozzle (CRDM) and Other Vessel Closure Head Penetrations." In response to the NRC generic letter, licensees developed susceptibility ranking models to relate the operating conditions (in particular, the operating temperature and time) for each plant to the plant's relative susceptibility to primary water stress corrosion cracking (PWSCC). The responses committed to surface examinations (i.e., eddy current) of the CRDM nozzles at the plants identified as having the highest relative susceptibility ranking. The surface examinations conducted prior to November 2000 identified only limited axial cracking and circumferential cracking below the weld in the base metal of CRDM nozzles but no circumferential cracking above the nozzle welds and no cracking in the Alloy 82/182 welds.

Inspections of the CRDM nozzles at Oconee Nuclear Stations 2 and 3 in early 2001 identified circumferential cracking of the nozzles above the J-groove weld. Circumferential cracking above the J-groove weld is considered a safety concern because of the possibility of nozzle ejection, should the circumferential cracking not be detected and corrected. On August 3, 2001, the NRC issued Bulletin 2001-01, "Circumferential Cracking of Reactor Pressure Vessel Head Penetration Nozzles." The bulletin described instances of cracked and leaking Alloy 600 vessel head penetration nozzles, including CRDM and thermocouple nozzles, at Oconee Nuclear Station 3. In response to the bulletin, pressurized water reactor (PWR) licensees provided their plans for inspecting the CRDM nozzles and/or the outside surface of the reactor pressure vessel (RPV) head to determine whether the nozzles were leaking.

Inspections at other PWRs continued to find leakage and cracks in CRDM nozzles or J-groove welds that required repairs or prompted the replacement of the RPV head. In response to the increasing number of reported occurrences, the NRC issued Order EA-03-009 on February 20, 2004, to require additional periodic inspections of RPV heads and associated penetration nozzles at PWRs as a function of the unit's susceptibility to PWSCC and, as appropriate, to address the discovery of boron deposits to provide reasonable assurance that plant operations do not pose an undue risk to the public health and safety.

To provide the data needed to address issues related to cracking of nickel-base alloys and degradation of reactor pressure vessel heads, the NRC and the Electric Power Research Institute (EPRI) initiated a collaborative research effort. CRDM nozzles and J-groove weldments were removed from the decommissioned North Anna Unit 2 reactor pressure vessel (RPV) head and shipped to Pacific Northwest National Laboratory (PNNL) in Richland, Washington, and Westinghouse Electric Company LLC in Pittsburgh, Pennsylvania, for study. The primary objectives of the research were to evaluate the effectiveness and reliability of nondestructive examination (NDE) methods as related to the in-service inspection of CRDM nozzles and J-groove weldments and to enhance the knowledge base of PWSCC through destructive characterization of the CRDM assemblies.

Extensive and detailed NDE of the North Anna Unit 2 reactor vessel head (RVH) during the 2002 fall outage identified crack indications in the Alloy 600 CRDM penetrations and associated Alloy 182 and 82 J-groove attachment welds. Given the extent of degradation found, the utility decided to replace the reactor vessel head (RVH). This decommissioned head was made available for research purposes.

Six CRDM penetrations were removed from the RVH and transferred to PNNL. Four of the CRDM penetrations were decontaminated to reduce individual radiation dose and contamination levels in preparation for NDE studies. Round-robin inspections were conducted by four NDE vendor companies. The vendors involved in the round-robin testing performed examinations on only the penetration tube. The vendors used eddy current and ultrasonic testing of the penetration tube and ultrasonic and eddy current testing of the annulus to detect signs of leakage. The purpose of the round robin inspections was to evaluate the CRDM assemblies in a laboratory environment and to perform some of the inspections with advanced technologies and methods.

The results of the round robin inspections were then analyzed. It was decided that PNNL would focus its laboratory studies on CRDM Nozzle 31 (which had cracks, as evidenced by through-wall leakage and the in-service inspection data) and Nozzle 59 (where an outer-diameter circumferential crack but no discernable leakage had been identified). In parallel, EPRI would study Nozzle 54 (which also had circumferential defect indications in the penetration tube outer diameter but no discernable leakage. After the data collection had been completed, the destructive evaluation (DE) efforts at PNNL focused on Nozzle 31.

Figure 1.1 is a diagram of a CRDM penetration-nozzle assembly showing the pressure vessel head, the penetration tube, and the J-groove weld. A description of these product forms can be found in Doctor et al. (2004). Most of the interface between the penetration tube and the vessel head is a simple interference fit and is not watertight. When a PWR is at operating pressures and temperatures, the pressure vessel head bulges slightly, further opening the interference fit in some regions. The only barriers between the primary coolant and the outside are the J-groove weld, buttering, and the penetration tube above the weld. Any cracks that propagate through these sections can lead to leakage.

One objective of this work was to provide information to the NRC on the effectiveness of NDE methods as related to the in-service inspection of CRDM nozzles and J-groove welds containing PWSCC. Thus, some of the selected NDE methods used in the laboratory examinations were based on standard industry techniques for conducting in-service inspections of CRDM nozzles and the crown of the J-groove welds and buttering to better enable a comparison of results. In addition, state-of-the-art NDE methods were employed to conduct inspections of the CRDM assemblies, with particular emphasis on inspecting the J-groove weld and buttering.

A secondary objective was to enhance the knowledge base for PWSCC through destructive characterization of the CRDM assemblies. Project efforts used the results from the NDE studies to guide the DE of the CRDMs. The purpose of the destructive analysis was to reveal the flaw morphology compared with NDE responses to determine what each NDE method detected or missed as well as how accurately each NDE technique characterized the detected flaws.

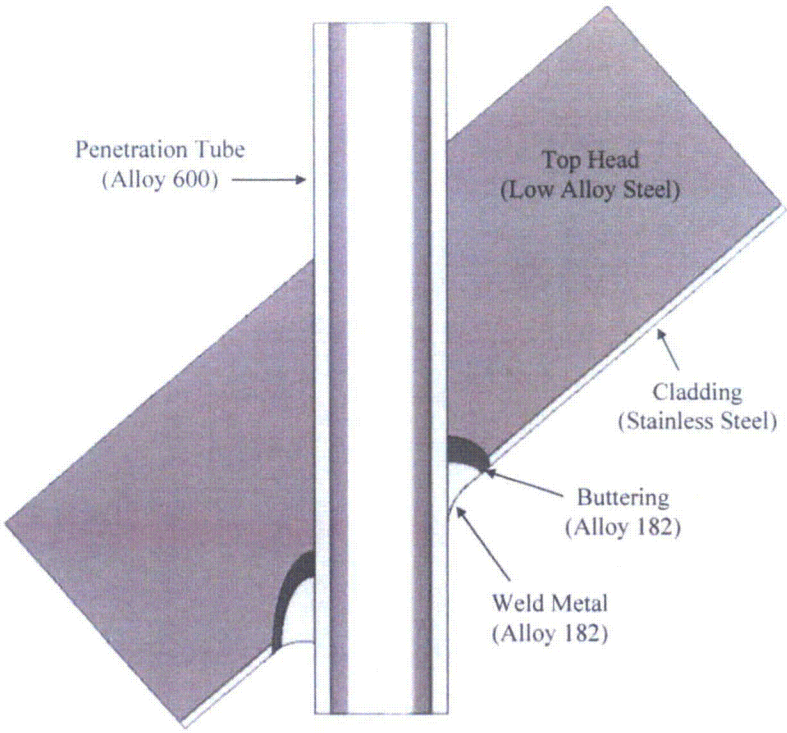

Figure 1.1 Control Rod Drive Mechanism Penetration-Nozzle Assembly

Figure 1.2 shows the program concept. There are two primary efforts: NDE and DE. Regarding NDE, the surfaces and volumes for the various product forms in the CRDM nozzle assemblies were evaluated. Nickel-based alloy product forms typically contain PWSCC. Four nondestructive testing modalities were used at PNNL on Nozzles 31 and 59—eddy current (ET), time-of-flight diffraction (TOFD), immersion ultrasonic testing (UT), and visual testing (VT). The NDE inspections were conducted in a laboratory environment using very high sensitivity to optimize flaw detection but were not performed to meet existing codes and standards.

The NDE data from all of the inspections were combined or fused into an assessment of degradation. This assessment was used to guide the development of a DE plan with subsequent sectioning and metallurgical study of the two CRDM nozzle assemblies.

Metallographic techniques, including micro-polishing and etching, were used on some materials removed from the two CRDM nozzle assemblies. Also, photographs and micrographs from an optical microscope were combined with electron images of exposed degradation from a scanning electron microscope (SEM). This work was performed to determine the "true state" of any fabrication flaws, conditions, and degradation to contribute to the knowledge base of PWSCC, especially its morphology and location.

During conduct of the second effort (i.e., DE), the location of degradation was recorded in the coordinate system used by the NDE inspections. These data were combined with images of the NDE responses. The purpose of this portion of the project was to quantify the sensitivity and specificity of the NDE to the shape and form of the degradation.

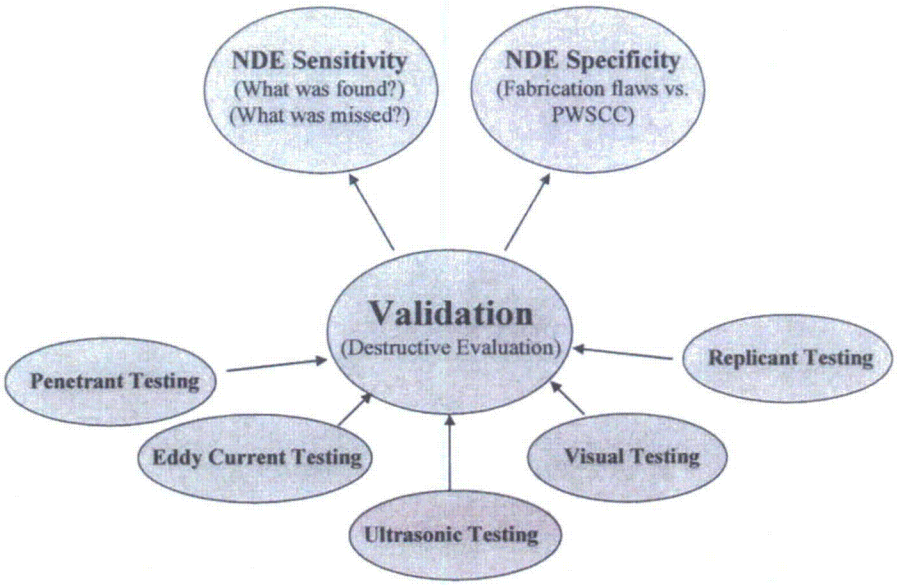

Figure 1.2 NDE Studies of CRDM Nozzle Assemblies Removed from Service

Figure 1.3 shows a CRDM penetration-nozzle assembly as received at PNNL after removal from the North Anna 2 reactor vessel head, wrapped, bolted, and strapped to the bottom of a shipping container. The outer wrapper for the assembly is taped to help prevent the spread of radioactive contamination. The portion of the CRDM nozzle assembly that would be above the top head of the vessel is shown on the left in the photograph resting on the lumber portion of the shipping fixture. On the right side of the photograph is a portion of the vessel top head, flame-cut from its location and surrounding a potentially degraded CRDM nozzle weldment.

In Figure 1.4, a CRDM nozzle assembly is shown being lifted from the container in which it was shipped to PNNL. The assembly is surrounded by additional wrapping to prevent escape of radioactive contamination that may have been dislodged during transport to PNNL facilities. The staff member shown is assisting by guiding the CRDM as it is lifted by an overhead crane (not shown).

This report documents the NDE of Nozzles 31, 54, and 59, which were removed from the decommissioned North Anna 2 RVH. Section 2 describes the decontamination activities at PNNL and shows a CRDM penetration-nozzle assembly prepared for removal of its radioactive oxide layer. The NDE probes and measurements used for the inspection of CRDM penetration assemblies and mapping of degradation are described in Section 3. The pre-inspection testing done using calibration pieces is described in Section 4. The results of the NDE examinations are described in Section 5. Section 6 details the process and results for the DE of Nozzle 31. The NDE and DE results for Nozzle 54 are summarized in Section 7. A discussion of all results is provided in Section 8, and conclusions are presented in Section 9.

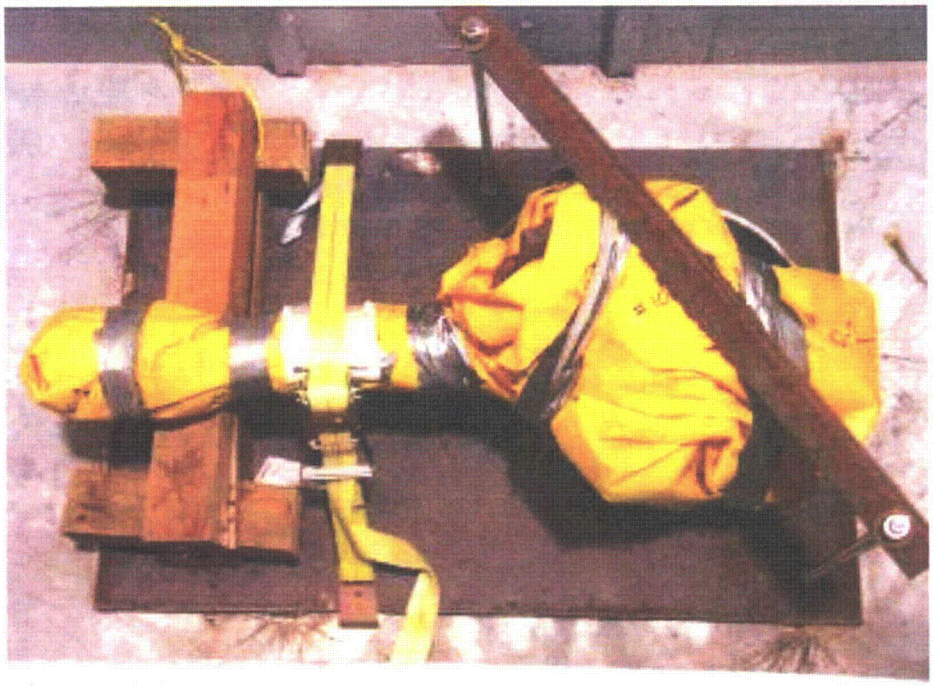

Figure 1.3 CRDM Penetration-Nozzle Assembly as Received at PNNL

Figure 1.4 CRDM Nozzle Assembly Being Removed from Shipping Container

2 Decontamination of Control Rod Drive Mechanism Nozzle Assemblies

The CRDM nozzle assemblies were decontaminated to minimize radiation exposure for PNNL personnel and the round-robin inspection teams during the NDE and DE. Figure 2.1 shows a CRDM penetration-nozzle assembly in a glove box. The flame-cut surface of the top head of the vessel is shown after being painted red to secure the remaining small amounts of contamination. The CRDM penetration tube that extends above the vessel top head can be seen clearly. This portion of the assembly was not wetted by the reactor primary coolant water and was largely free of radioactive contamination. The wetted surfaces of the inside of the top head and the penetration tube were coated with a highly radioactive, hard oxide layer. PNNL decontaminated the CRDM using a carbon dioxide (CO_2) pellet blasting process and repeated application of replica material. These worked well for removing the loose contamination but did not reduce the dose level. Thus, it was concluded that the oxide layer must be removed to further reduce the dose. This hard oxide layer was removed by repeated application of a commercially available etchant-gel. The gel typically dries after application in about 2 hours, and then the etched portion of the dissolved reactive oxide layer can be wiped away with a cloth.

Figure 2.1 CRDM Penetration-Nozzle Assembly in Glove Box

The decontamination gel was effective at removing the contamination on the surface of the CRDMs and at reducing the radiation dose rate near the CRDMs. The contamination levels on Nozzle 59 went from well over 1 million decays per minute (dpm) per 100 square centimeters (dpm/100 cm^2) at the most contaminated areas to less than 100,000 dpm/100 cm^2. Similar results were obtained on Nozzle 31, with the lowest contamination levels remaining at around 200,000 dpm/100 cm^2. The contact dose levels also were reduced significantly. The decontamination results for different locations for Nozzle 59 and Nozzle 31 are given in Tables 2.1 through 2.4.

Table 2.1 Effects of Etchant Gel Decontamination on Removable Contamination Levels for Nozzle 59

Location	Removable Contamination (dpm/100 cm^2)/1000		
	Initial	Application 1	Application 8 (Final)
Dry surface (pressure vessel)	500	50	5
OD nozzle – dry side	200	40	1.5
ID nozzle – dry side	>1000	>1000	1
Wetted surface (pressure vessel)	200	800	40
OD nozzle – wetted side	300	900	65
ID nozzle – wetted side	600	800	45

Table 2.2 Effects of Etchant Gel Decontamination on Contact Dose Levels for Nozzle 59

Location	Contact Dose Rate (mRem/hr)	
	Application 1	Application 8 (Final)
ID nozzle – dry side	270	40
Dry side surface	250	90
ID nozzle – wetted side	3000	1100
Wetted side surface	1200	580

Table 2.3 Effects of Etchant Gel Decontamination on Removable Contamination Levels for Nozzle 31

Location	Contact Dose Rate (mRem/hr)	
	Application 1	Application 13 (Final)
Dry surface (pressure vessel)	5	<MDA[a]
OD nozzle – dry side	5	<MDA
ID nozzle – dry side	1000	<MDA
Wetted surface (pressure vessel)	300	10
OD nozzle – wetted side	130	200
ID nozzle – wetted side	450	200

(a) Less than minimum detectable activity.

Table 2.4 Effects of Etchant Gel Decontamination on Contact Dose Levels for Nozzle 31

Location	Contact Dose Rate (mRem/hr)	
	Application 1	Application 13 (Final)
ID nozzle – dry side	300	40
Dry side surface	400	70
ID nozzle – wetted side	2100	1400
Wetted side surface	1200	500

Note: After Application 9, the dose rate at 30 cm ranged from 6 to 37 mrem/hr.

3 Nondestructive Examinations of North Anna 2 Nozzles

The North Anna 2 nozzles have been the subject of three series of nondestructive examinations. The first series was the in-service examination regime at North Anna 2 that determined the need to replace the pressure vessel head. After the head was removed from service and the suspect nozzles cut out and shipped to PNNL, a round-robin examination of the penetration tubes was performed at PNNL but was administered by EPRI as part of the cooperative agreement between the NRC and industry. The final and most extensive series of examinations also was performed at PNNL under laboratory-quality and controlled conditions. This section describes the in-service and round-robin testing briefly, as the specifics of the probes and techniques used to examine the nozzles are proprietary. The examinations performed by PNNL are described in much more detail because all of the information generated by the laboratory examinations under NRC contract is publicly available.

3.1 In-Service Examination

In 2001, a bare metal visual examination of the North Anna 2 top head showed that three nozzles were leaking. The nozzles were examined using penetrant, ultrasound, and eddy current testing; repaired using 152/52 weld metal; and put back into service. In 2002, a bare metal visual examination of the top head showed that 2 penetrations were leaking, 4 penetrations were suspected of leaking, and 21 nozzles were masked by boric acid deposits from other sources to the point where it was impossible to determine if they were leaking. The North Anna 2 CRDM penetration nozzles were examined using eddy current techniques on the J-groove weld surface and the interior of the penetration tube, ultrasonic examinations of the penetration tube, ultrasonic examinations of the annulus to try to find evidence of a leakage path, and penetrant testing of the J-groove weld surface. The ISI techniques used in service are given in Table 3.1.

Table 3.1 ISI NDE Techniques Used to Study CRDM Nozzle Assemblies

NDE Technique	Product Form	Examination Area
Eddy current testing	Alloy 600 penetration tube	Near-surface examination
	J-groove weld	(1–3 mm depth of penetration)
Ultrasonic examination	Alloy 600 penetration tube	Volumetric examination of nozzle
Ultrasonic examination	Interference fit (annulus)	Leakage path measurement of annulus

After the nozzles were cut from the pressure vessel head and shipped to PNNL, a round-robin test was performed on the nozzles. The round robin was performed at PNNL in 2004 and was designed to determine how effective different techniques were at finding the possible degradation in the nozzles. As the weld geometry is complicated and posed a challenge to the round-robin examinations, all examinations were limited to the interior of the penetration tubes. The round-robin examinations included ultrasonic and eddy current testing of the penetration tube, as well as ultrasonic and eddy current measurements to try to detect a possible leakage path in the annulus above the weld. The round-robin tests were performed from below the nozzles in a field-like geometry but with a lower radiation dose rate and without any interference that would have been caused by nearby nozzles. As previously discussed, the round robin inspections were administered by EPRI. The purpose was to perform inspections under

laboratory conditions to address questions raised during the in-service inspections, such as whether certain indications were truly PWSCC. Conducting the laboratory examinations also provided an opportunity to make judgments regarding the effectiveness and reliability of NDE as currently performed. It was not the purpose of this exercise to evaluate individual inspectors or inspection teams. Thus, the combined results for all teams were made available for this report. The NDE techniques used in the round-robin testing are given in Table 3.2.

Table 3.2 Round-robin Testing NDE Techniques Used to Study CRDM Nozzle Assemblies

NDE Technique	Product Form	Volumetric or Surface
Eddy current testing	Alloy 600 penetration tube	Near-surface examination (1–3 mm depth of penetration)
Ultrasonic examination	Alloy 600 penetration tube	Volumetric examination
Deep penetrating eddy current testing	Interference fit (annulus)	Leakage path measurement of annulus
Ultrasonic examination	Interference fit (annulus)	Leakage path measurement of annulus

3.2 Nondestructive Testing at PNNL

The six NDE techniques used for studying the CRDM penetration nozzle-assemblies removed from service are listed in Table 3.3. Eddy current testing was used to detect surface-breaking flaws on the inside of the Alloy 600 tube of both nozzles and on the J-groove weld of Nozzle 31. The ET technique examines the near-surface region with a depth of penetration that varies between 1 to 3 mm (0.04 in. to 0.12 in.), depending on the frequency of coil excitation and size of the coil. Ultrasonic testing with spherically focused probes was applied from the inside of Alloy 600 nozzles of both nozzles to inspect the fusion zone of the J-groove weld with the nozzle and beyond, into the weld metal. Time-of-flight diffraction (TOFD), an ultrasonic technique, was applied to the volume of the Alloy 600 nozzle from the inside surface of the tube. Visual testing was performed on replicas of the surface of the J-groove weld and buttering using a high-resolution camera. The J-groove weld of Nozzle 31 was examined using penetrant testing, and all relevant indications found in the J-groove weld of Nozzle 31 were photographed directly using a high-resolution camera.

Table 3.3 PNNL NDE Techniques Used to Study CRDM Nozzle Assemblies

NDE Technique	Product Form	Volumetric or Surface
Eddy current testing	Alloy 600 nozzle J-groove weld	Near-surface examination (1–3 mm depth of penetration)
Time-of-flight diffraction	Alloy 600 nozzle	Volumetric examination
Spherically focused probe ultrasound	J-groove weld and buttering	Volumetric examination
Visual testing via replicant	J-groove weld crown Alloy 600 of Nozzle of 59	Surface examination
Bare metal visual testing	J-groove weld crown of 31	Surface examination
Penetrant testing	J-groove weld crown of 31	Surface examination

3.2.1 Scanners

The CRDM nozzles presented two regions of interest for scanning—the interior of the penetration tube and the wetted surface of the J-groove weld crown and buttering. These different regions required different scanners, which are described in this section.

3.2.1.1 Theta-Z Scanner

The Theta-Z scanning apparatus for examining the inner diameter (ID) of the penetration tubes was constructed by Brockman Precision Machine and Design, Kennewick, Washington. The ID scanner was designed for inner-surface scanning by both ET and UT probes. Figure 3.1 shows the scanner sitting on a laboratory bench and in use on Nozzle 31 in a walk-in hood at PNNL. The scanner has a linear (vertical) axis and a rotational axis. The range of linear motion is 40 cm. The rotational motion is continuous, with no hard limits, but is practically constrained to approximately 1.5 revolutions by the cables attached to the motor drivers and the NDE probes.

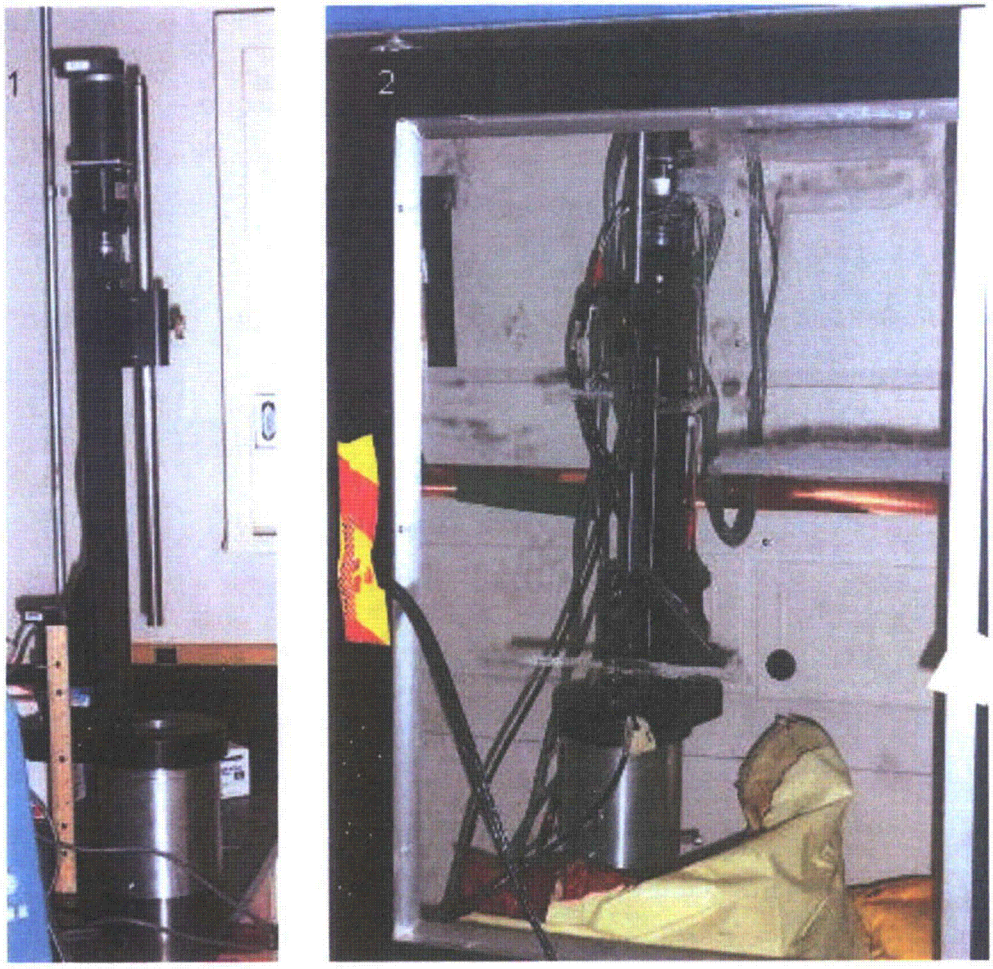

Figure 3.1 CRDM Scanner on Laboratory Bench with 30-cm Scale (left) and in Use on CRDM Nozzle 31 in PNNL Walk-In Hood (right)

3.2.1.2 *x-y* Scanner

The eddy current data acquisition system is based on a computer-controlled linear *x-y* scanner as shown in Figure 3.2 and an eddy current instrument and probe. The scanner was designed to allow examination of the welded surface of a CRDM nozzle assembly. The probe, described later, is attached to the scanner, held on to the specimen with spring loading, and scanned over the piece while magnitude and phase data are recorded from the material over the defined scanning grid. Raster scanning of the surface of the sample consists of line scans in *x* (left to right) while incrementing in *y* (back to front). The scanner was manufactured by Parker Hannifin Corporation, Motion Control Systems, North America. The scanner assembly was mounted in an aluminum tray. A Plexiglas box beneath the scanning bridge holds the sample and provides additional containment to reduce the spread of contamination inside the fume hood. Additionally, a lock-down turntable (shown as light brown) with marked increments of 5 degrees was fabricated and is seen in Figure 3.2 holding the cutout nozzle section inside the Plexiglas box. The turntable facilitated rotational or circumferential positioning of the nozzle assembly for inspection.

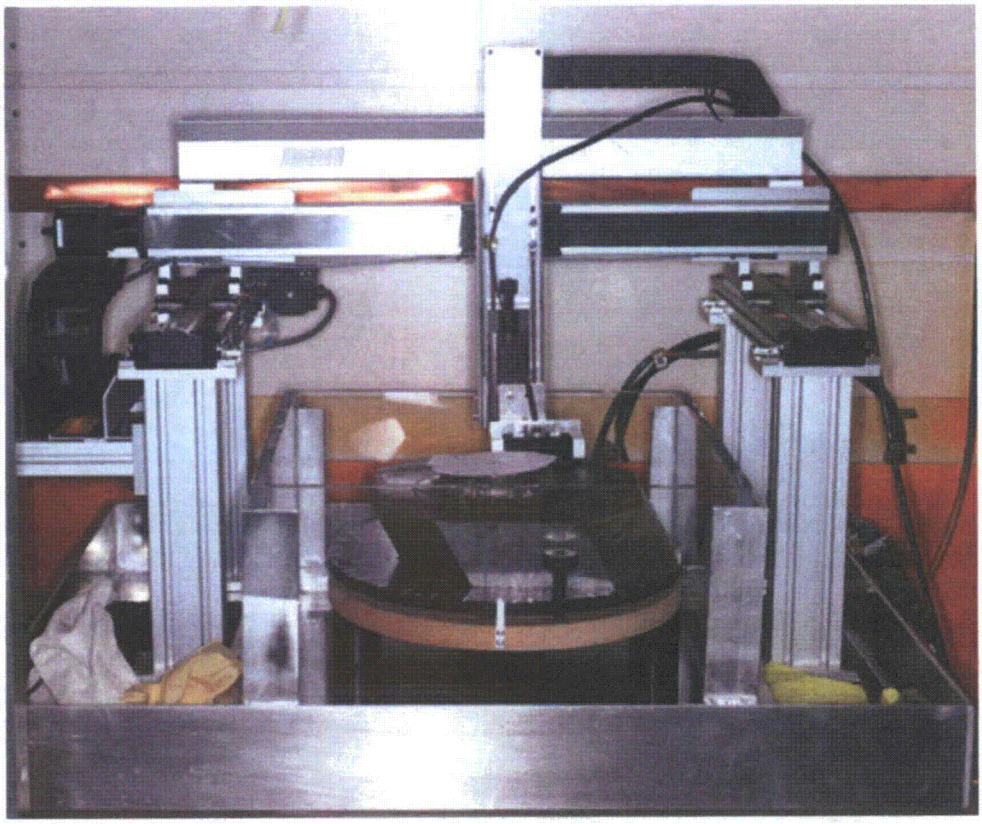

Figure 3.2 Eddy Current Scanner with Attached Probe on a Cut-Down Version of CRDM Specimen 31 from the North Anna 2 Plant

3.2.2 Eddy Current Probe Assembly and Sensors

The sensitivity of the ET probes as a function of angle is shown in Figure 3.3. The data for this graph were acquired by scanning the sensors across two scribe marks in the calibration piece (one axial and one circumferential). The sensors were rotated 1/16 turn (22 ± 5 degrees) between scans, over a range of 1/4 turn (90 ± 5 degrees).

The ET data collection apparatus is shown in Figure 3.4. The apparatus consists of a Zetec MIZ-27 ET instrument, a Gateway GP7-800 computer, and motor control electronics. The computer uses a National Instruments 16-bit digitizer card (PCI-MIO-16XE-10) and counter-timer card (PCI-6602) to digitize data from the ET instrument analog output. The counter-timer uses signals from encoders on the linear axis motors to synchronize data-taking with probe position.

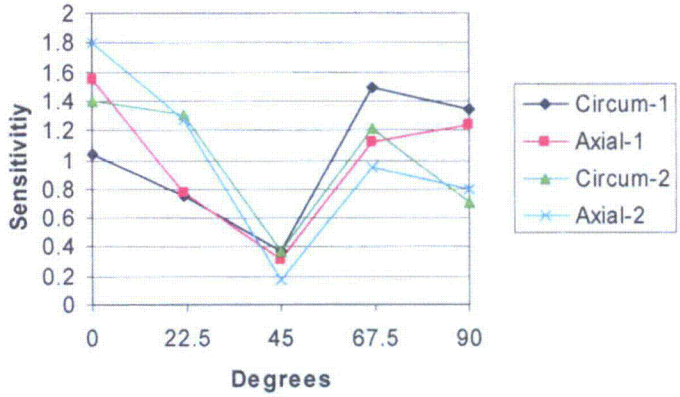

Figure 3.3 Eddy Current Probe Sensitivity as a Function of Angle, Normalized to Yield Average of 1.0 for Each Set of Measurements

Figure 3.4 Data Collection Apparatus: Zetec Eddy Current Instrument (left), Computer (lower right), and Control Electronics (bottom center)

3.2.2.1 Eddy Current Using the Theta-Z Scanner

The ET probe assembly consists of a housing with two sensor seats and is shown in Figure 3.5. The sensors used were differential plus-point probes supplied by Zetec, Inc. The plus-point probe is preferentially sensitive to localized features such as cracks but is relatively insensitive to irregular surface features that may cause "lift-off." These probes are also direction-sensitive. For this reason, two sensors were used, one oriented at 45 degrees to the other. This provided consistent and uniform detection for cracks in any orientation. The probe design uses spring-loaded ball bearings to hold the probe assembly centered in the penetration tube to account for variations in the inside diameter of the nozzles. Figure 3.6 shows how the probe assembly fits into the penetration tube for scanning.

Figure 3.5 Redesigned Probe Assembly Showing Roller Bearings and Both Sensors

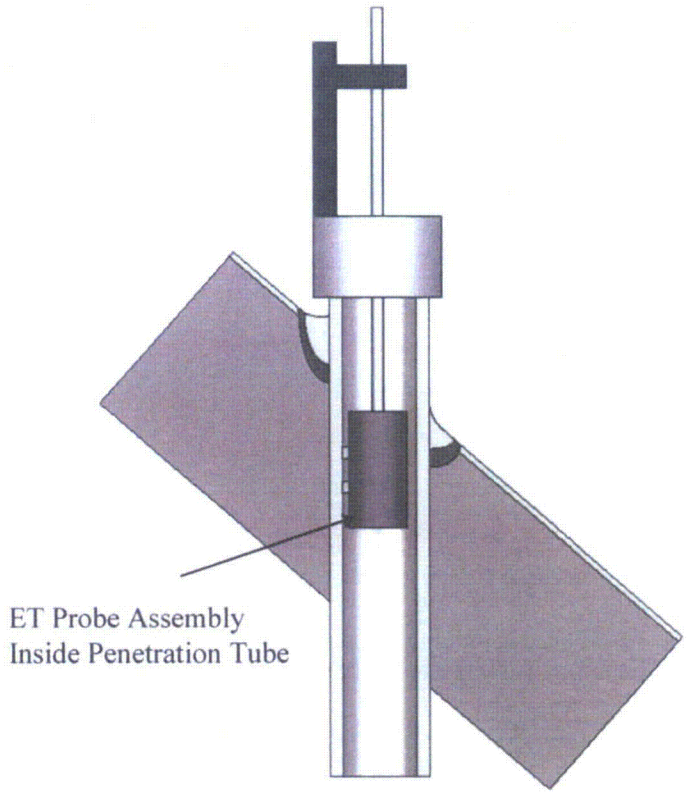

Figure 3.6 How the ET Assembly Fits in the Penetration Tube

3.2.2.2 Eddy Current Using the *x-y* Scanner

The ET probe assembly consists of a rectangular housing held onto the piece using a spring-loaded slide. The sensor used was a differential plus-point probe supplied by Zetec, Inc. The spring-loaded slide is shown in Figure 3.7. The spring-loaded slide holds the probe on the part while allowing the probe to ride over surface irregularities. The probe and probe holder are shown in Figure 3.8. This holder provides a spring-controlled up-and-down motion for the probe as well as wheels for smooth left and right movement. Additionally, the probe holder is mounted to the vertical slide with a horizontal aluminum piece that pivots on the slide. This pivoting action, the probe up and down motion, and the wheels provide increased stability and more uniform coupling to the material over rough and welded surfaces.

This portable scanner assembly was developed on a benchtop and moved to the Radiochemical Processing Laboratory (RPL) where the North Anna 2 CRDM nozzle assembly was evaluated.

Figure 3.7 Spring-Loaded Slide Assists in Holding the Probe on the Specimen

Figure 3.8 Plus-Point Probe in a Spring-Loaded Holder (left) and the Probe Holder Assembly Attached to the Scanner Vertical Slide at a Pivot Point (right)

3.2.3 Time-of-Flight Diffraction Probe Assembly and Transducers

Two sets of TOFD probes were used for data acquisition on the nozzles. The transducers used were Krautkramer round probes, 6 mm (0.25 in.) in diameter, attached to screw-in wedges. A 5-MHz, 60-degree longitudinal pair, the industry standard for the TOFD technique, and a 7.5-MHz, 60-degree longitudinal pair were used. The probe holder with two transducers is shown in Figure 3.9. When mounted on the search tube, the probe orientation is vertical with a top and bottom transducer. Each probe is individually pushed out via spring loading to provide contact with the inner surface of the nozzle wall. A water line for coupling is shown to the left of the transducer. This holder was later modified to provide an additional coupling water line to the right transducer. Signal consistency and quality were improved with this modification. Water dripped along the inside wall of the nozzle and was collected in a pan under the CRDM. A peristaltic pump in the tubing loop circulated approximately 2 L/min of water

from the drip pan to the TOFD probes. Secondary water containment was provided by a large plastic berm that held the entire CRDM assembly, including the CRDM support frame, all water lines, and the pump. Figure 3.10 shows how the probe would fit into the penetration tube for scanning.

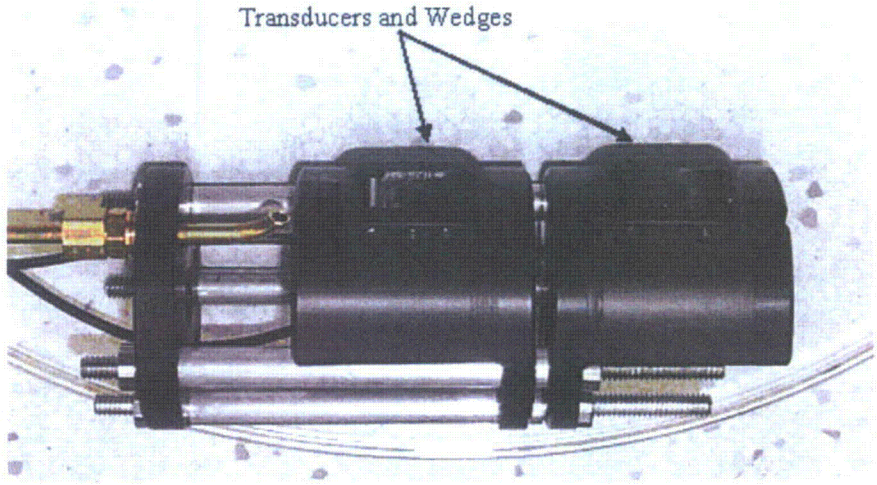

Figure 3.9 Time-of-Flight Diffraction Transducers Mounted in Holder Assembly with Signal and Water Lines

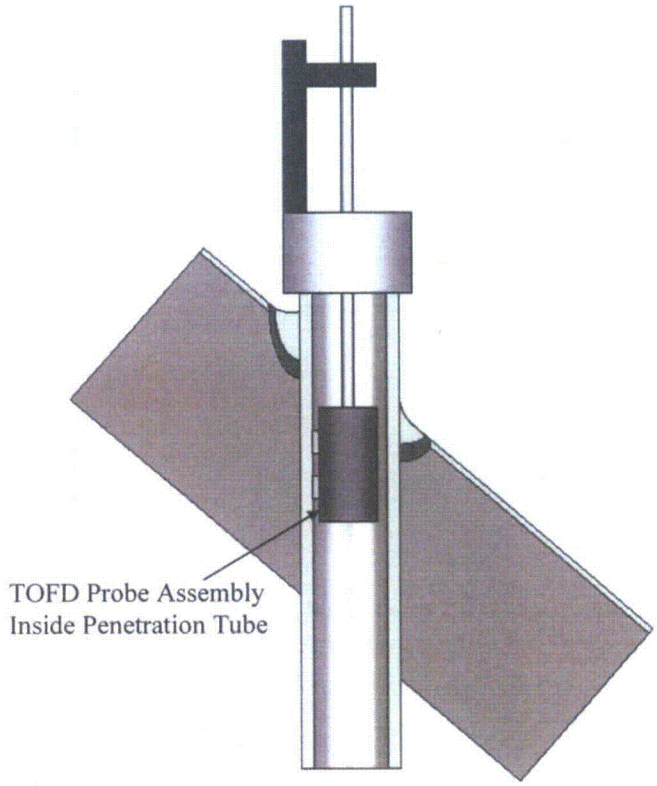

Figure 3.10 How the TOFD Assembly Fits in the Penetration Tube

3.2.4 Immersion Ultrasonic Probe Assemblies and Transducers

Immersion UT data at a 0-degree incident angle (perpendicular to the penetration tube ID surface) were acquired on Nozzles 59 and 31 at frequencies of 500 kHz, 1 MHz, 2.25 MHz, and 5 MHz. Two of the transducers and a probe in the large-diameter mirror assembly are shown in Figure 3.11. The reflective mirror provided a 0-degree incident angle for the inspection. To inspect a nozzle, a plug was placed in the bottom of the CRDM assembly (ID) for the CRDM in the orientation shown in Figure 3.10. A cap was placed over the nozzle outer diameter (OD) that extended approximately 50 mm (2 in.) axially and was secured with a hose clamp. This provided double containment of the water in the nozzle. Additionally, a catch basin was kept under the CRDM assembly, and a large berm held the entire assembly. Once the nozzle was sealed, water was added to bring the fill level to approximately 25 mm (1 in.) below the top surface. An inadvertent small tilt in the vertical position of the CRDM assembly helped to prevent an air bubble from becoming trapped on the transducer surface as it was lowered into the water. The bubble formation was a potential problem for the 5-MHz focused probe (100-mm focus) with its concave surface 19 mm (0.75 in.) in diameter. The 2.25-MHz probe had a 6-mm (0.25-in.) diameter and was unfocused (flat). Both the 1-MHz and 500-kHz transducers were 12.5 mm (0.5 in.) in diameter and unfocused. The data were processed using the synthetic aperture focusing technique (SAFT) and envelope-detected prior to data analysis.

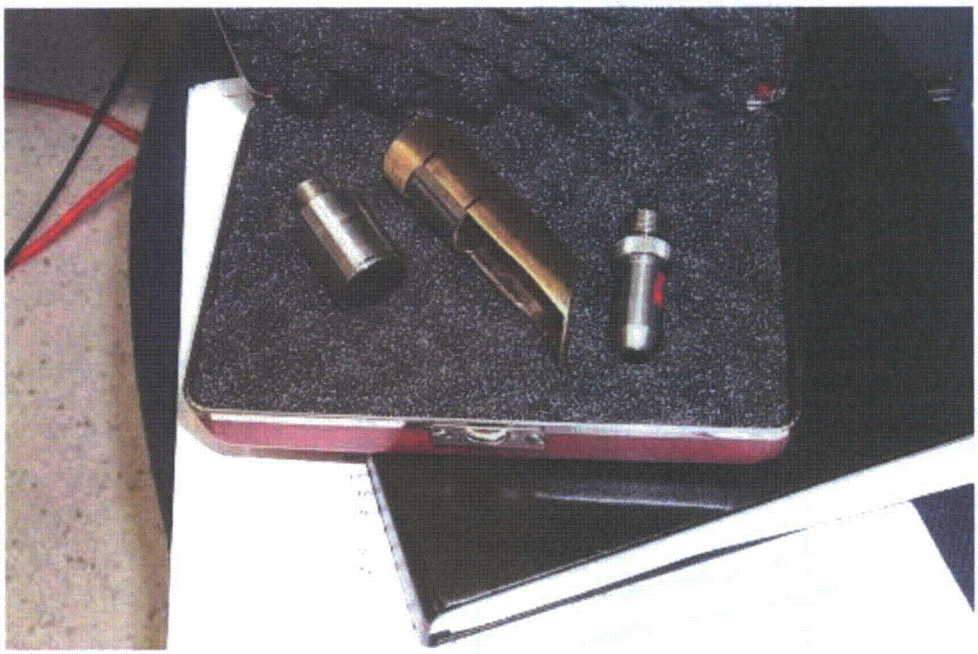

Figure 3.11 Two Immersion Ultrasonic Transducers with Mirror Assembly in Center. The mirror provided a 0-degree incident angle for the inspection.

3.2.4.1 Front Surface Alignment

A variable water path distance to the inner surface of the nozzle was noted in the immersion UT data. This was due to weld shrinkage and the tilt of the CRDM assembly in the metal frame holder. The tilt from a vertical position likely caused the transducer at the end of the search tube to slightly wander from its center position as the scanner moved circumferentially around the CRDM assembly. To correct for this misalignment, each A-scan in the data file was threshold-detected and shifted in time (or depth), if necessary, to place all the ID nozzle surface signals at the same zero start position in time. This alignment step is critical for subsequent data analysis to ensure that indications are mapped to the correct depth.

3.2.4.2 Signals and Areas of Interest

The areas investigated with immersion UT were from the ID out: the nozzle material, the first fusion zone, the J-groove weld, the second fusion zone, the buttering, the third fusion zone, and the top head carbon steel material. The Alloy 600 nozzle wall is approximately 16 mm (0.63 in.) thick. The J-groove weld varies around the penetration tubes and nominally is approximately 13 to 18 mm (0.5 to 0.7 in.) thick, and the buttering layer is approximately 10 mm (0.4 in.) thick. The lower frequencies penetrated deeper into the material and could potentially detect flaws out in the buttering material and beyond, while the higher frequencies provided better resolution at shallower depths.

3.2.4.3 Visual Testing of J-Groove Weld Surface

Enhanced VT, when applied properly, can be a useful tool in detecting and characterizing component surface features. To achieve a proper level of resolution with the system, one needs a high–pixel-count camera system, a high-quality lens, and a proper lighting arrangement. A low-resolution camera or incorrect lighting can greatly reduce the reliability of a visual system. For the visual tests, PNNL used a Canon 1Ds Mk 2 camera with a 180-mm 1:1 macro lens. The camera with the 180-mm lens was able to resolve 41 lines/mm using a 1951 Air Force resolution target.

This magnification is very useful for detecting and identifying cracks. Stress corrosion cracks of the PWSCC style (called interdendritic stress corrosion cracking or IDSCC by some) in nickel alloys typically have widths of 0–120 μm (0–0.05 in.) with median widths of 31 μm (0.0012 in.) (MacDonald 1985; Ekström and Wåle 1995). The Canon camera system using diffuse lighting has a pixel size of 7 μm (0.0003 in.) and would be able to, under ideal conditions, detect a crack as narrow as 5 μm (0.0002 in.) and definitively identify it as a crack at the higher magnification.

3.2.4.4 Replicant Testing

Because the CRDMs are highly radioactive and contaminated and have a complex geometry, the VT of the J-groove weld was performed using a replica of the weld region. An epoxy-like polymer (Microset Products Ltd., Warwickshire, UK) was applied on a surface as a liquid; it then hardened, making a high-resolution replica of the surface. The replica was then peeled from the surface and examined. This surface replication captured details of as small as 0.1 μm (0.000004 in.). Images of cracks on the order of 10–100 μm (0.0004–0.004 in.) wide were captured by the replica.

When the replicas were being photographed, the camera was mounted on a graduated slide bar and a graduated tripod. The camera and slide-bar arrangement is shown in Figure 3.12. This arrangement allowed for precise raster scanning of the sample. The replicas were mounted on a flat board, and the camera slide bar was set parallel to the board at a distance that gave 1:1 macro focusing. The slide bar and tripod height were adjusted to put the camera at the top left-hand corner of the sample and then indexed across, taking a photograph every 33 mm (1.3 in.). When the length of the sample was scanned, the tripod height was lowered by 19 mm (0.8 in.), the camera repositioned at the left-hand edge of the sample, and the next indexed series across the replica was photographed. This procedure allowed for complete coverage of the sample with very high resolution and some overlap on the edges. The images were then examined at 100%–200% magnification on a high-resolution monitor.

Figure 3.12 High-Resolution Camera Mounted on a Slide Bar and Tripod

3.2.4.5 Penetrant Testing

To find cracks that were too small or camouflaged for replicant testing, penetrant testing was used to examine the J-groove weld surface of Nozzle 31. Because PWSCC was suspected to be very tight and challenging to PT, PNNL selected high-sensitivity fluorescent dye. To meet these parameters, Magnaflux Zyglo ZL-27A dye was used along with Spotcheck SKC-S cleaner and SKD-S2 developer. A dwell time of at least 30 minutes was used to ensure that the dye had sufficient time to be drawn into possible cracks.

4 Pre-Inspection Calibration and Testing

Before the CRDMs were examined, PNNL researchers characterized the NDE equipment and experimental methods to be used for the NDE methods. The pre-inspection tests were performed also to provide practice with the procedures in a nonradioactive environment to work out any problems and gain familiarity with the techniques. The test pieces used to calibrate and set inspection sensitivity are described in Section 4.1 for each NDE technique employed. Section 4.2 documents the responses for each NDE technique on the calibration pieces.

4.1 Test Pieces

The equipment and procedures for each NDE technique were tested and characterized prior to use on the removed-from-service CRDMs. The ET and TOFD equipment was tested using an Alloy 600 tube with machined notches and holes. The immersion UT was tested using a nonradioactive CRDM cut from the Midland Nuclear Power Plant pressure vessel head that was cancelled and never irradiated. The VT equipment was tested using cracked steel samples with a variety of crack sizes and surface conditions.

4.1.1 Penetration Tube Test Piece

The calibration standard for the ET and TOFD systems consists of a 100-mm-OD (4-in.) Alloy 600 tube with 12 electrical discharge-machined (EDM) notches cut into the inner- and outer-diameter surfaces. Each EDM notch was 25 mm (1 in.) long and 0.38 mm (0.015 in.) wide. Three 1-mm-diameter (0.04-in.) flat-bottom holes were drilled from the outside surface, terminating at 10.4, 6.9, and 1.3 mm (0.41, 0.27, and 0.05 in.) from the inner surface. The locations of the EDM notches are shown in Figure 4.1; the notches are described further in Table 4.1.

4.1.2 Immersion UT Test Piece

The immersion testing equipment and scanning technique were characterized using the Midland CRDM. The Midland CRDM has no service-induced or machined flaws, but it contains several fabrication flaws in the weld. This allowed PNNL to determine which UT frequencies and SAFT processing parameters were needed to effectively examine different regions of the J-groove weld. The Midland CRDM is shown in Figure 4.2.

4.1.3 Visual Testing Test Piece

The high-resolution camera and scanning equipment were tested using replicated surfaces made from stainless steel sample surfaces. The stainless steel samples were produced to be similar to stainless steel reactor internal surfaces (not clad) and have a variety of artificial cracks implanted in them. The crack opening dimensions range from less than 10 μm (<0.0005 in.) wide to 150 μm (0.006 in.) wide. The surfaces of the samples have been machined smooth, but some contain grinding marks that make VT much more challenging. Two of the stainless steel samples employed in this work are shown in Figure 4.3.

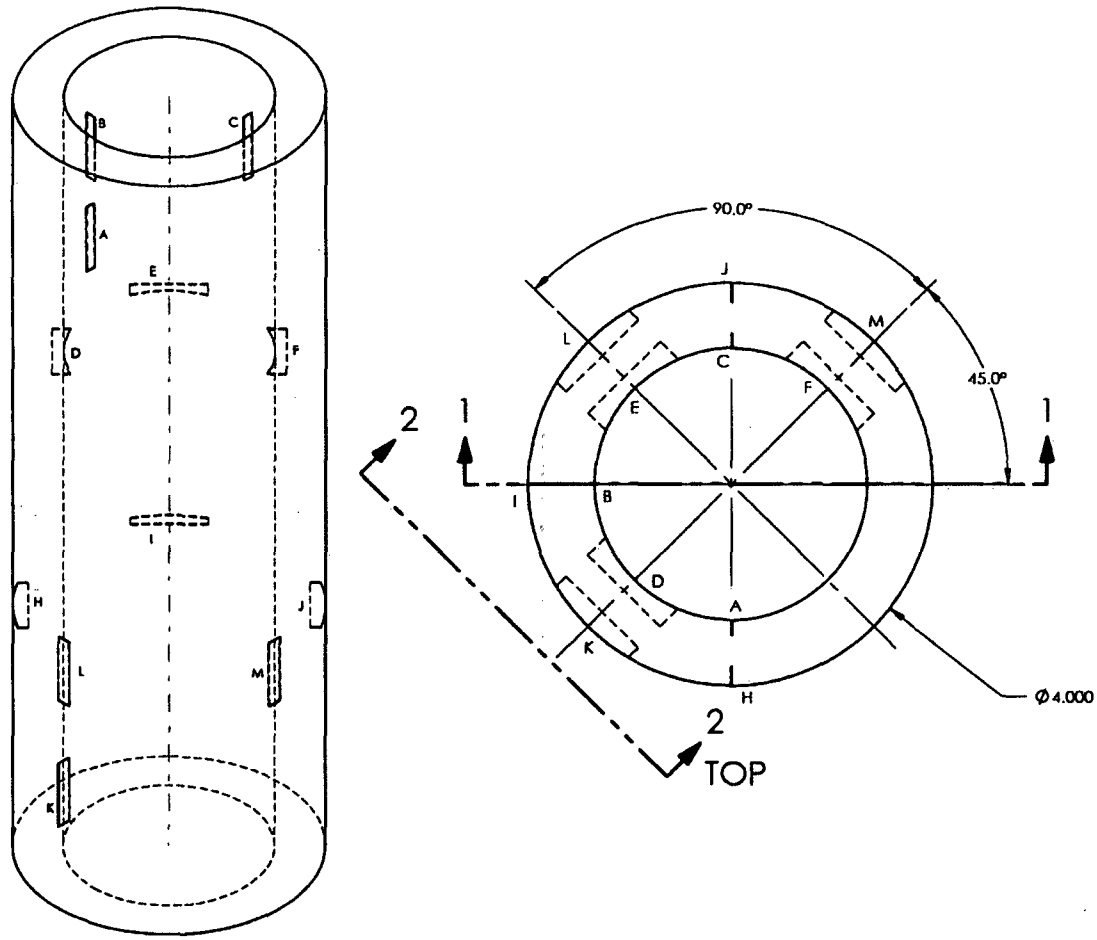

Figure 4.1 Penetration Tube Calibration Standard Isometric and Top View

Table 4.1 Calibration Tube Flaw Descriptions

Notch Designation	Surface	Orientation	Depth
A	ID	Axial	2 mm (0.08 in.)
B	ID	Axial	4 mm (0.16 in.)
C	ID	Axial	8 mm (0.31 in.)
D	ID	Circumferential	2 mm (0.08 in.)
E	ID	Circumferential	4 mm (0.16 in.)
F	ID	Circumferential	8 mm (0.31 in.)
H	OD	Circumferential	2 mm (0.08 in.)
I	OD	Circumferential	4 mm (0.16 in.)
J	OD	Circumferential	8 mm (0.31 in.)
K	OD	Axial	2 mm (0.08 in.)
L	OD	Axial	4 mm (0.16 in.)
M	OD	Axial	8 mm (0.31 in.)

Figure 4.2 Midland Control Rod Drive Mechanism Used for Testing Immersion UT Equipment and Techniques

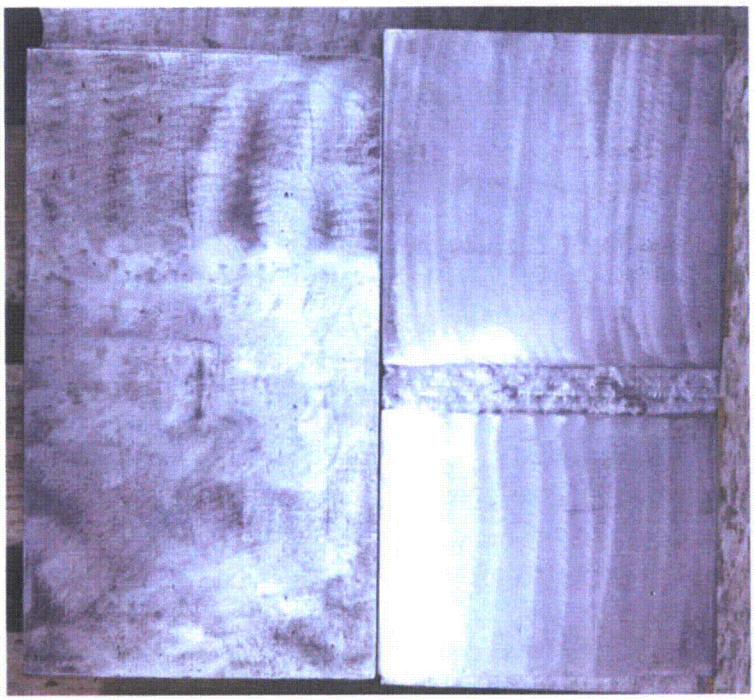

Figure 4.3 Two Cracked Stainless Steel Samples Used To Test Visual Testing Procedures and Equipment Using Replicas

4.1.4 Notched Plate Piece

At the beginning and end of a series of scans using the *x-y* scanner, a calibration check was made using an EDM notch "I" in an Alloy 600 plate 5.88 mm (0.625 in.) thick (Figure 4.4). The notch was 0.3 mm wide and 25 mm long with a 100% through-wall depth. Notch response variations were monitored to ensure a uniform system performance throughout the test period.

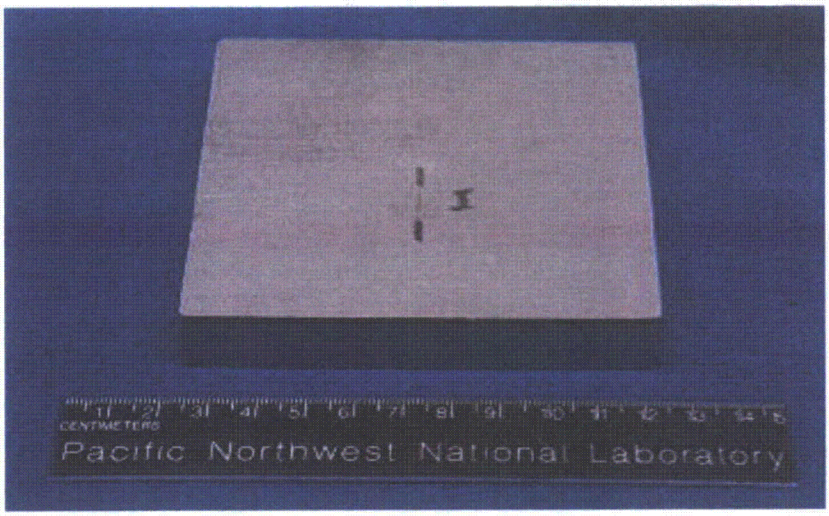

Figure 4.4 Calibration Notch "I" in Alloy 600 Plate Material Used To Assess Equipment Performance or Calibration

4.2 Nondestructive Evaluation Results from the Test Pieces

4.2.1 Eddy Current Responses to Artificial Flaws

The EDM notches for testing the ET procedure were on the inside surface of the Alloy 600 cylinder. The inner-surface EDM notches consisted of two sets of three each—an axially oriented set and a circumferentially oriented set. All were 25 mm (1 in.) long and 0.4 mm (0.015 in.) wide. Their depths were 2, 4, and 8 mm (0.08, 0.16, and 0.31 in.). In addition, three flat-bottom holes were drilled from the outside surface, terminating at 10.4, 6.9, and 1.3 mm (0.41, 0.27, and 0.05 in.) from the inner surface.

Eddy current testing responses to all the inner surface notches were very large. None of the outer-surface notches was detectable by ET. Only the flat-bottom hole terminating 1.3 mm (0.41 in.) from the inner surface was detectable. Figure 4.5 shows the response of the 0-degree ET probe to the notches. The axis of the cylinder runs from lower left to upper right; thus, the left-hand set of notches is axial and the right-hand set is circumferential. Two images of the 2-mm-deep (0.08-in.) axial notch, at 90 degrees and at 270 degrees (58 mm and 175 mm), can be seen, although the second image is truncated by the end of the scan. Figure 4.6 shows the ET response to scribe marks as well as to the notches when high gain was used.

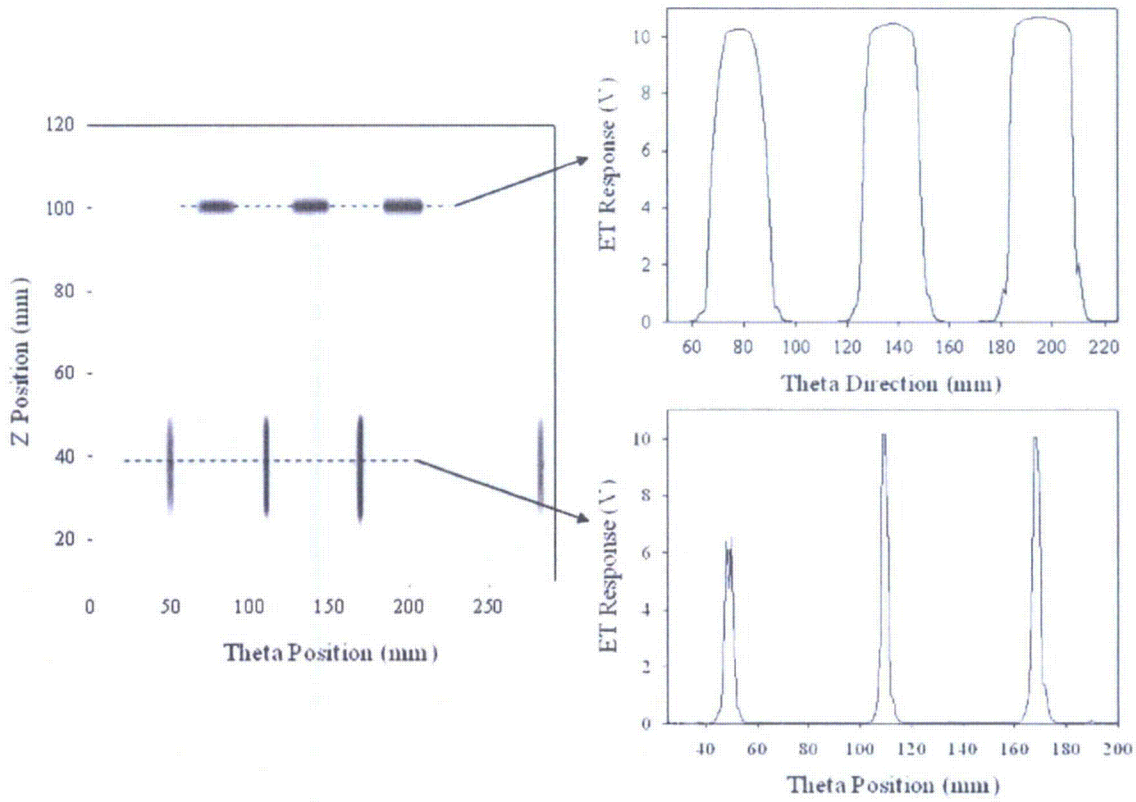

Figure 4.5 Eddy Current Response to 2-, 4-, and 8-mm (0.08-, 0.16-, and 0.31-in.) EDM Notches in Calibration Tube at 350 kHz, 15 dB Gain, and 0 Degrees Probe Rotation

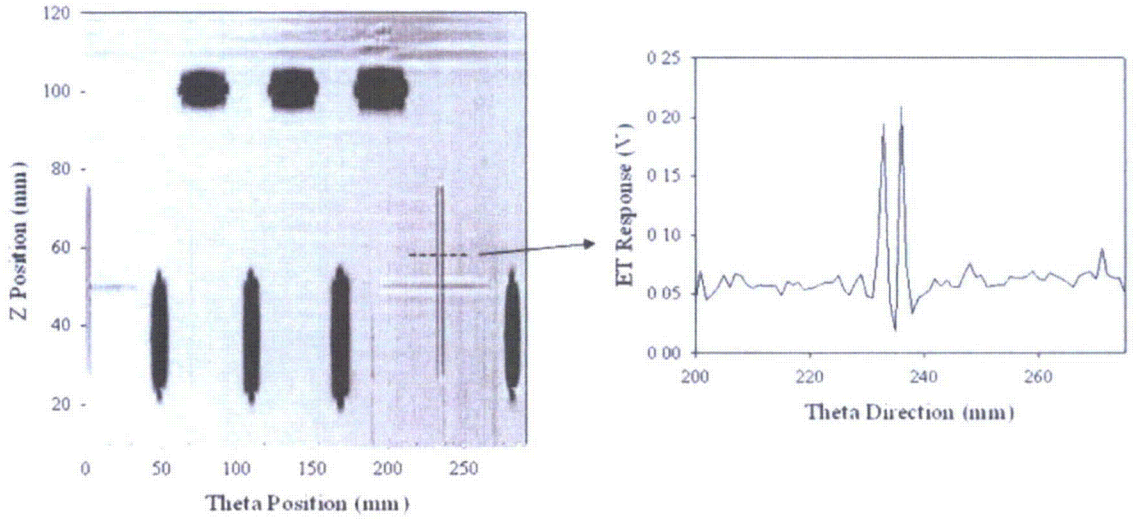

Figure 4.6 Eddy Current Response in the Calibration Tube to Scribe Marks at 350 kHz, 15 dB Gain, and 0 Degrees Probe Rotation

Figure 4.7 shows the response of the 45-degree plus-point sensor to the 0- and 90-degree notches. The amplitudes are much lower, and the peaks are often at the ends of the notches. The only difference between the 0-degree and 45-degree sensors is how the probes are oriented in their holders. Figure 4.8 shows the response of the 45-degree probe at high gain, 150 kHz. The response to a far-side flat-bottom hole, terminated at 1.3 mm (0.050 in.) below the surface, is visible at 200 mm (7.9 in.) horizontal (axial) and at 0 and 233 mm vertical (0 and 9.2 in.) (circumferential). The response to the scribe lines at lower left is visible mainly at the tip of each line, as is expected for a 45-degree orientation of the plus-point probe.

Typical voltage magnitudes and phases for various artificial flaws, for the 0-degree probe at 15 dB gain, are as shown in Table 4.2, from the calibration reference scan performed after inspection of Nozzle 31. Because the person who needed to move the scanner from the test piece to the CRDM was physically required to be in a radiation field during the pre-scan calibration, a complete one-hour calibration scan was not performed immediately before the inspection. A shorter scan over a notch with a known response was taken to ensure that the equipment was working properly.

A complete scan of the calibration piece was not performed for the calibration scans before or after the inspection of Nozzle 59. The available data from two notches (0-degree probe) show 3 V at 240 degrees for an axial notch 2 mm (0.08 in.) deep and 3 V at 62 degrees for a circumferential notch 2 mm (0.08 in.) deep.

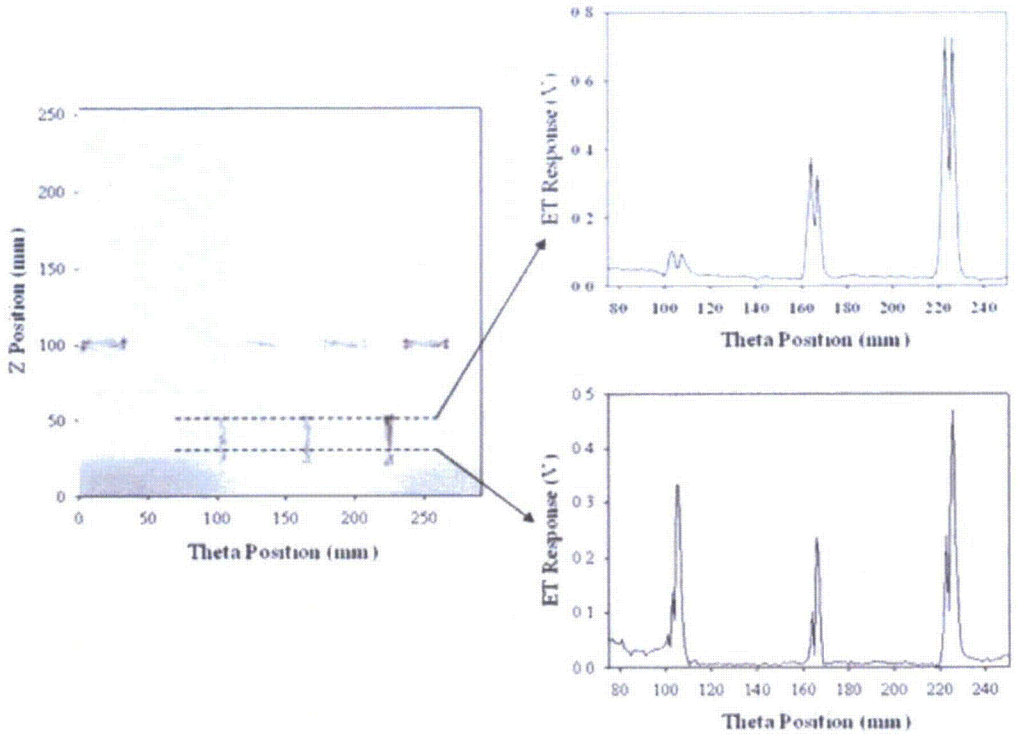

Figure 4.7 Eddy Current Response to 2-, 4-, and 8-mm (0.08-, 0.16-, and 0.31-in.) EDM Notches in Calibration Tube at 350 kHz, 15 dB Gain, and 45 Degrees Probe Rotation

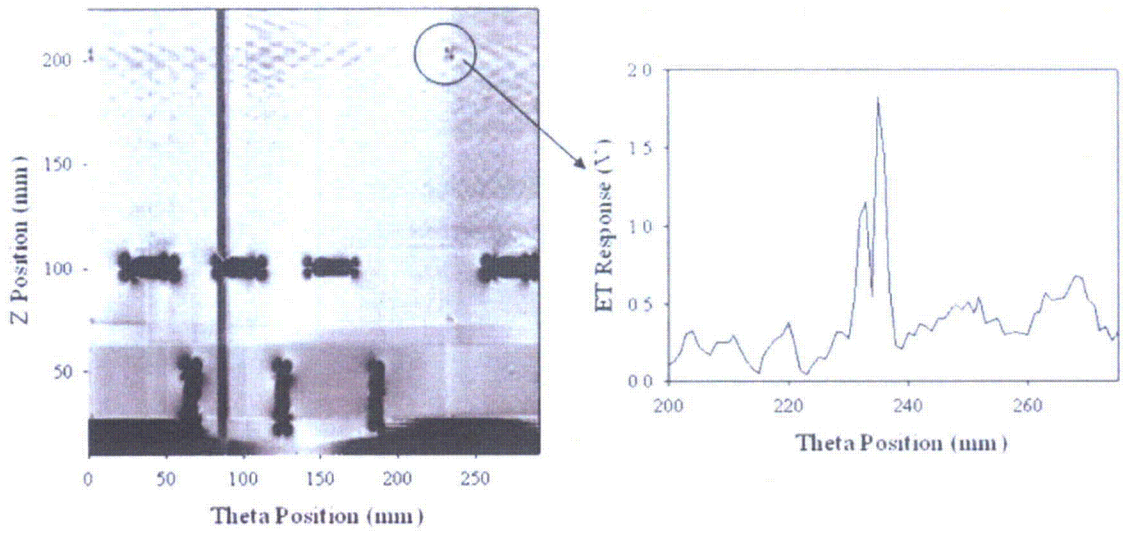

Figure 4.8 Calibration Check of the Calibration Tube Using 150 kHz and 35 dB Gain

Table 4.2 Typical Eddy Current Artificial Flaw Responses at 15 dB Gain (Nozzle 31 Post-Inspection)

	Axial		Circumferential	
Depth (mm)	Magnitude (volts)	Phase (degrees)	Magnitude (volts)	Phase (degrees)
2	9	170	10	345
4	10	165	10	340
8	10	170	11	340
Scribe mark	0.2	185	0.1	185

The results for the eddy current scans of the EDM notch in the Alloy 600 flat-plate sample were similar to the result in the Alloy 600 tube. The peak voltage across the notch at 350 kHz and 15 dB gain was 10.3 V with the probe oriented favorably, and the peak voltage is much lower (2 V at the ends and 0.6 V in the middle) if the probe was oriented at 45 degrees to the notch. The ET results for the EDM notches with the probes at 0 degrees and 45 degrees are shown in Figures 4.9 and 4.10.

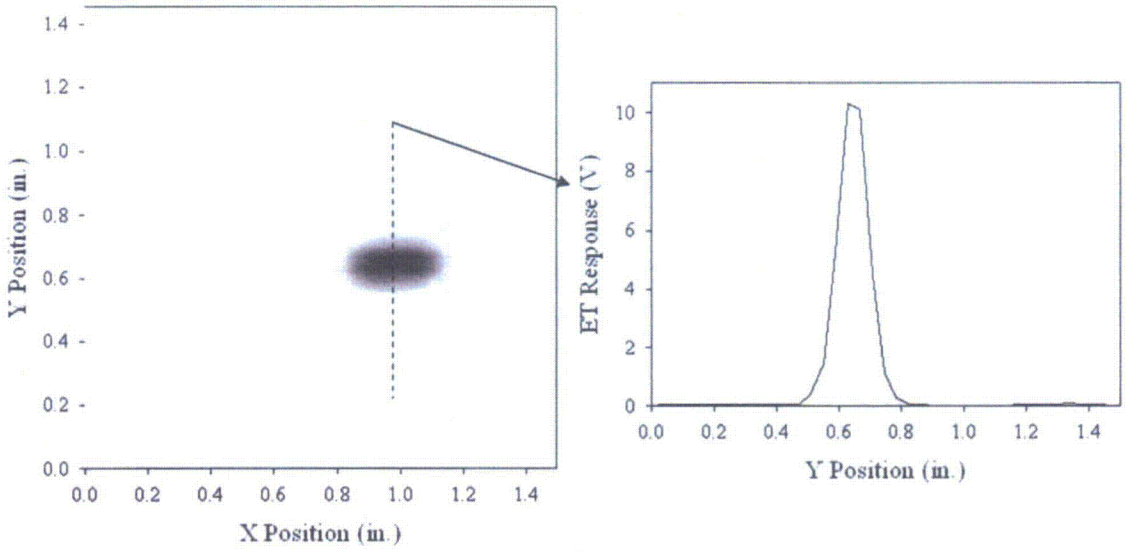

Figure 4.9 Eddy Current Calibration Check of 0-Degree Probe on Calibration Plate, 350 kHz, and 15 dB Gain

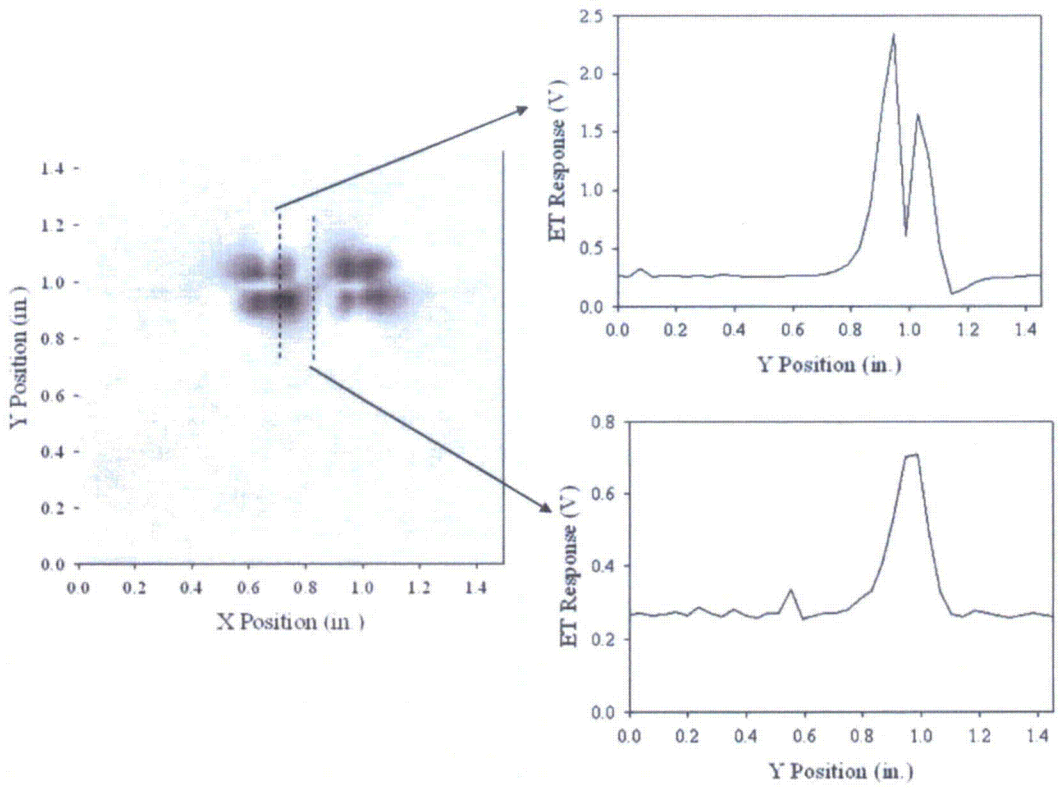

Figure 4.10 Eddy Current Calibration Check of 45-Degree Probe on Calibration Plate, 350 kHz, and 15 dB Gain

4.2.2 Time-of-Flight Diffraction Responses to Calibration Notches

The calibration cylinder was examined using TOFD. Data were acquired at 7.5 MHz in a laboratory setting, and the signal responses from the notches with depths of 2, 4, and 8 mm (0.08, 0.16, and 0.31 in.) were recorded. Figure 4.11 shows rectified data from an axial OD notch 4 mm (0.16 in.) deep. The four views in Figure 4.11 are from top left and going clockwise as follows: A-scan data, a B-scan side view, a B-scan end view, and a C-scan or plan view. The A-scan view shows three main reflections. They are, from left to right, the lateral wave signal, the notch signal, and the back surface signal. A red marker line is placed on the peak response from the notch signal, allowing a measurement of the amplitude. In this data set, the response is –6.4 dB. This response is relative to the lateral wave response, which was chosen as a reference signal for each data file. Both the side and end views also show the lateral wave, notch, and back surface responses. The lateral wave is at the top of the side view image and at the left in the end view. A TOF shape, typical for a notch, is seen in the side view of the data. The TOF shape in the end view is very narrow for an axial notch but is discernable in the data set. Finally, the C-scan view locates the notch relative to the entire scan (horizontal) and increment (vertical) axes at the intersection of the two red lines.

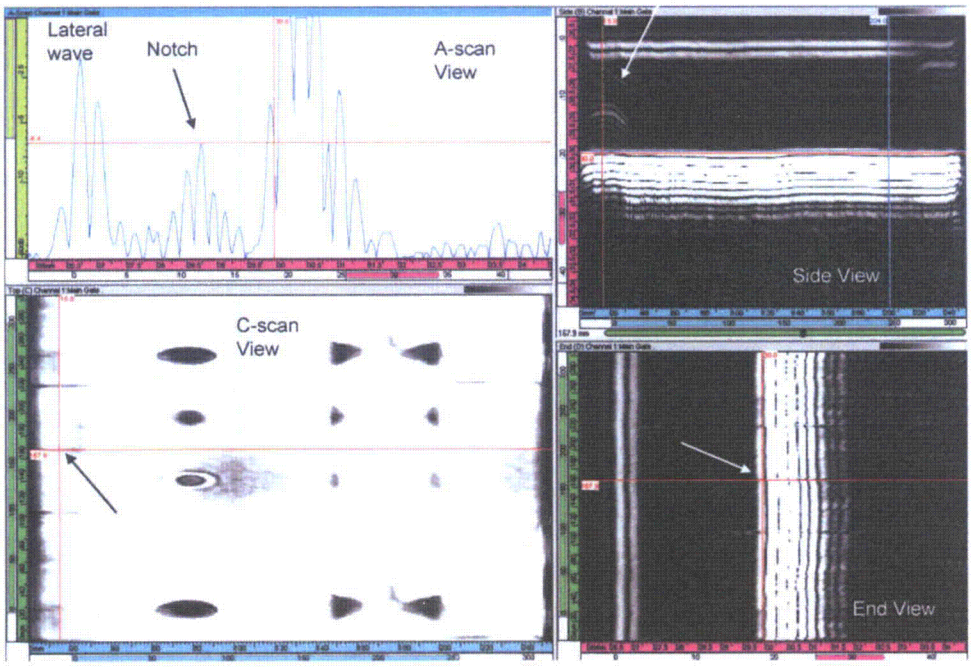

Figure 4.11 Time-of-Flight Diffraction Data from Axial Outside-Diameter Calibration Notch 4 mm (0.16 in.) Deep, at 167.9 mm (31.1 in.) Horizontal, 15 mm (0.59 in.) Vertical, and −6.4-dB Response. The arrows locate the notch signal in the various views.

The TOFD responses from several notches are listed in Table 4.3. These response levels were used as a baseline for comparison of signals from Nozzles 59 and 31.

Table 4.3 Time-of-Flight Diffraction Responses from Notches in Alloy 600 Calibration Cylinder

Flaw Orientation	Flaw Location	Depth	Response (dB)
Circumferential	Outer Diameter	2 mm (0.08 in.)	1.7
		4 mm (0.16 in.)	4.2
Axial	Outer Diameter	2 mm (0.08 in.)	-4.5
		4 mm (0.16 in.)	-6.4
		8 mm (0.31 in.)	-6.8
Axial	Inner Diameter	2 mm (0.08 in.)	Not Detected
		4 mm (0.16 in.)	-0.4
		8 mm (0.31 in.)	-3.8

4.2.3 Immersion Ultrasonic Testing Responses from Fabrication Flaws

Although the Midland CRDM specimen contains no cracks, the weld contains several fabrication flaws in the fusion zone between the penetration tube and the weld metal. These fabrication flaws are isolated and point-like and likely are very small lack-of-fusion defects or slag inclusions. The immersion UT was able to penetrate into the weld and was sensitive to features such as the small differences in reflectivity along the weld beads. Figure 4.12 shows a 2.25-MHz UT scan of the Midland CRDM focused first on the fusion zone and then deeper into the weld. The wetted tube is to the left and shows up in the left-hand image as pink. The interference fit is to the right and also shows up as pink. The blue stripe in the middle of the figure is the J-groove weld. The fabrication flaws show up as green or red spots in the blue stripe (left-hand image). In the section focused deeper into the weld, the weld passes are visible, demonstrating good sensitivity for flaws in the weld.

The immersion UT is expected to have a very high sensitivity for circumferentially oriented cracks through the weld metal. Axial cracks may be difficult to detect, as they would present a very small cross section to the UT beams.

4.2.4 Visual Testing Results from Cracks in Calibration Standards

The VT results on replicas of the cracked stainless steel samples showed that on a surface containing deep grinding marks, only cracks with a crack opening dimension (COD) larger than 100 μm were readily detected. On very smooth surfaces, cracks as small as 10 μm (0.0004 in.) wide were detected easily. On surfaces with some machining marks, cracks from 10–25 μm (0.0004–0.001 in.) wide were detectable with difficulty. The crack orientation relative to the machining marks and other surface textures also strongly affects the crack visibility. A crack ranging from 10–25 μm (0.0004–0.001 in.) wide that follows the machining marks on a machined surface is shown in Figure 4.13. A crack 28 μm (0.001 in.) wide that is perpendicular to the machining marks is shown in Figure 4.14.

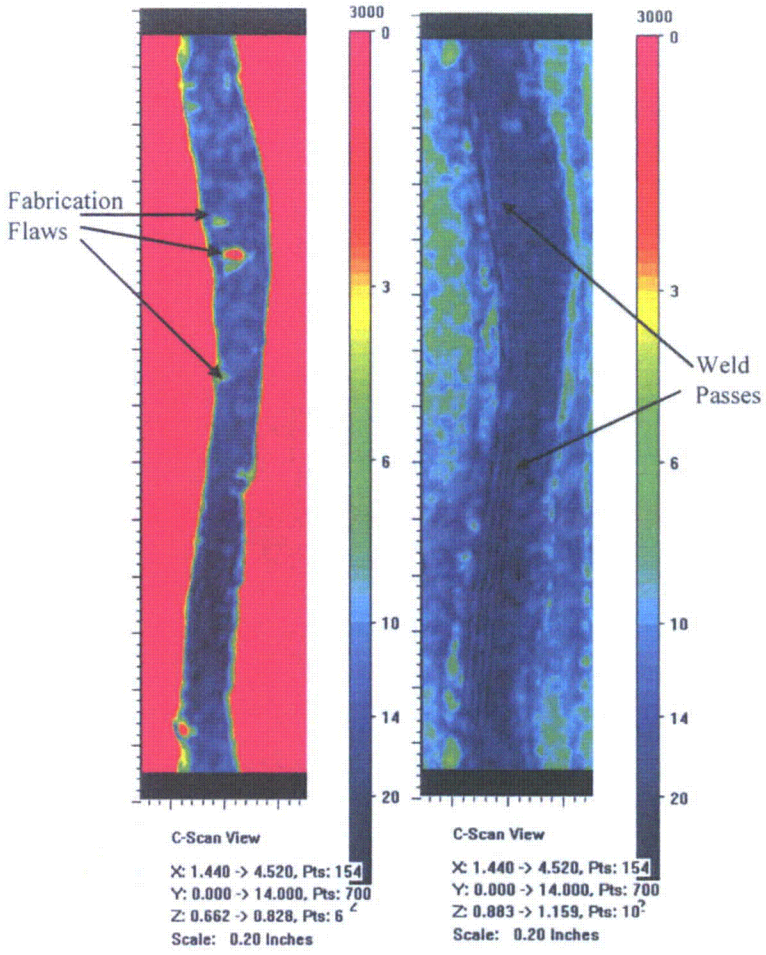

Figure 4.12 Ultrasonic Testing Responses for 2.25-MHz in Midland Control Rod Drive Mechanism. The first image shows the fusion zone of the weld where fabrication flaws were detected. The second image shows the J-groove weld area where the individual weld passes were detected.

The metal J-groove weld on Nozzles 59 and 31 have not been ground down and show the topography common to as-built welds but have relatively smooth surfaces. Based on the work on the replicas of the stainless steel samples, one would expect high sensitivity for crack detection on cracks that cut across the weld passes or that occur in the middle of a weld bead. The smooth weld surface allows for very good crack visibility. One would expect very low sensitivity for detecting cracks that follow weld beads, as the cracks easily could be hidden by the topography of the weld. This suggests that VT will be highly sensitive to axially oriented cracks and relatively insensitive to circumferentially oriented cracks that initiate at the boundaries of weld beads.

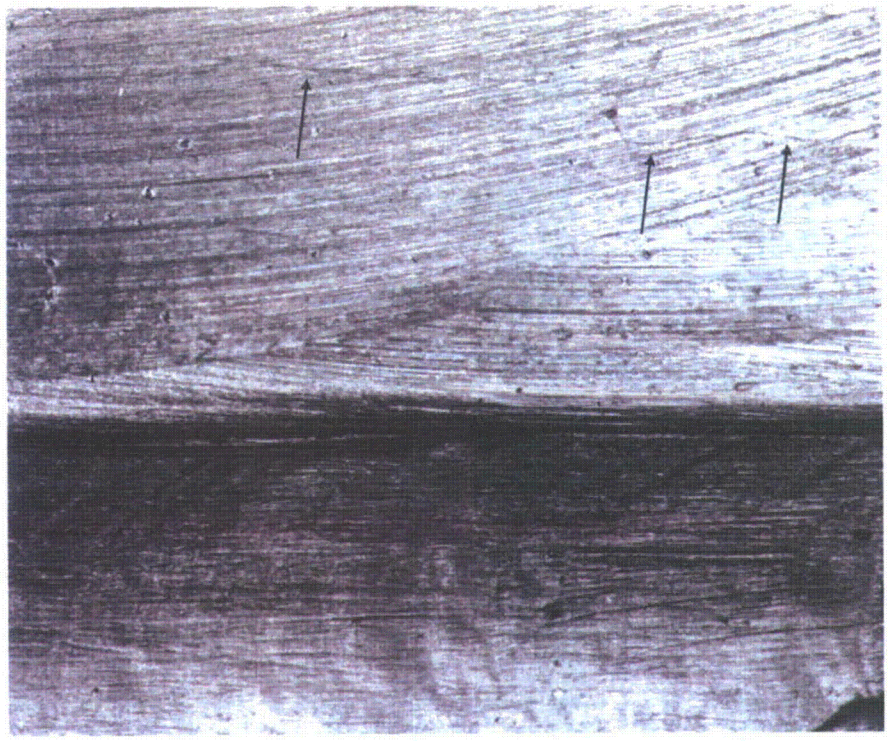

Figure 4.13 Narrow Crack Ranging 10–25 μm (0.0004–0.001 in.) Wide on a Machined Surface. The crack is easy to see when it cuts across machining marks and is difficult to see when it follows the marks.

Figure 4.14 A Crack 28 μm (0.001 in.) Wide Cutting Perpendicularly Across Machining Marks

5 Nondestructive Examination Results

As described in Section 3, the North Anna 2 CRDM nozzles were inspected in three stages. The first set of examinations was the in-service inspections performed during the scheduled outage in 2002. The inspections conducted by the licensee were consistent with the guidance provided in NRC Bulletin 2001-01, "Circumferential Cracking of Reactor Pressure Vessel Head Penetration Nozzles." The second set of examinations was performed at PNNL in 2004 by selected ISI vendors as part of an EPRI round-robin examination. The methods and procedures used by the ISI vendors were the same as those used for the in-service inspections. The final set of laboratory-quality nondestructive examinations was performed at PNNL by PNNL staff in 2005–2006.

The in-service inspections were performed as part of the planned maintenance of the reactor. The North Anna 2 pressure vessel head showed clear evidence of leakage during bare metal visual examinations of the head. Boric acid deposits were present on top of the head, with some nozzles showing the classic "popcorn" boric acid pattern. The in-service inspections included ultrasonic and eddy current examinations of the interior of the penetration tube and eddy current examinations of the accessible sections of the wetted surface of the J-groove weld. Also performed were ultrasonic examinations of the interference fit regions of the nozzles to detect signs of the damage that would be caused by leaking water passing through the annulus, if a leak were present. All examinations were performed from underneath the pressure vessel head in a high radiation field and with a challenging geometry characterized by nearby nozzles interfering with access to the nozzle being examined. Although the results of the ISI examinations were made available, many details remain proprietary. Consequently, this report will focus on the results and not the specifics of the probes used and the inspection parameters.

After the pressure vessel was removed from service, several nozzles were flame cut from the pressure vessel head, shipped to PNNL, and examined as part of an EPRI-administered round-robin test. The vendors involved in the round-robin testing performed examinations on only the penetration tube. The vendors used ET and ultrasonic testing of the penetration tube and ultrasonic and ET of the annulus to detect signs of leakage.

PNNL staff examined the CRDM nozzles from July 2005 through January 2006. The nozzles were examined individually after being placed into optimum positions for each examination, allowing for the best possible access to the areas being examined. The decontamination described in Section 3 resulted in a much lower dose rate. Nozzle 59 was first examined with ET, as it required no coupling fluid. The nozzle was then examined using TOFD. After the TOFD examination was completed, the bottom of the penetration tube was plugged and filled with water for the immersion UT. Finally, the J-groove weld was covered in Microset polymer, and the replica was set aside for later VT. This procedure was repeated with Nozzle 31.

The results of all three nondestructive examinations of Nozzle 59 and 31 are presented in this section. The NDE inspection results for Nozzle 59 are presented in Section 5.1; those for Nozzle 31 are presented in Section 5.2. The NDE results for both nozzles are summarized in Section 5.3.

5.1 Control Rod Drive Mechanism Nozzle 59

5.1.1 In-Service Inspection Results

The in-service inspection of Nozzle 59 was inconclusive in determining if it had leaked during service. The bare metal visual examination showed that the nozzle was masked by boric acid that had flowed over the nozzle from another source. The ultrasonic examination of the penetration tube found two strings of indications at the tube outer diameter from 345 degrees to 65 degrees and from 155 degrees to 205 degrees. A single indication was found in the penetration tube ID above the weld at 160 degrees. ET of the wetted surface of the J-groove weld found two strings of small indications ranging from 50 to 135 degrees and from 255 to 305 degrees. The ET of the penetration tube found an ID defect at 145 degrees close to the ID defect found by ultrasound. The ISI results are summarized in Table 5.1.

Table 5.1 In-Service NDE Results for Nozzle 59

Description	Angle	Location
Ultrasound indications	345–65°	Penetration tube OD, middle of weld
	155–205°	Penetration tube OD, top of weld
	160°	Axial indication on penetration tube ID, above weld
Eddy current indications	50–135°	Outer portion of J-groove weld wetted surface
	255–305°	Outer portion of J-groove weld wetted surface
	145°	Penetration tube ID middle of weld

5.1.2 Round-Robin Nondestructive Examination Results

The round-robin testing focused entirely on the penetration tube. The round-robin ultrasonic examinations found strings of indications from 345 to 60 degrees and from 155 to 205 degrees. A defect was found above the weld at 160–175 degrees as well. The round-robin results are summarized in Table 5.2.

Table 5.2 Round-Robin NDE Results for Nozzle 59

Description	Angle	Location
Ultrasonic Indications	345-60°	Penetration Tube OD, Middle of Weld
	155–205°	Penetration Tube OD, Top of Weld
	160–175°	Axial Indication on Nozzle ID, Above Weld
	0°	Axial Indication in Penetration Tube Below Weld
	210–220°	Axial Indication Across Weld

5.1.3 PNNL Nondestructive Examination Results

5.1.3.1 Eddy Current Testing

The scanning protocol was as follows:

- Data were taken on a grid having 1-mm (0.4-in.) spacing.
  - This was exact in the axial direction because the drive mechanics use metric threads.
  - This was approximate in the circumferential direction, assuming an inner diameter of 74.2 mm (2.9 in.) (in which case 360 degrees corresponds to 233 mm).
- Data were recorded only while the probe was moving down. Because the CRDM nozzle was inverted in the fixture, the data were taken from bottom to top (inner end to outer end) of the part.
- Between vertical scans, the probe was indexed clockwise. Initially, the plan had been to rotate counterclockwise, but it was found that the probe assembly would sometimes become unscrewed from the center shaft.
- The scan covered 450 degrees (291 mm, 11.5 in.), providing overlap on 25% of the part. This provided a check on the consistency of the data and facilitated spatial registration with the ultrasonic data.

The data presentations in this section show the cylinder axis from left to right and the circumferential direction from top to bottom, so the data are presented as if unwrapped and viewed from the outside of the nozzle.

Data from Nozzle 59 showed some high-amplitude indications, as shown in Figure 5.1 (150-kHz data). The horizontal line is shown to mark 360 degrees (233 mm, 9.2 in.), where the data begin to repeat. Figure 5.2 shows data at 350 kHz from the same scan.

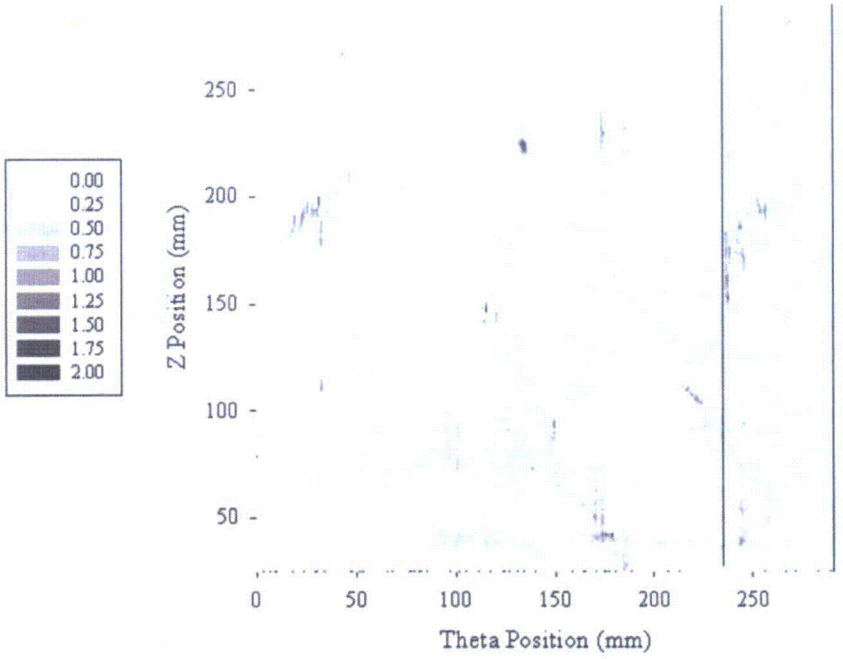

Figure 5.1 **Eddy Current Data (150 kHz) on Nozzle 59. Indications are shown in grey to white scale. Horizontal line shows 360 degrees (233 mm, 9.2 in.). Indications in grey-black are greater than 1 V.**

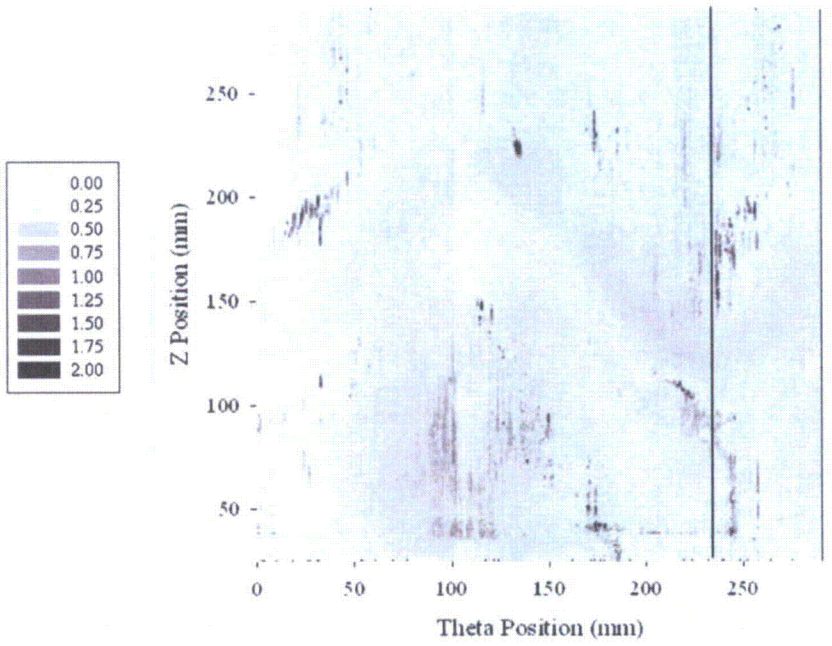

Figure 5.2 **Eddy Current Data (350 kHz) on Nozzle 59. Indications are shown in grey to white scale. Vertical line shows 360 degrees (233 mm, 9.2 in.). Indications in grey-black are greater than 1 V.**

5.1.3.2 Time-of-Flight Diffraction Results

The TOFD data were reviewed for relevant indications. An interesting indication was defined as one with a TOF shape or one with amplitude large enough to stand out. The amplitude cutoff was not firmly fixed but was approximately 10 to 12 dB less than the lateral wave response. This range is nearly double the response level sensitivity measured from the axial OD notches on the calibration cylinder.

Figures 5.3 through 5.5 show weld repair intrusions in Nozzle 59. The C-scan view in the lower left portion of Figure 5.3 shows the weld image in the data. The start of the scan is in the lower left corner of the C-scan, with the axial scan direction proceeding left to right and the circumferential increment proceeding from bottom to top. A weld repair intrusion indication is marked by arrows in both the C-scan and B-scan side views. The side view, top right, shows the TOF shape expected from a flaw. The C-scan view locates the repair intrusions near the start of the scan at 24 mm (0.95 in.) counterclockwise (CCW) from the reference position (start of the scan). An axial position is also given. Figure 5.4 shows a second area with weld repair intrusion indications. This region is 122 mm (4.8 in.) CCW from the start. The third area with weld repair intrusion indications shown in Figure 5.5 is at 231 mm (9.1 in.) CCW from the start. This is a repeat of the first area because the data overlap circumferentially starting at 224 mm (8.8 in.). Response levels from these signals are approximately 5 to 7 dB below the lateral wave signal. From the C-scan (plan) views, it appears that the weld repair intrusion condition is occurring near the axial top and bottom extremes of the weld.

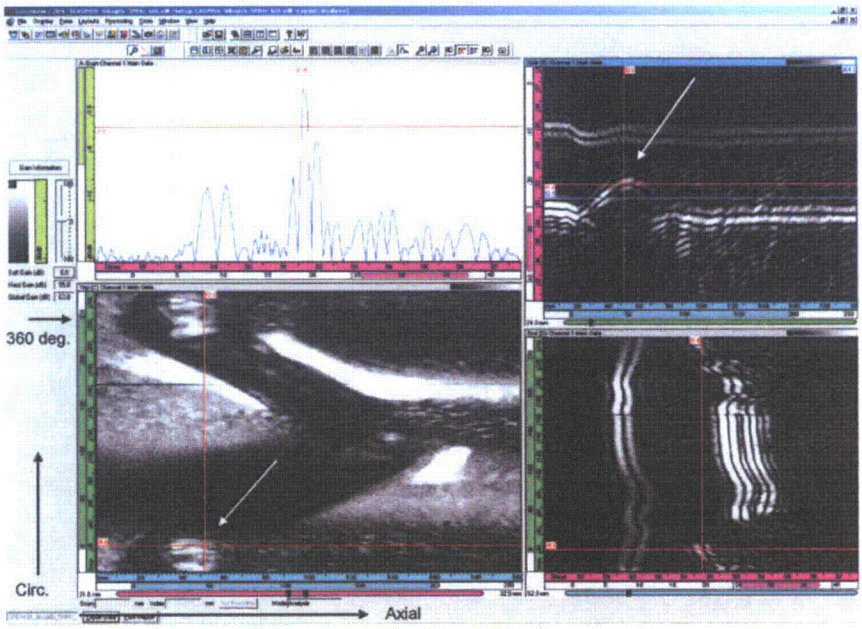

Figure 5.3 Nozzle 59 Weld Repair Intrusion Indication Detected with Time-of-Flight Diffraction at 24 mm (0.95 in.) CCW, 52 mm (2 in.) Axial, with a −5.6-dB Response. The axial and circumferential axes are also noted. One revolution (360 degrees) was represented by 224 mm (8.8 in.) circumferentially.

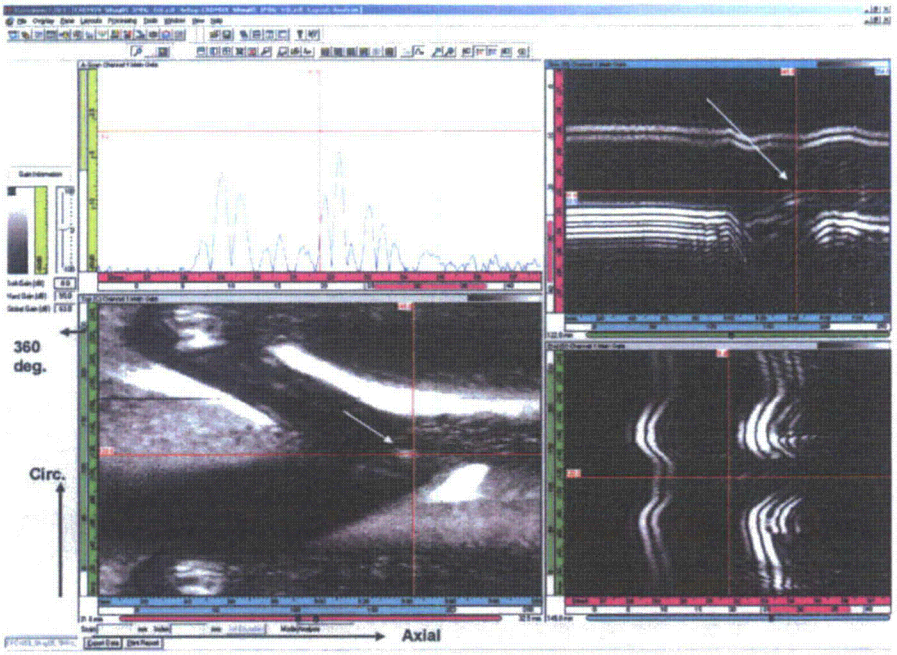

Figure 5.4 Nozzle 59 Weld Repair Intrusion Indication Detected with Time-of-Flight Diffraction at 122 mm (4.8 in.) CCW, 145 mm (5.7 in.) Axial, with a −7-dB Response

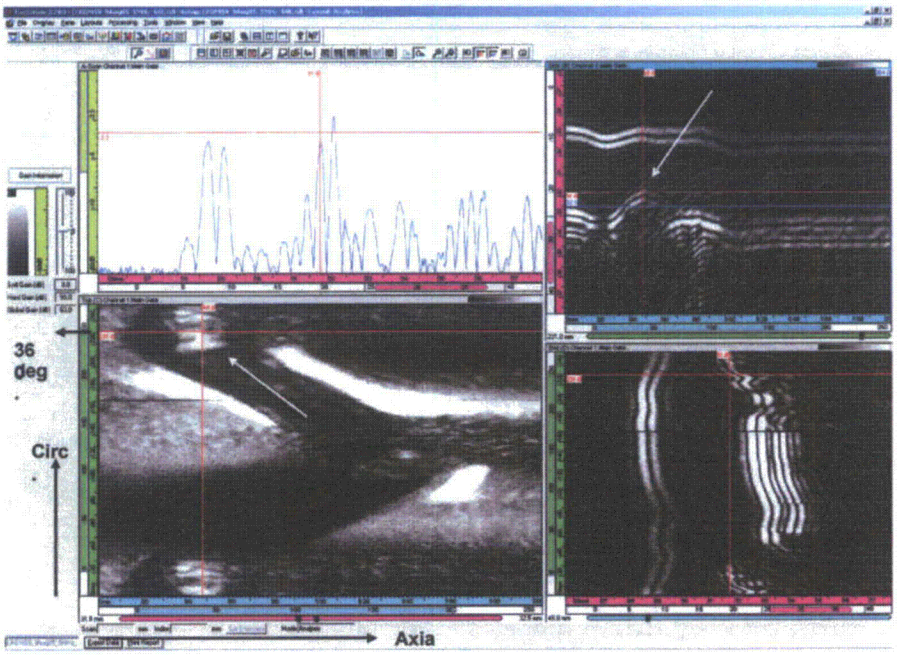

Figure 5.5 Nozzle 59 Weld Repair Intrusion Indication Detected with Time-of-Flight Diffraction at 231 mm (9.1 in.) CCW, 48 mm (1.9 in.) Axial, with a −5.7- to −6.8-dB Response

Interesting indications or regions with many indications based on response were noted from the 5- and 7.5-MHz data. No TOF shapes were seen in Nozzle 59 data outside of the weld repair penetration indications. Additionally, the indications appeared to be axial and did not break the inner surface, noted by a lack of lateral wave interruption. Two typical indications are shown in Figures 5.6 and 5.7. The indication in Figure 5.6 is closer to the back surface signal, while the indication in Figure 5.7 is closer to the front surface lateral wave signal. Figure 5.7 also shows a region with numerous indications with approximately double the response amplitude of the indication in Figure 5.6.

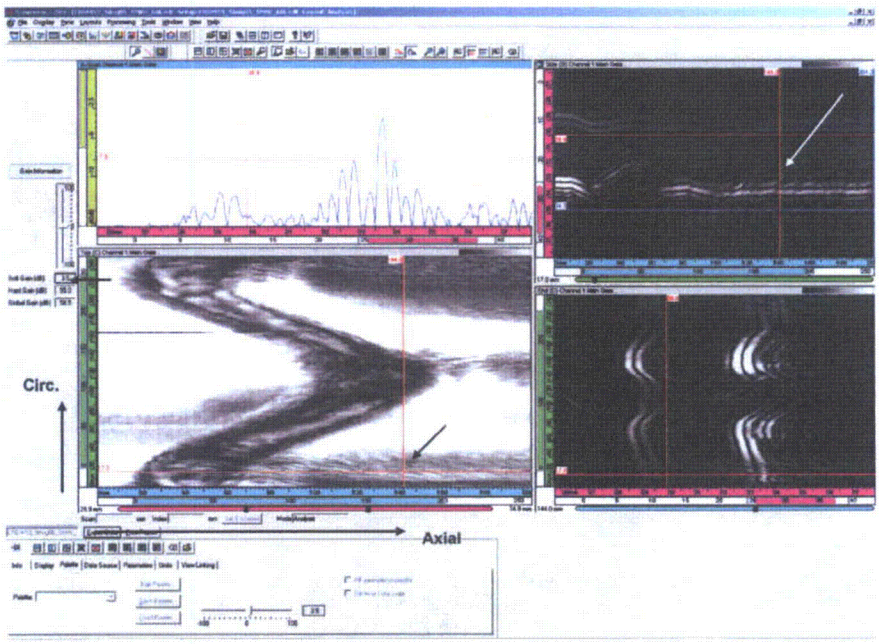

Figure 5.6 Nozzle 59, 5-MHz Time-of-Flight Diffraction Data Showing Typical Indication. The indication is at 17 mm (0.67 in.) CCW, 144 mm (5.7 in.) axial, with a response of −7.5 dB.

5.1.3.3 Immersion Ultrasonic Testing Results

C-scan images of Nozzle 59 with the four frequencies are shown in Figures 5.8 through 5.12. The 5-MHz data focus on the penetration tube and the fusion zone between the penetration tube and the weld metal. The 2.25-MHz data focus clearly on the fusion zone and slightly into the weld metal. The 1-MHz data focus deeper into the weld metal, and the 500-kHz data penetrate very well through the weld. Figure 5.8 shows an indication that possibly starts in the nozzle material. Figures 5.9 through 5.12 show lack-of-fusion types of indications in the J-groove weld material at the four different frequencies. The 5-, 2.25-, and 1-MHz data presented in Figures 5.9 through 5.11, respectively, are best and show similarity in locating two areas with lack of fusion. With the decreasing frequency, however, the resolution drops as expected. The 500-kHz data in Figure 5.12 shows a different area that is possibly lack of fusion at approximately 89 mm (3.5 in.) circumferentially.

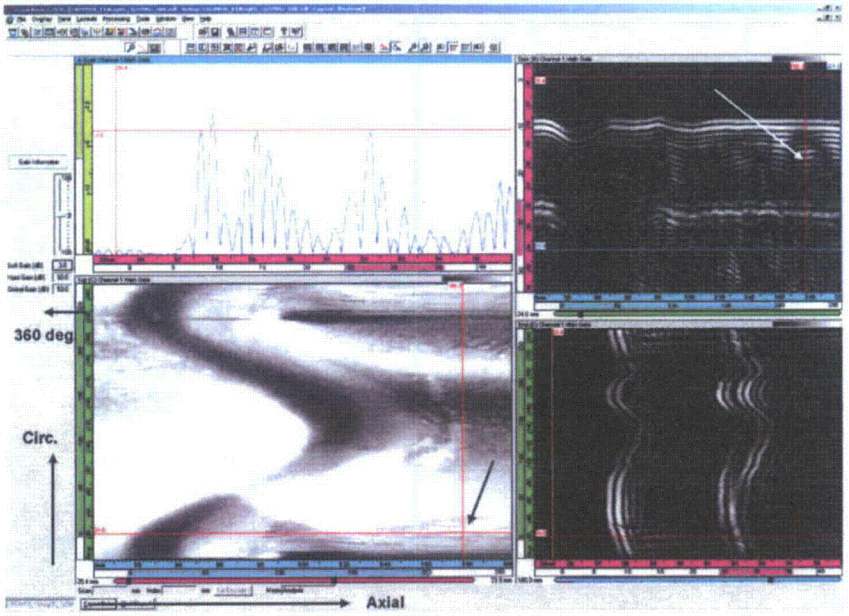

Figure 5.7 **Nozzle 59, 7.5-MHz Time-of-Flight Diffraction Data Showing Interesting Indication. This indication is at 24 mm (0.95 in.) CCW and 180 mm (7.1 in.) axial position with a response of −3.8 dB in a region with many indications.**

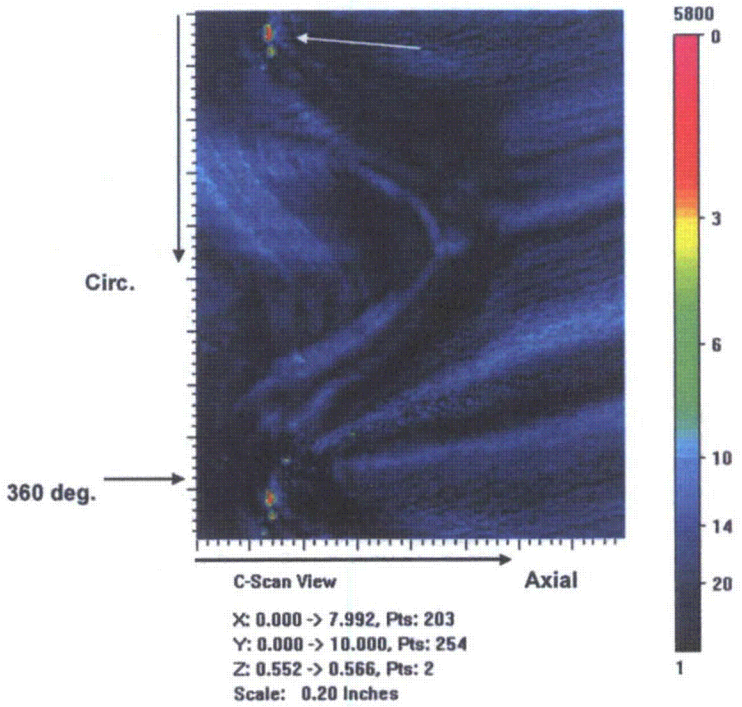

Figure 5.8 **Nozzle 59, 5-MHz Immersion Data Showing Potential Indications Starting in the Nozzle Material**

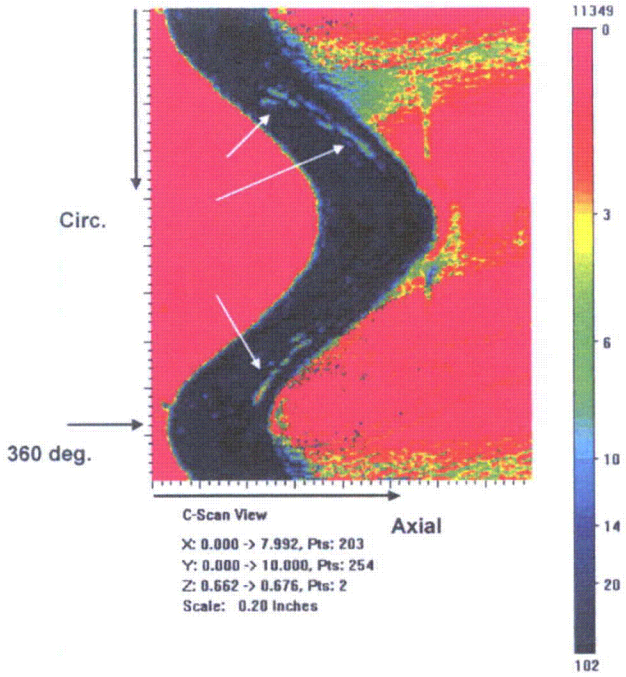

Figure 5.9 Nozzle 59, 5-MHz Immersion Data Showing Indications That Respond Like Lack of Fusion Starting in the J-Groove Weld Material

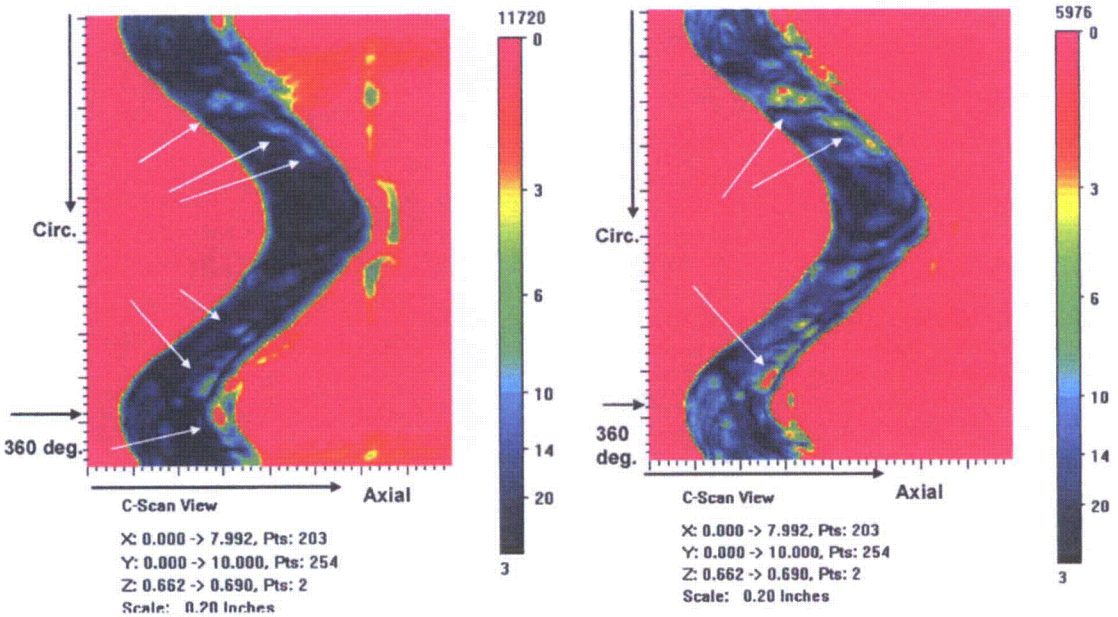

Figure 5.10 Nozzle 59, 2.25-MHz Immersion Data Showing Indications That Respond Like Lack of Fusion Starting in the J-Groove Weld Material at Two Different Displayed Amplitude Settings

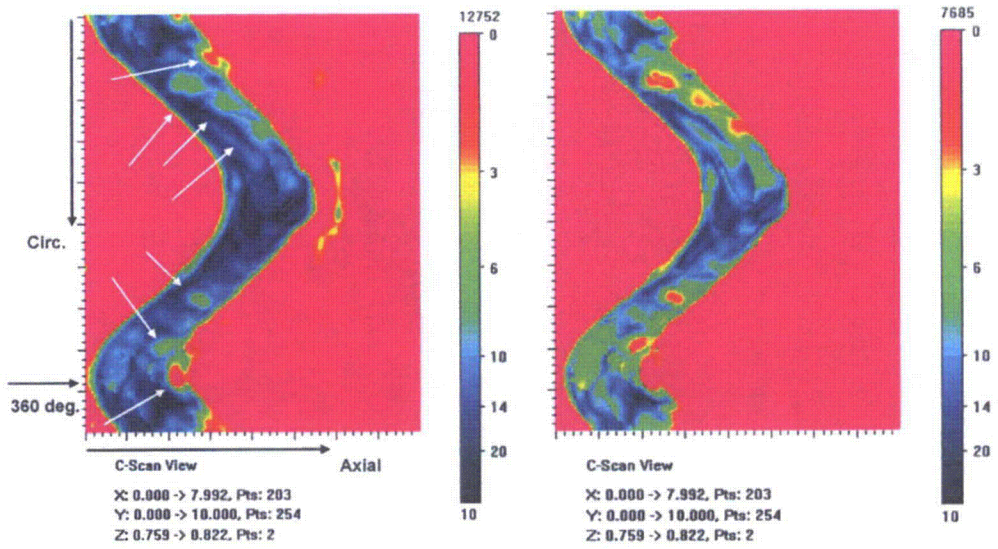

Figure 5.11 Nozzle 59, 1-MHz Immersion Data Showing Indications That Respond Like Lack of Fusion Starting in the J-Groove Weld Material at Two Different Displayed Amplitude Settings

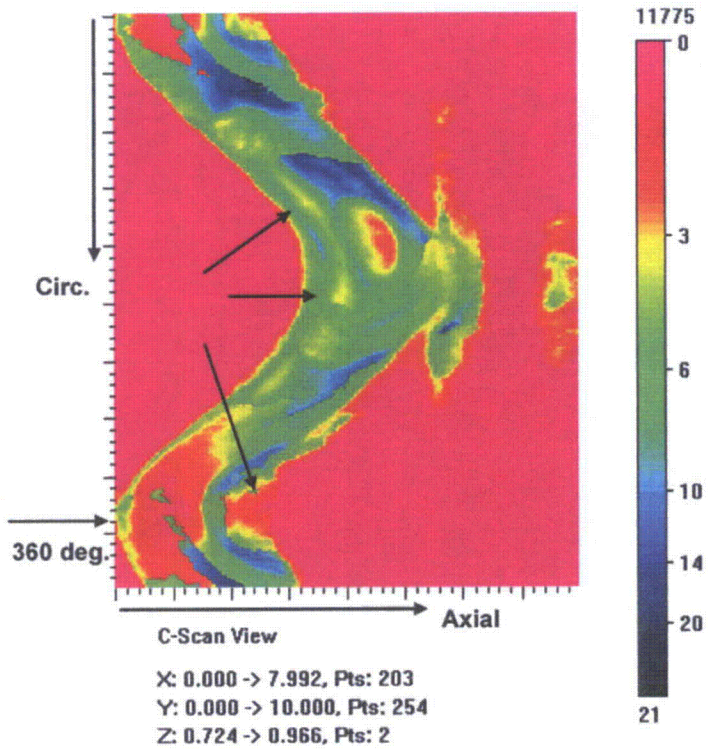

Figure 5.12 Nozzle 59, 500-kHz Immersion Data Showing Possible Lack-of-Fusion Indications Starting in the J-Groove Weld Material

5.1.3.4 Visual Testing Results

5.1.3.4.1 Penetration Tube Interior

Based on the strong ET responses for the penetration tube of Nozzle 59, a replica of the interior was recovered and examined. This Microset replica was made as part of the initial decontamination of the nozzles during a previous series of examinations on the nozzles. The Microset replica of the interior was in the form of a continuous tube approximately 254 mm (10 in.) long. The tube was cut lengthwise, stretched out, and pinned to a foam core board. The replica was then photographed in sections using the slide bar and tripod arrangement described in Section 3.5.

A 0-degree mark had been scribed onto the interior surface of the penetration tube in previous tests, and this mark was found and used to orient the results from the visual tests. The 0-degree mark was very shallow and wide, which is likely why it did not show up in the eddy current tests. The 0-degree mark is shown in Figure 5.13.

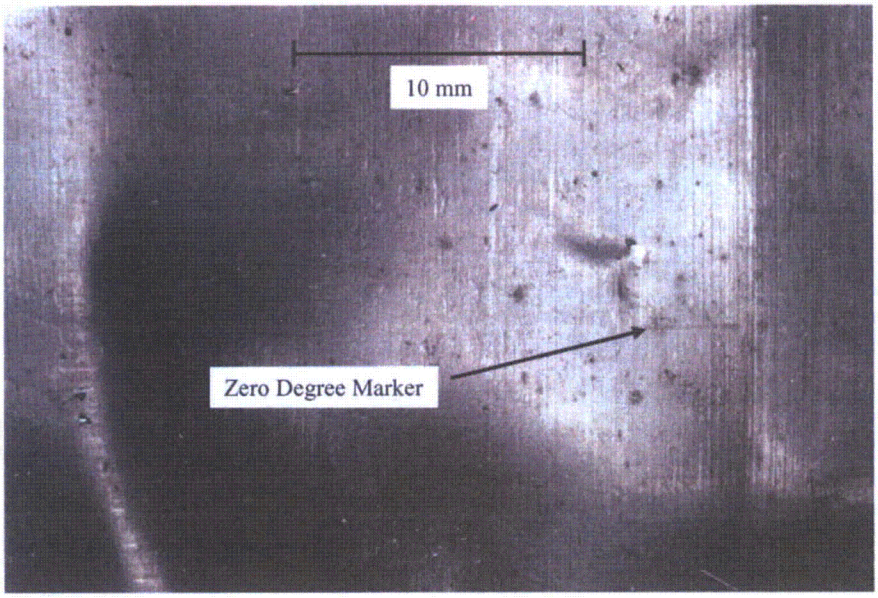

Figure 5.13 Zero-Degree Marker and Wetted End of Penetration Tube Imaged Using Replicant

The photographs were examined individually at 100% magnification using a variety of sharpness, brightness, and contrast settings. The interior of the tube showed regular circumferential machining marks and many axial scratches. Some of the deepest axial scratches were coincident with the larger voltage responses seen using ET. Figure 5.14 shows deep axial scratches cutting through the circumferential machining marks.

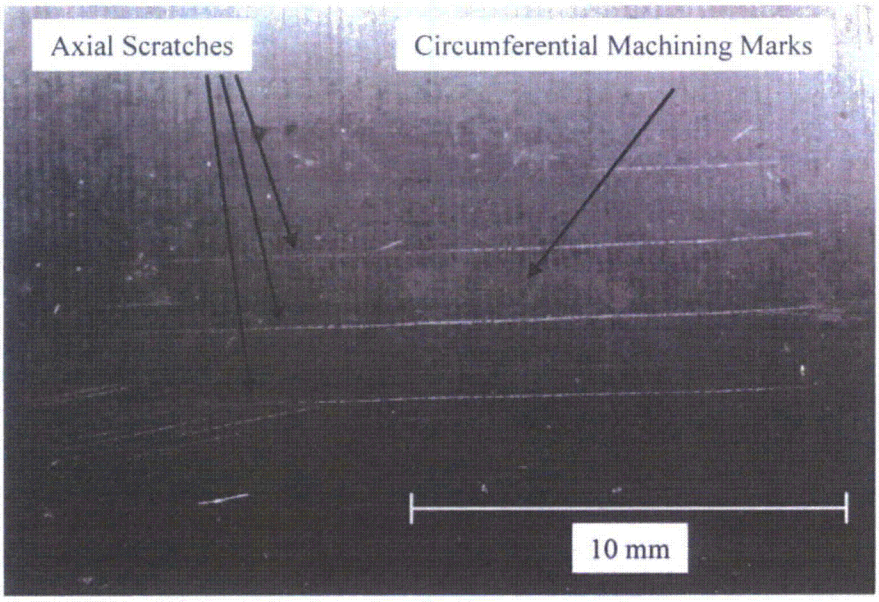

Figure 5.14 Machining Marks and Axial Scratch-Like Indications on the Interior of the Penetration Tube in Nozzle 59

Evidence for pitting or inclusions was seen in the interior of the penetration tube. It is impossible to know from the images if the pits observed are the result of inservice corrosion or are fabrication flaws. It should be noted again that this replica was taken before the etchant gel was used on the interior surface of the tube, so the pits were not caused by the acid gel. It is likely that these indications could be partially responsible for the ET responses seen in Nozzle 59. The pitting is dispersed throughout the inner surface of the tube and exists in some clusters such as the one shown in Figure 5.15. Another interesting indication was detected at close to 180 degrees, 200 mm (7.9 in.) axially into the tube. This indication appeared to be a 1.5–mm-long (0.06-in.) rough section in the tube. This section corresponds almost exactly in location to the "bright spot" ET indication seen at close to 180 degrees and below the weld line. Because the Microset polymer compound applied to the interior of the penetration tube was not of uniform thickness, thin regions stand out slightly from thicker regions when the replica is stretched out. This results in a "mottled" texture and appearance that does not reflect the topography of the interior surface of the penetration tube.

One very crack-like indication was detected in the replica of the penetration tube. Unlike the axial scratches commonly seen in the tube, this indication is curved and at an angle to the tube. It is also in a region with several large pit-like indications. This crack-like indication, at 140 mm (5.5 in.) axially into the penetration tube, is shown in Figure 5.16. Another interesting area was a rough patch in the penetration tube with possible micro-cracking. The tube appears to have undergone some sort of degradation in this region. The general area is shown in Figure 5.17; an enlargement of possible micro-cracks is shown in Figure 5.18.

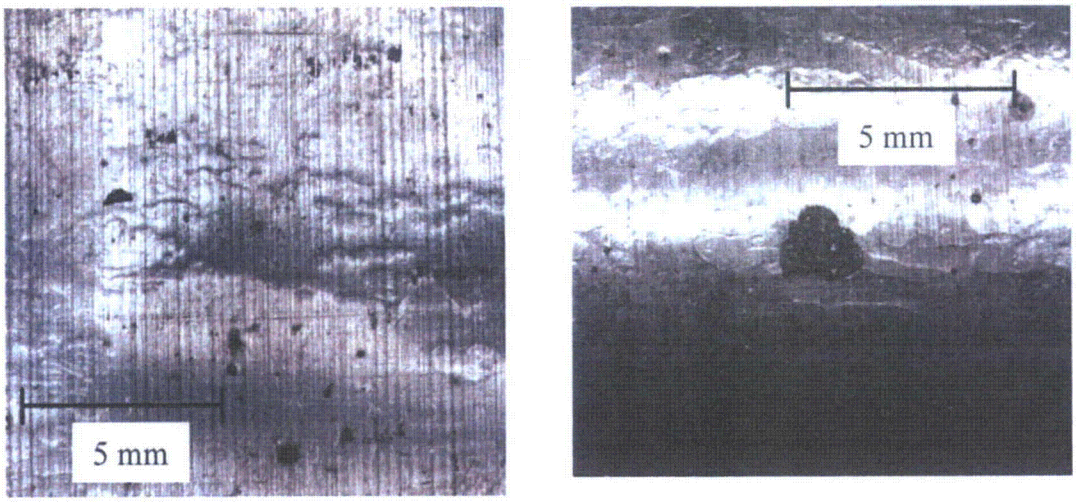

Figure 5.15 Pit-Like Indications and a Rough Patch Imaged Using High-Resolution Photographs of the Replicated Surface. The pit-like indications are located throughout the tube, while the rough patch is located at close to 180 degrees and 200 mm (7.9 in.) axially.

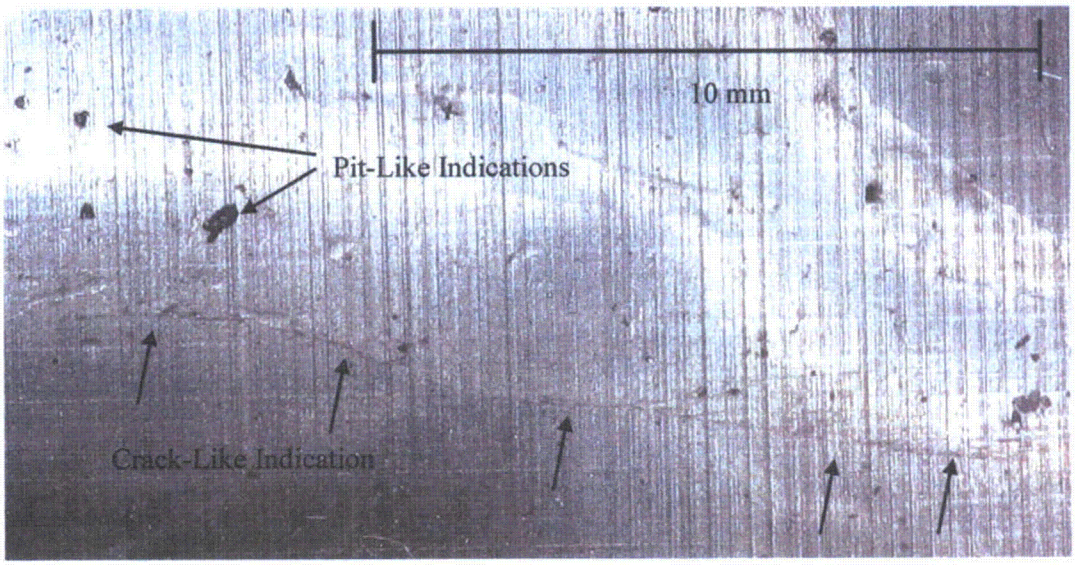

Figure 5.16 Crack-Like Indication Located at 315 Degrees Clockwise Rotation and 140 mm (5.1 in.) Axially in the Penetration Tube

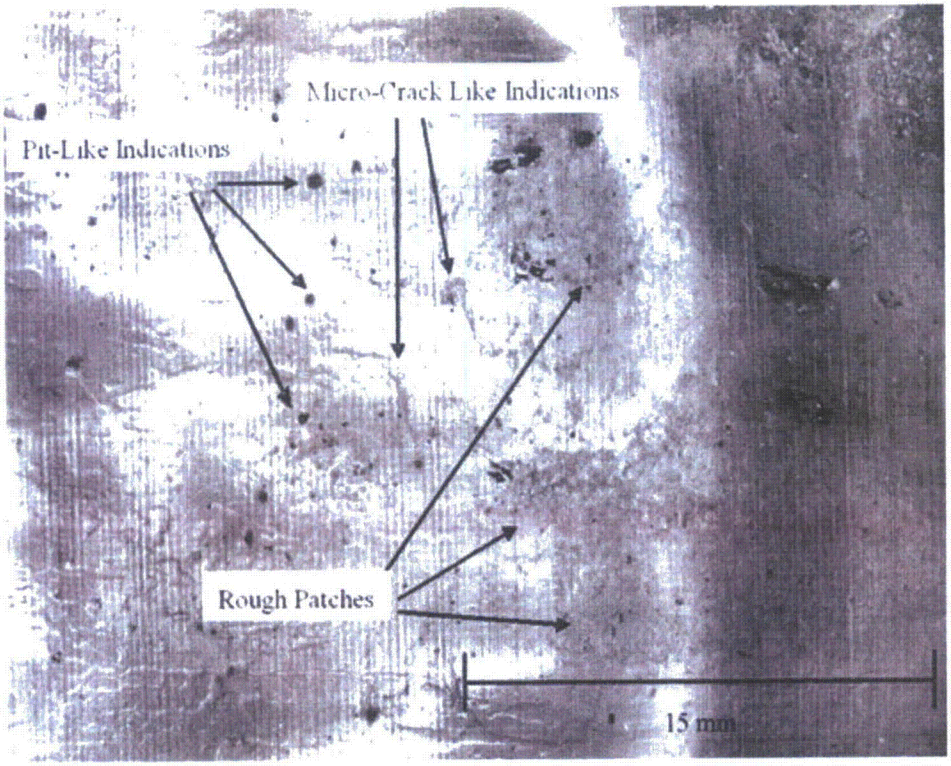

Figure 5.17 Rough Section and Possible Micro-Cracks in the Penetration Tube Interior

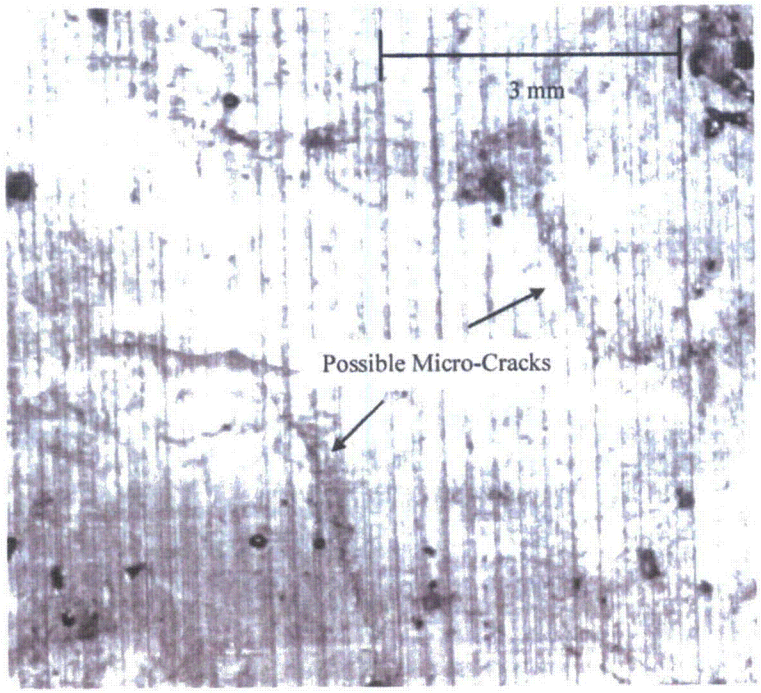

Figure 5.18 Micro-Crack–Like Indications in the Penetration Tube of Nozzle 59

5.1.3.4.2 J-Groove Weld and Buttering

A replica of the J-groove weld was taken and examined using the high-resolution camera. The surface of the J-groove weld showed no evidence of grinding but did show a lot of texture and features related to the welding process—that is, visible weld passes and ridges between the weld passes. The texture of the weld would make it difficult to find cracks that follow a string of weld beads but also would make it very easy to detect a crack that cuts across several weld beads.

No large cracks were detected in the J-groove weld material. Several small crack-like indications were detected. The small cracks are typically on the order of 1–5 mm (0.04–0.20 in.) in length and are aligned circumferentially along individual weld beads. It is difficult to determine if these indications are actual cracks or tortuous lines on the weld beads. The small crack-like indications are found primarily from 112 to 135 degrees. Two examples are shown in Figure 5.19.

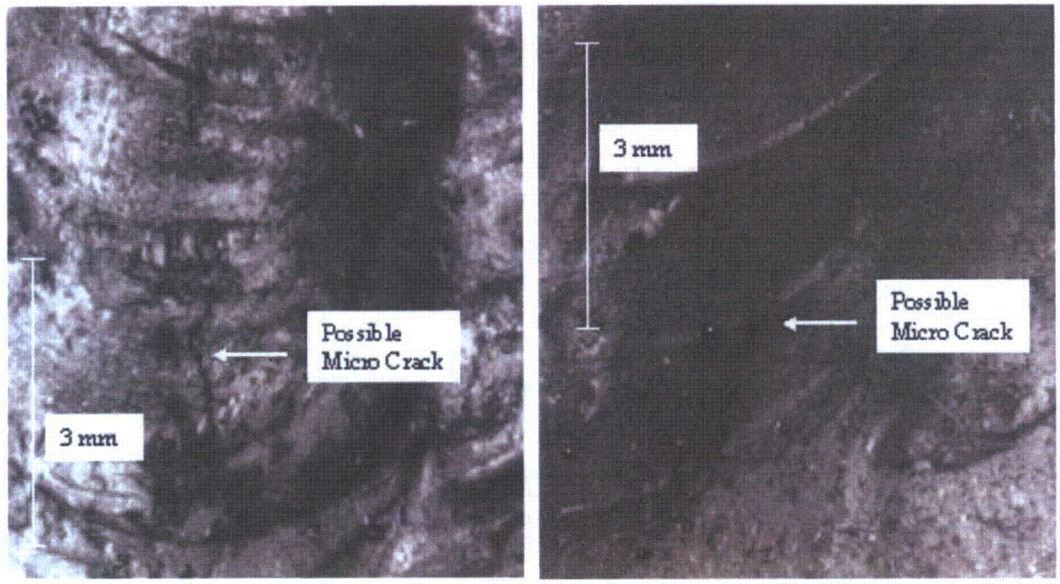

Figure 5.19 Small Crack-Like Indications near 120 Degrees in the J-Groove Weld Replica, Nozzle 59

The largest detected crack-like indication in the J-groove weld of Nozzle 59 was 10 mm (0.4 in.) long and located at 225 degrees. This indication cut across three weld beads and showed a jagged path (Figure 5.20).

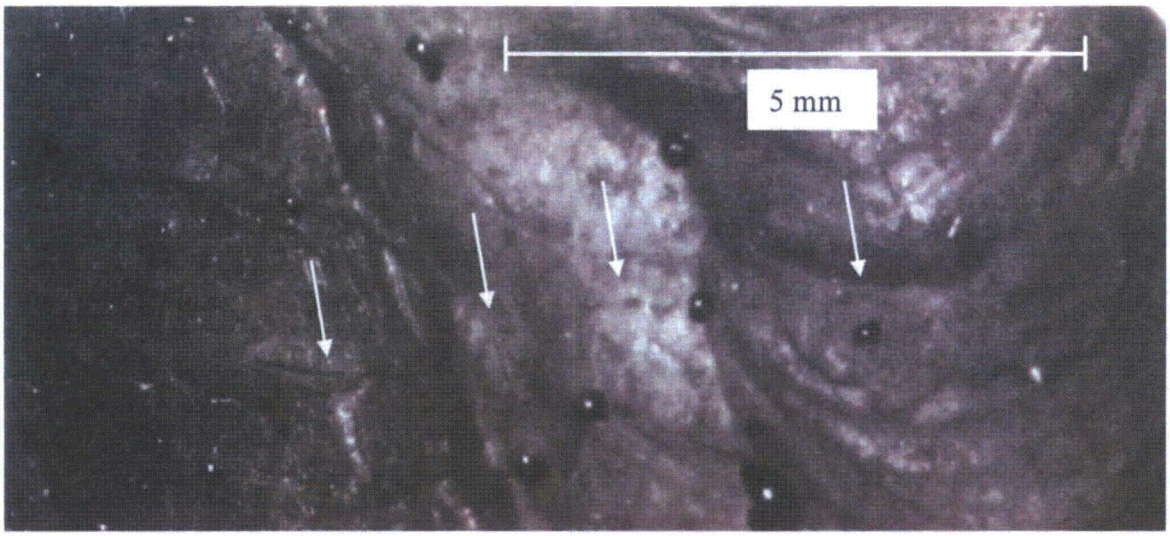

Figure 5.20 Crack-Like Indication in the J-Groove Weld Replica, of Nozzle 59 at 225 Degrees

5.2 Control Rod Drive Mechanism 31

5.2.1 In-Service Nondestructive Examination Results

The North Anna 2 pressure vessel head showed clear evidence of leakage, with boric acid present on the head and with some nozzles showing the classic "popcorn" boric acid pattern. The in-service inspections had identified Nozzle 31 as one that seemed to have leaked. The ISI results are summarized in Table 5.3.

Table 5.3 In-Service Inspection Results for Nozzle 31

Technique	Angle	Location
UT leak path measurement	80–120°	Above weld in interference fit
Ultrasonic indications	300–305°	Nozzle mid wall location
Eddy current indications	155°	Weld surface axial indications
	210°	Weld surface axial indications
	235°	Weld surface axial indications
	265°	Weld surface axial indications

The in-service inspections had also found an apparent leakage path through the annulus. The characteristic ultrasonic fingerprint for a leakage path is like a "river delta" and a path to the outside of the annulus. The ultrasonic data for the leakage path examination were provided for this report by the ISI vendor and are shown in Figure 5.21.

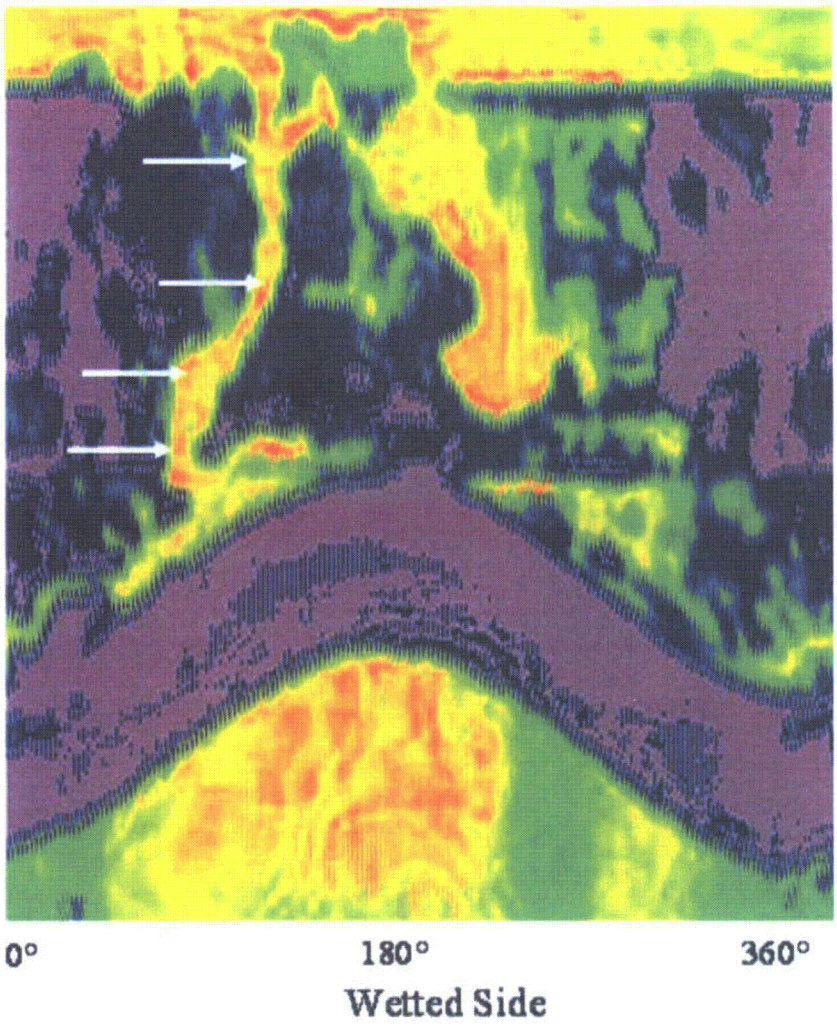

Figure 5.21 Industry-Acquired ISI Data Taken to Detect and Characterize the Presence of Any Leakage Path in Nozzle 31. The leakage path called by the ISI team is shown with the white arrows.

5.2.2 Round-Robin Nondestructive Examination Results

Three vendors examined Nozzle 31 in the round robin conducted at PNNL. The vendors were aware that indications had been detected in this particular nozzle assembly during the in-service inspections, but the vendors did not have detailed information in this regard. The examinations included eddy current scans of the penetration tube, ultrasonic examination of the penetration tube, and electromagnetic acoustic transducer techniques. No examination of the wetted weld surface was performed, however. Indications of leakage were found by deep-penetrating eddy current technique close to the region identified as a possible leakage path by ISI ultrasonic examinations. New ultrasonic indications were found in the penetration tube at 25–35 degrees and at 355–75 degrees. The round-robin indications are summarized in Table 5.4.

Table 5.4 Round-Robin Results for Nozzle 31

Description	Angle	Location
Eddy current leak path	30–155°	Above weld in interference fit
	90–140°	Above weld in interference fit
	300–330°	Above weld in interference fit
UT leak path measurement	65–150°	Region directly above weld
	65–140°	Region directly above weld
UT indication	25–35°	Close to weld/interference fit interface (new)
	355–75°	Close to weld/interference fit interface (new)

5.2.3 PNNL Nondestructive Examination Results

5.2.3.1 Penetration Tube Eddy Current Results

Nozzle 31 had only low-level indications (Figure 5.22). The rectangular indication at the left corresponds to a visible 0-degree mark, repeated at 360 degrees (233 mm). The set of diagonal indications, extending from 50 to 150 mm (2 to 5.9 in.) circumferential and 220 to 270 mm (8.7 to 10.6 in.) axial, corresponds to a visibly scratched region. The scan with the probe oriented at 45 degrees displayed a low-level linear indication (boxed in Figure 5.23), but it was not visible in either of the scans with the probe oriented to 0 degrees.

5.2.3.2 Eddy Current Examination of J-Groove Weld

The J-groove weld area of Nozzle 31 was examined using a plus-point differential eddy current probe. The scan was conducted by performing a series of rectangular scans using the *x-y* scanner. The rectangular scans were made every 30 degrees to cover the weld surface with a large degree of overlap in the scans. The scans were taken as close to the penetration tube as possible and, in general, covered the buttering and 12–15 mm (0.5–0.6 in.) of the weld taper. The scans were made with the probe in the normal position and with the probe rotated to 45 degrees to ensure good coverage of the weld with high sensitivity. The rectangular scans were assembled into an ellipse to show the locations of areas of interest. The assembled ellipses for the 0- and 45-degree rotations are given in Figures 5.24 and 5.25.

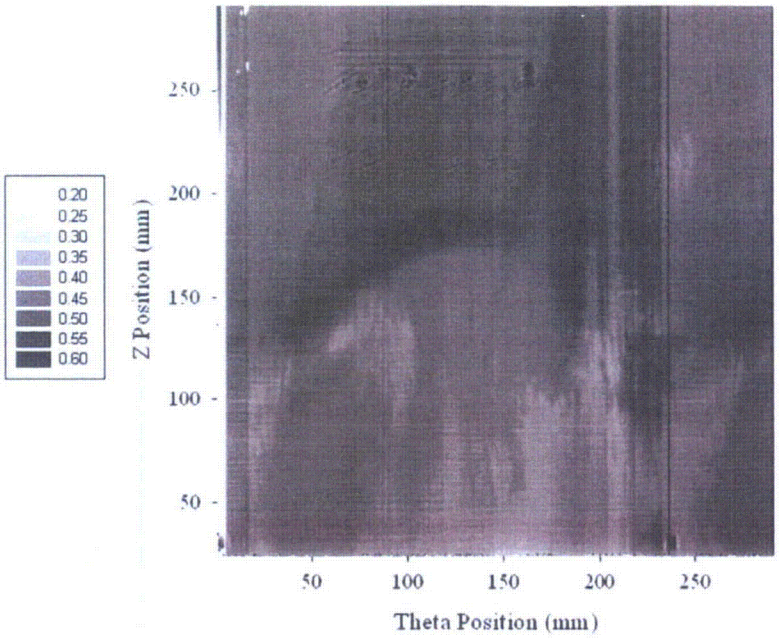

Figure 5.22 Nozzle 31, Scan Taken with Probe Oriented to 0 Degrees, 350 kHz, with the Image Set To Display Scratches

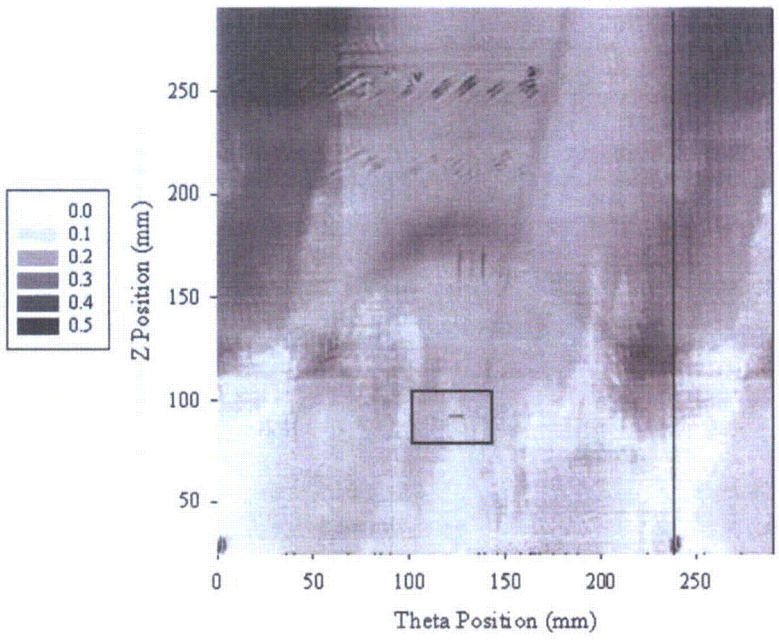

Figure 5.23 Nozzle 31, 45-Degree Rotated Probe Scan, 350 kHz, Showing Linear Indication (centered in box, about 125 mm [4.9 in.] circumferential and 100 mm [3.9 in.] axial)

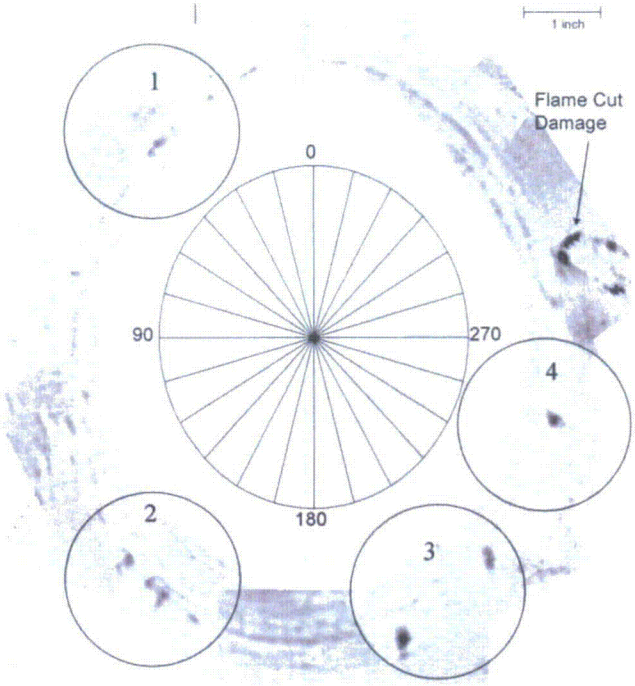

Figure 5.24 **Eddy Current Results for 0-Degree Scan of the J-Groove Weld of Nozzle 31. Four areas of interest were found at close to 60, 150, 215, and 270 degrees.**

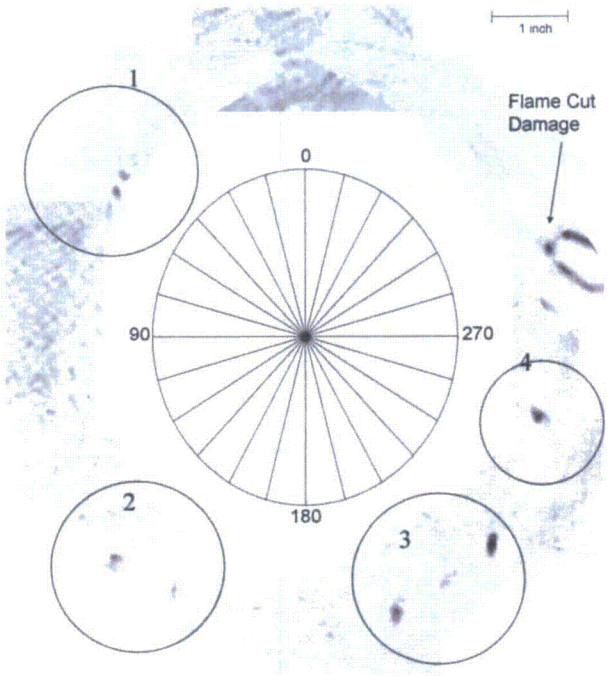

Figure 5.25 **Eddy Current Results for 45-Degree Scan of the J-Groove Weld of Nozzle 31. Four areas of interest were found at close to 60, 150, 215, and 270 degrees.**

Four areas of interest were found in these data. The areas of interest are at 60, 150, 215, and 270 degrees. These areas were examined again in more detail to quantify the indications. The scans were made using 0.5-mm steps and were repeated until no signs of lift-off or other possible scanning errors were present in the scan. This scanning regime yielded a total of 16 indications considered crack-like. These ET responses, their locations, lengths, and ET response strengths are given in Table 5.5. The ET responses given in the table are the maximum response found during scanning and re-scanning the areas of interest at a variety of probe rotation angles. This ET response strength, 1.8 V with a gain of 15 dB, was determined by using the ET response strength of ET indication 14, which was confirmed as a crack via PT testing (see Section 5.2.6.).

The area near 60 degrees has seven indications between 2 to 5 mm (0.08 to 0.2 in.) in length and with ET responses from 1.8 V to 3.3 V over a 50-mm (2-in.) range at the weld/buttering interface. The flaws appear to be point-like or circumferential, and the responses from the flaws are strongly affected by the probe direction. This cluster of seven indications is unique in the J-groove weld, and no such indications are present at the mirror-image position at 300 degrees, which should have a similar stress field while in service. These indications are numbered 1 through 7 from Table 5.5. Figure 5.26 shows the 0-degree and 45-degree rotation scans of the region near 60 degrees.

Table 5.5 Comprehensive Eddy Current Testing Responses on the J-Groove Weld of Nozzle 31

Indication	Angle	Length	Max Voltage	% EDM Notch
1	45°	2 mm (0.078 in.)	2.1	20
2	50°	5 mm (0.20 in.)	1.9	18
3	55°	4 mm (0.16 in.)	3.3	32
4	65°	2 mm (0.078 in.)	1.8	18
5	70°	4 mm (0.16 in.)	2.2	21
6	75°	3 mm (0.12 in.)	2.5	24
7	80°	3 mm (0.12 in.)	2.3	22
8	130°	4 mm (0.16 in.)	2.3	22
9	145°	10 mm (0.39 in.)	3.2	31
10	155°	8 mm (0.31 in.)	3.3	32
11	160°	14 mm (0.55 in.)	4.1	40
12	170°	5 mm (0.20 in.)	2.6	25
13	200°	8 mm (0.31 in.)	4.6	45
14	215°	10 mm (0.39 in.)	1.8	18
15	225°	9 mm (0.35 in.)	4.6	45
16	255°	7 mm (0.28 in.)	4.2	41

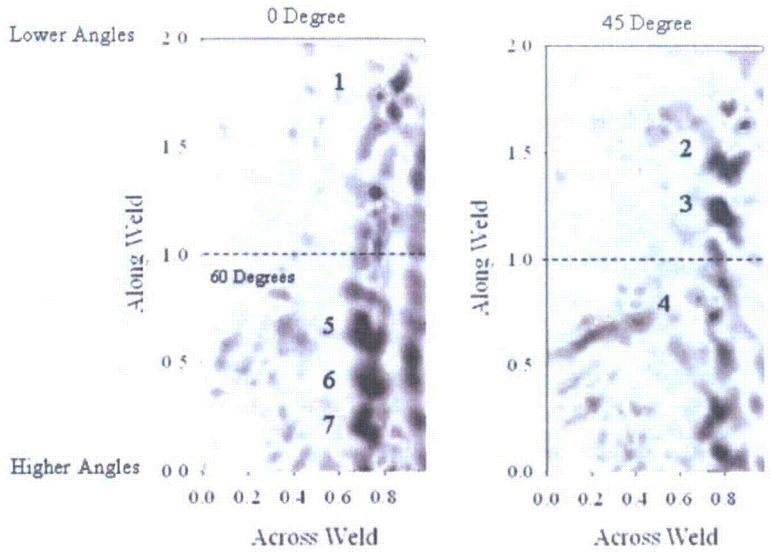

Figure 5.26 0- and 45-Degree Scans Centered on 60 Degrees on the J-Groove Weld of Nozzle 31

The area near 150 degrees was also re-scanned to quantify the indications in this area. Five indications were found at the weld/buttering interface, ranging from 4 mm to 14 mm and from 2.3 V to 4.1 V. Two of the indications—8 and 12—were point-like, and three—9, 10, and 11—were linear. Only indication 9 gave a significant ET response to both probe rotations. It is worth noting that indications 9, 10, and 11 are axial and are angled slightly toward 180 degrees. The ET results for this region are given in Figure 5.27.

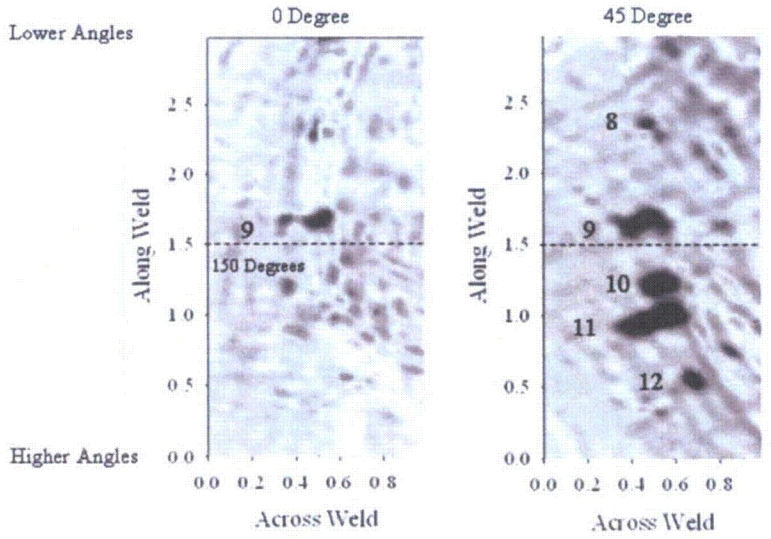

Figure 5.27 0- and 45-Degree Scans Centered on 150 Degrees on the J-Groove Weld of Nozzle 31

The next region of interest was centered around 210 degrees at the weld/buttering interface. Three indications were found—13 through 15 from Table 5.5. Indications 13 and 15 are 8–9 mm (0.3–0.35 in.) long and have responses of 4.6 V. Indications 13 and 15 show up clearly in both probe orientations. Both indications are axial in orientation but are also slightly angled toward 180 degrees, much like the indications centered around 150 degrees. Indication 14 is circumferential, has an ET response of 1.8 V, and has a discernable response only when the probe is oriented at 45 degrees. The ET results for this region are given in Figure 5.28.

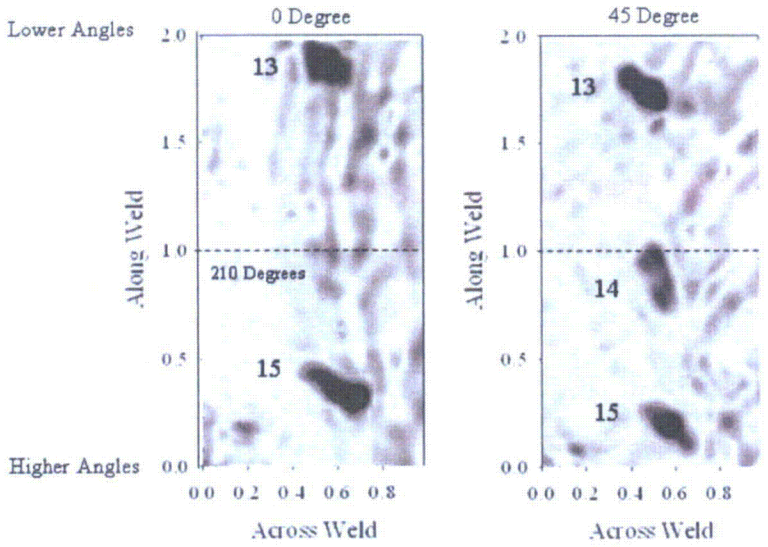

Figure 5.28 0- and 45-Degree Scans Centered on 210 Degrees on the J-Groove Weld of Nozzle 31

The last ET indication was found at 255 degrees at the weld/buttering interface. This indication is 8 mm (0.3 in.) long and has an ET response of 4.2 V. The indication is much more pronounced when the probe is at 0 degrees but is still present at 45 degrees. The ET results for this region are given in Figure 5.29. It should be noted that while the scans show indications at certain locations in the penetration tube wall or weld, the indications shown in a particular scan may not be indicative of leakage. For example on Nozzle 31, volumetric inspection of the J-groove weld was not able to detect the through-weld crack, and eddy current testing also exhibited inconsistencies.

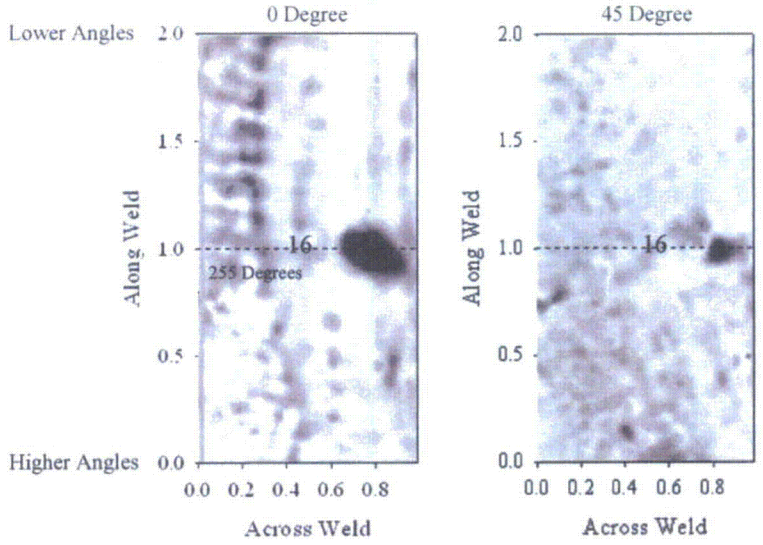

Figure 5.29 0- and 45-Degree Scans Centered on 255 Degrees on the J-Groove Weld of Nozzle 31

5.2.3.3 Time-of-Flight–Detected Indications for Nozzle 31

In general, the higher-frequency 7.5-MHz probe set generated many more responses than the 5-MHz set. Figure 5.30 shows a weak TOF-shaped indication located at 91 mm (3.6 in.) from the start. A stronger indication without the TOF shape acquired also at 5 MHz is shown in Figure 5.31. Figure 5.32 shows a TOF shape and two other indications acquired at 7.5 MHz. The TOF-shaped indication in Figure 5.26 is lower in amplitude at −7.2 dB than the other two indications in Figures 5.33 and 5.34, with responses of −5.3 and −3.0 dB, respectively. These response levels are comparable to the responses from the axial calibration notches shown earlier in Table 4.3.

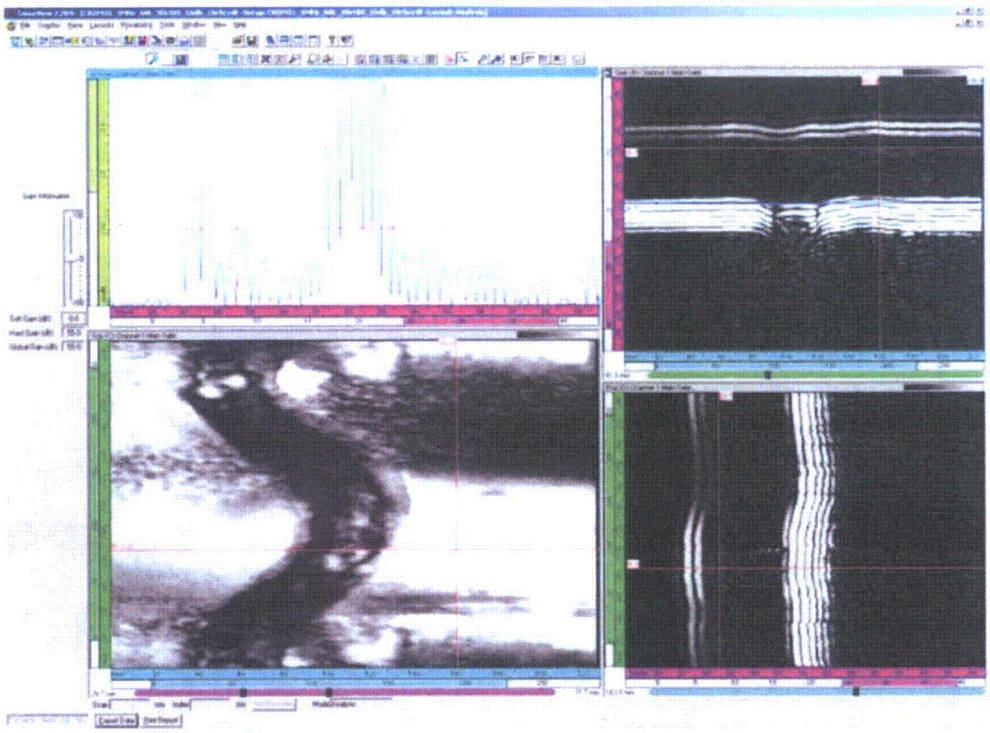

Figure 5.30 Time-of-Flight Shape in 5-MHz Time-of-Flight Diffraction Data from Nozzle 31 at 91 mm (3.6 in.) CCW, 163 mm Axial, with −9.4-dB Response

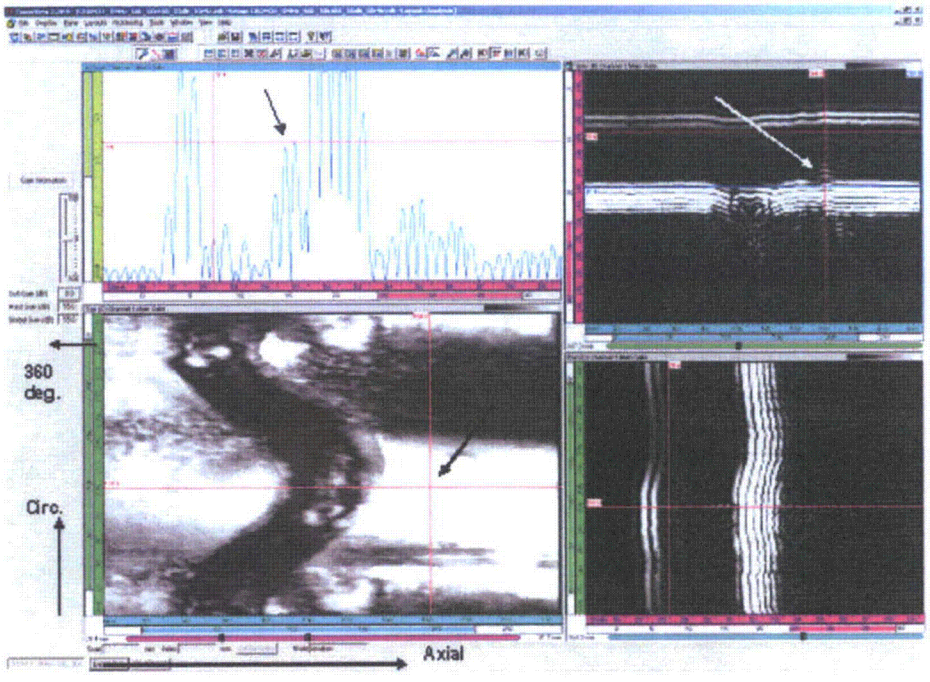

Figure 5.31 Interesting 5-MHz Time-of-Flight Diffraction Indication from Nozzle 31 at 107 mm (4.2 in.) CCW, 164 mm (6.5 in.) Axial, with −3.6-dB Response

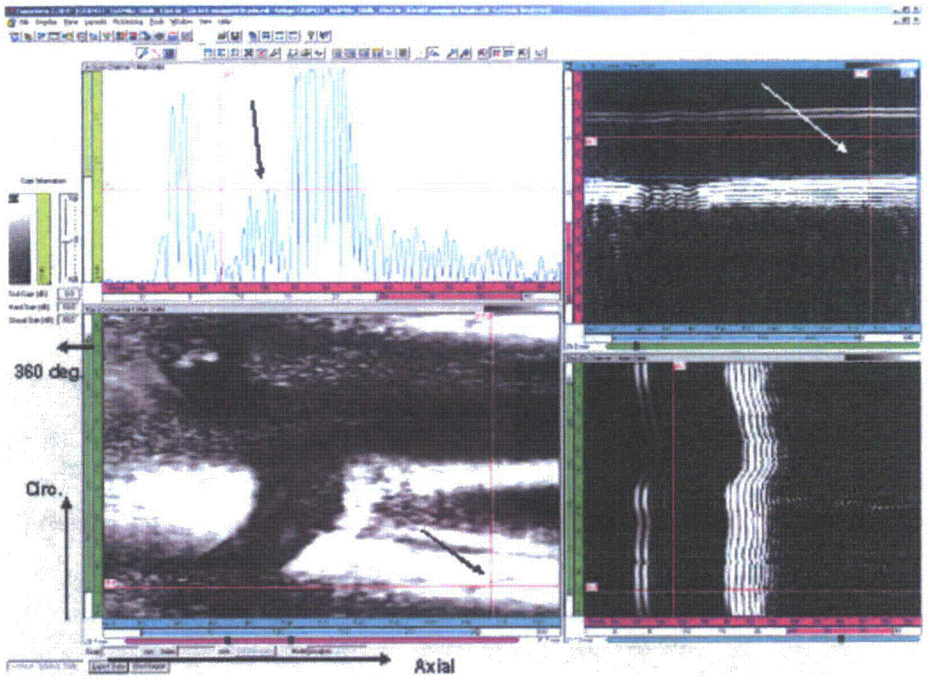

Figure 5.32 Time-of-Flight Shape in 7.5-MHz Time-of-Flight Diffraction Data from Nozzle 31 at 25 mm (1 in.) CCW, 217 mm (8.5 in.) Axial, with −7.2-dB Response

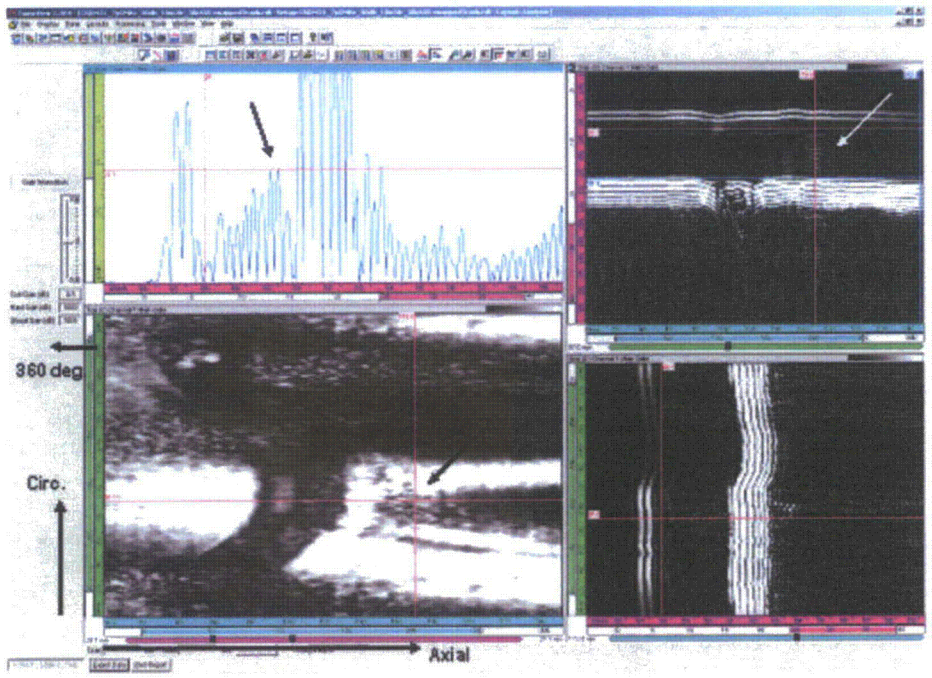

Figure 5.33 Interesting 7.5-MHz Time-of-Flight Diffraction Indication from Nozzle 31 at 97 mm (3.8 in.) CCW, 173 mm (6.8 in.) Axial, with −5.3-dB Response

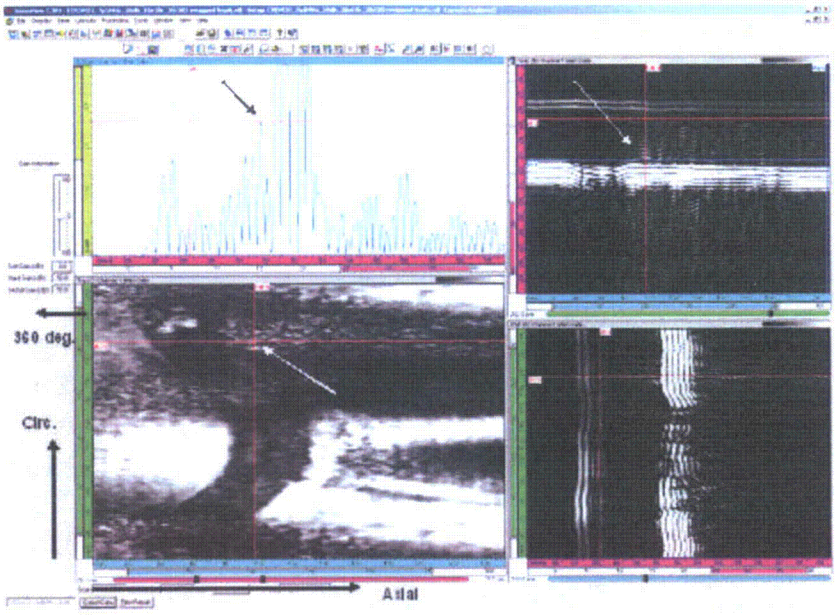

Figure 5.34 Interesting 7.5-MHz Time-of-Flight Diffraction Indication from Nozzle 31 at 202 mm (8 in.) CCW, 100 mm (3.9 in.) Axial, with −3.0-dB Response

5.2.3.4 Immersion Ultrasonic Testing Results

Numerous indications at all depths were found by UT immersion inspection in Nozzle 31 that map out the weld, as do the indications from Nozzle 59. Most of the indications started in the J-groove weld metal.

C-scan images of indications from the J-groove weld material at the four inspection frequencies are shown in Figures 5.35 through 5.39. The 5-MHz data in Figure 5.35 show a large-amplitude indication near 360 degrees. This same indication is seen also in the 2.25-, 1.0-, and 0.5-MHz data (Figures 5.36 through 5.39). Although in almost all cases the SAFT process was able to improve the signal-to-noise ratio without causing any significant change to the shape or nature of the indications, the 2.25-MHz data showed some interesting elongated indications prior to SAFT process application that became rounded when SAFT was applied. Figure 5.37 shows the unprocessed data. The elongated indications are at 90 degrees and from 270 to 300 degrees and appear to start in the weld metal, not the penetration tube. It should be noted that the Z data shown in Figure 5.26 are not compatible with the others, as the data in Figure 5.37 were not processed in the same way and there is no correction for the curvature of the data. The lower-amplitude lack of fusion indications at 178 mm (7 in., 286 degrees) in the circumferential direction are seen at all frequencies except 500 kHz.

5.2.3.5 Visual Testing Results

Microset polymer was applied to the J-groove weld surface of Nozzle 31. The replica covered the entire weld, including the buttering and 10 mm (0.4 in.) up the penetration tube. The examination of the replicas of the J-groove weld of Nozzle 31 showed two crack-like indications and two possible micro-crack-like indications. Figure 5.40 shows what appears to be a very wide crack cutting across several weld passes. Penetrant dye testing and ET testing did not confirm this as a crack, however; it is possibly an irregularity in the weld. Bare-metal photography of this area was inconclusive.

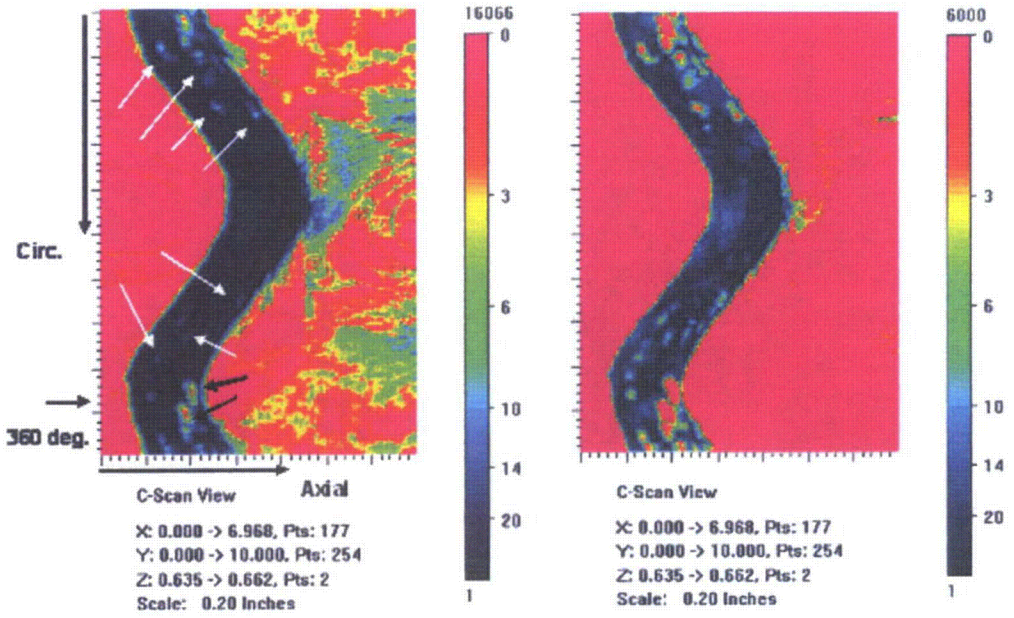

Figure 5.35 Nozzle 31, 5-MHz Immersion Data Showing Indications in the J-Groove Weld Material at Two Different Displayed Amplitude Settings

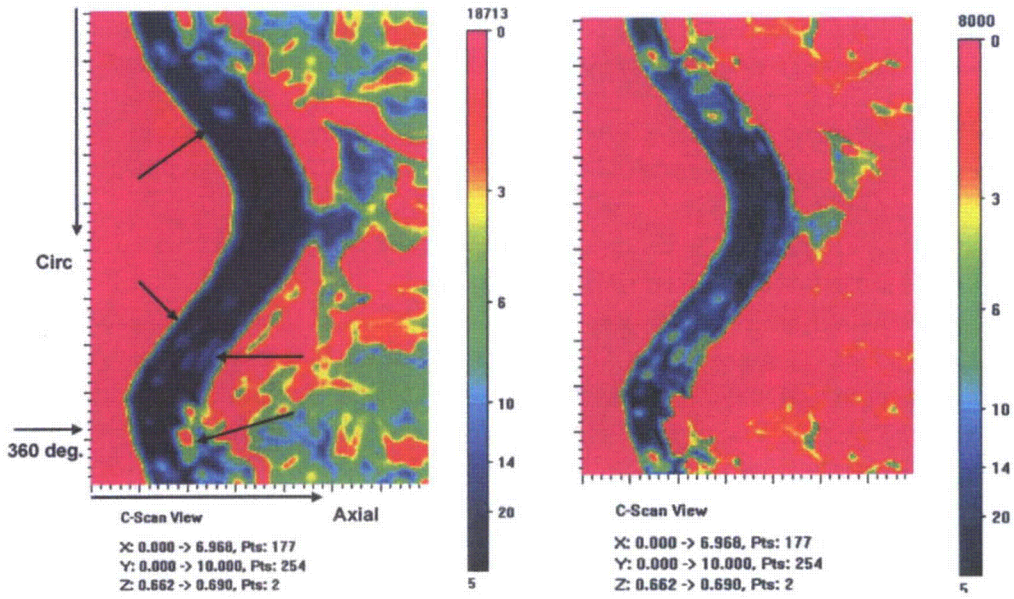

Figure 5.36 Nozzle 31, 2.25-MHz Immersion Data Showing Indications in the J-Groove Weld Material at Two Different Displayed Amplitude Settings

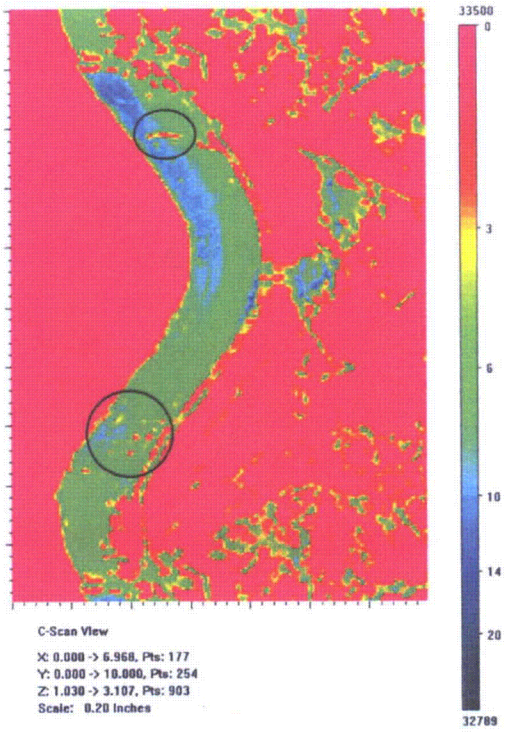

Figure 5.37 Unprocessed 2.25-MHz Data Showing Elongated Indications at 90 Degrees and from 270 to 300 Degrees (circled). These elongated indications are rounded by the SAFT processing.

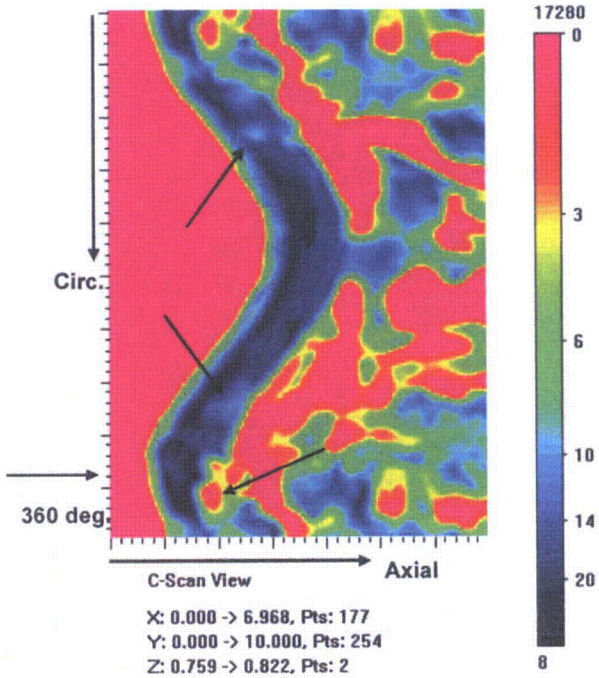

Figure 5.38 Nozzle 31, 1-MHz Immersion Data Showing Indications in the J-Groove Weld Material

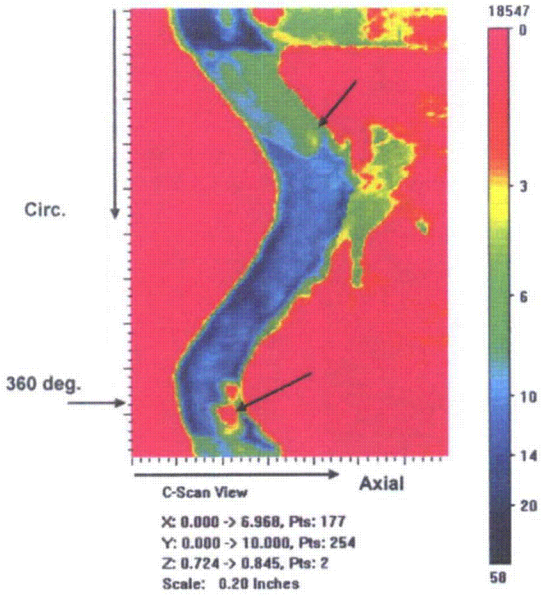

Figure 5.39 Nozzle 31, 500-kHz Immersion Data Showing Indications in the J-Groove Weld Material

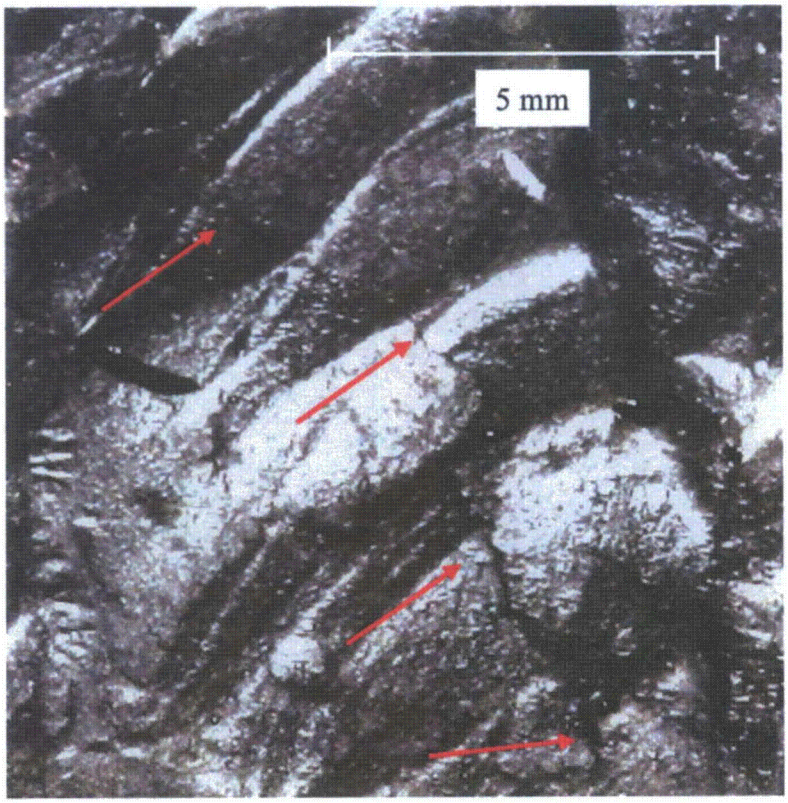

Figure 5.40 Crack-Like Indication 10 mm (0.0004 in.) Long at 145 Degrees CCW

A possible crack was found also at close to 135 degrees. This indication cuts across two weld passes but is very faint, and an indication this weak is common for only very tight cracks. This indication is shown in Figure 5.41. This indication was not confirmed by either PT or ET and is possibly a scratch or an irregularity in the weld. Bare-metal photography of the area was inconclusive.

Another region showing crack-like indications was detected at 275 degrees. This indication shows several small cracks, two of which appear to link. The region and the cracks are small, only 10 mm (0.4 in.) across, and could be craze cracking in the weld. This region is shown in Figure 5.42. A red piece of debris picked up by the Microset polymer is seen in Figure 5.42 as well. These indications are not confirmed by either PT or ET and are possibly a scratch or an irregularity in the weld. Bare-metal photography of the area was inconclusive.

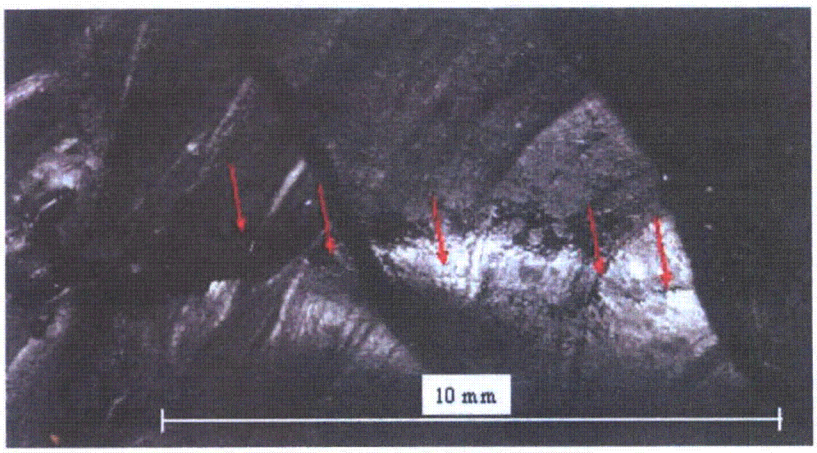

Figure 5.41 Crack-Like Indication at 135 Degrees CCW, 5 to 10 mm (0.0002 to 0.0004 in.) Long

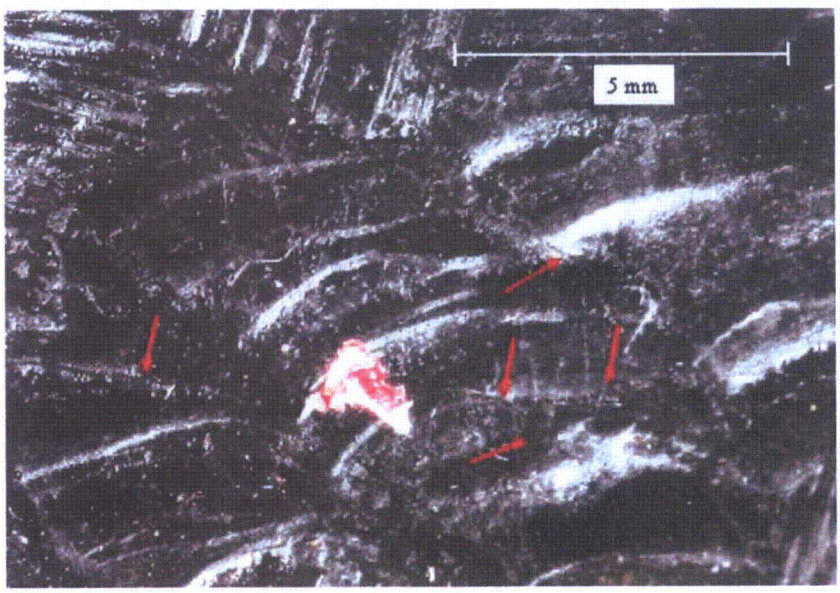

Figure 5.42 Cracked Area at 275 Degrees CCW. This branched crack-like indication traverses through the area. The cracked region is 1 cm^2.

Finally, a longer crack-like indication was detected at close to 270 degrees. This indication was longer, at least 15 mm (0.6 in.) long and possibly 20 mm (0.8 in.) in length. The indication has a low contrast against the black replica, and there are two possible "ends" for the crack. This crack-like indication is shown in Figure 5.43. This crack-like indication was not confirmed with either PT or ET. Bare-metal photography of the area showed it to be a deep scratch and not a crack.

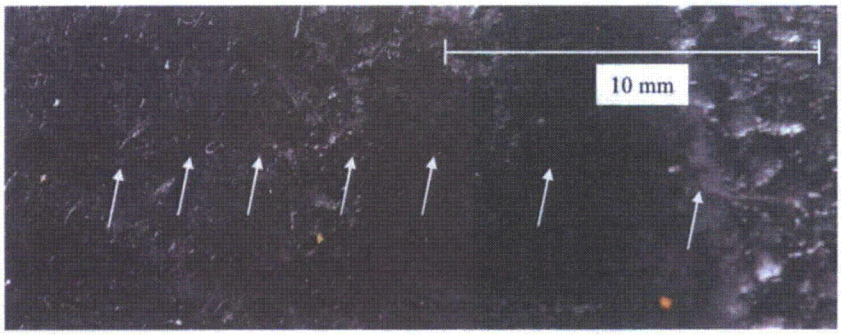

Figure 5.43 Crack-Like Indication at 270 Degrees CCW. The indication leaves the J-groove weld and propagates into the buttering. The indication is 15–20 mm (0.6–0.8 in.) long.

5.2.3.6 Penetrant Testing Results

Penetrant testing was applied to the surface of the J-groove weld of Nozzle 31. This was done to verify cracks found earlier using Microset polymer and bare-metal photography and to find any cracks missed by these techniques.

The PT testing showed that the major indications found by the examination of the J-groove weld using a replicate were scratches, not cracks. Two short crack-like indications were found using PT, one at 200 degrees and one at 225 degrees. A pore-like indication was found at 190 degrees, and a small linear indication was found at 215 degrees as well. These indications are shown in Figure 5.44. After the penetrant developer was cleaned off, these areas were re-photographed with the 16.7-megapixel Canon camera using the macro lens. The pore at 190 degrees and the linear indication at 215 degrees could not be detected, but the cracks at 210 and 235 degrees were confirmed using the photographs. Figure 5.44 shows these crack-like indications and the pore-like indication.

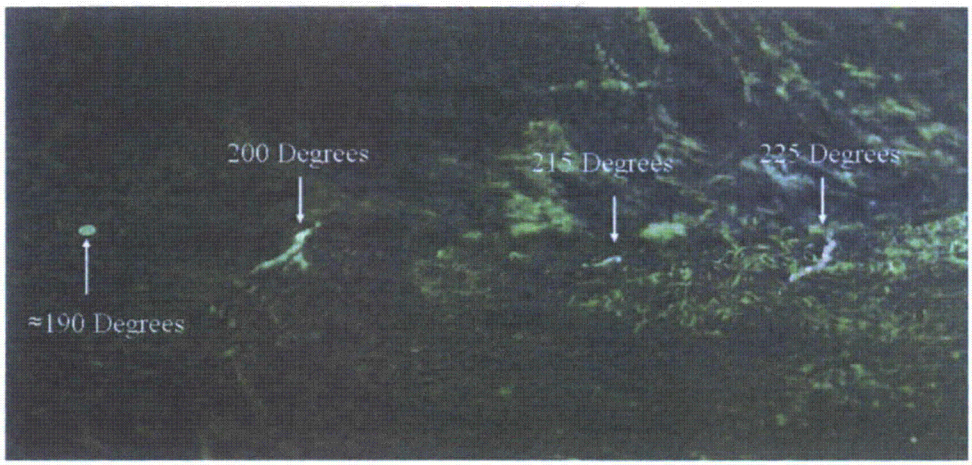

Figure 5.44 Penetrant Results at the Weld/Butter Interface Around 210 Degrees

5.2.3.7 Direct Photography

The cracked areas identified via VT of surface replicas, ET, and PT were photographed in detail in an attempt to confirm the presence of cracking. No images of cracks were detectable near 60 or 150 degrees or at 255 degrees. Crack-like indications were confirmed by direct photography at 200 and 225 degrees. Both crack-like indications are at the weld/buttering interface and extend primarily into the buttering. These crack-like indications are shown in Figures 5.45 and 5.46. It is difficult to measure the length of

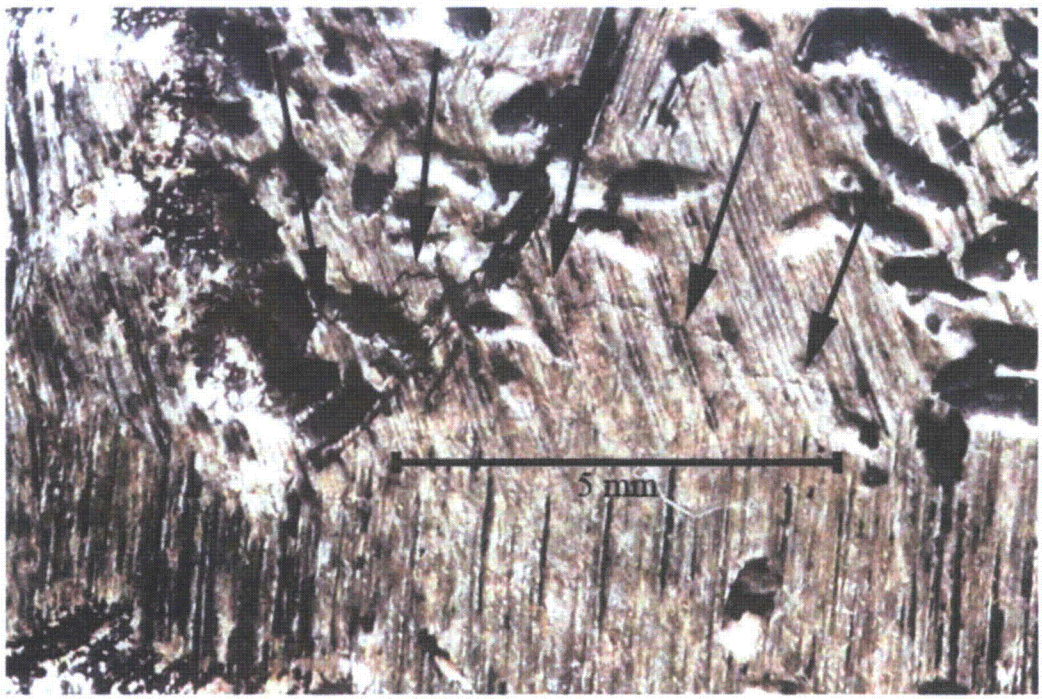

Figure 5.45 Crack-Like Indication Imaged Via Visual Testing at the Weld/Buttering Interface at 200 Degrees

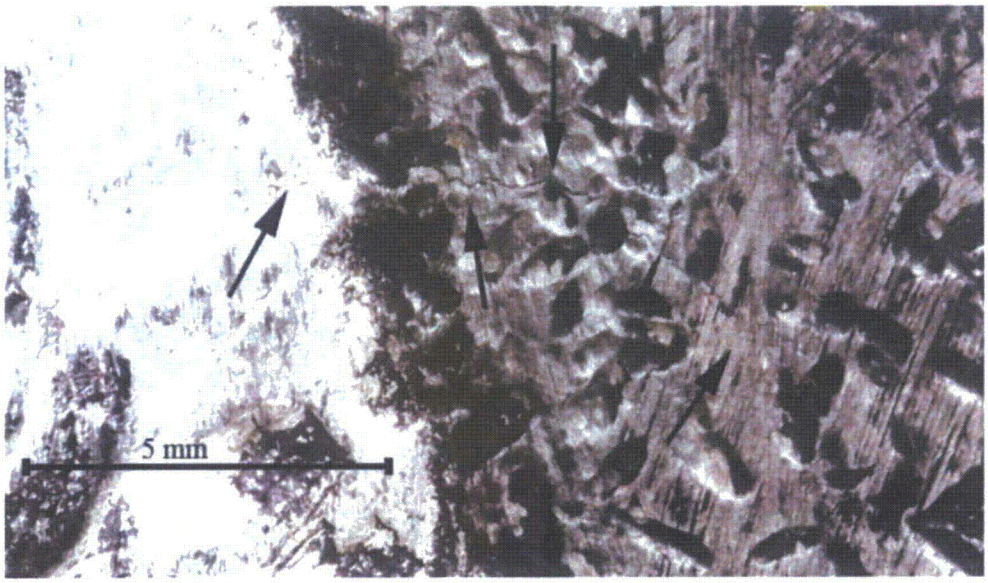

Figure 5.46 Crack-Like Indication Imaged Via Visual Testing at the Weld/Buttering Interface at 225 Degrees

the indications, as the beginning and end of the flaws are too tight and the surface is not ideal. The best approximation is that the crack-like indication at 200 degrees is 7 mm long, which is shorter than the 10 mm determined via ET, and the crack-like indication at 225 degrees is 9 mm long, which is the same length as determined by ET.

5.3 Nondestructive Examination Results Summary

The NDE techniques found many indications in the two nozzles, and the task of analyzing the data for a possible leakage path is challenging and complicated. In very few cases did more than one technique agree on any one location as being potentially cracked. However, there was some agreement between the results of the ISI, round robin, and PNNL NDE. It is also important to focus efforts on finding cracks in areas that would lead to leakage. There are two potential leakage paths through the nozzle. The path with the least material between the primary coolant and the outside of the reactor is through the wetted side of the penetration tube to the interference fit. The tube also presents a large surface area for cracking. The second path is through the J-groove and buttering weld metal to the interference fit. This area, which is thicker and has less area than the tube, is a weld and has heat-affected areas and areas where the weld metal has mixed with the carbon steel. The weld also will have residual stresses and service-induced stresses. This section focuses on the areas likely to lead to leakage and presents the data fusion used as part of the data analysis.

5.3.1 Nozzle 59 Penetration Tube

The penetration tube of Nozzle 59 was examined using ET, TOFD, and visual testing via replicas created with Microset polymer. The Nozzle 59 penetration tube contained many ET, TOFD, and VT indications that suggest cracking. One would expect that a crack that penetrates into the tube from the inner surface

should show up in each NDE method, while innocuous features are less likely to appear on all three techniques. An embedded volumetric flaw such as an inclusion or a void in the penetration tube would be detectable by TOFD but not by ET or VT. Deep scratches in the surface of the tube would be detected by ET, identifiable as scratches and not cracks by VT, and not detectable by TOFD. TOFD would detect this by loss of the lateral wave if it is a deep scratch.

The combined results of all three techniques are shown in Figure 5.47. The TOFD data have been reversed from what was shown in Section 5.1.3.2 to allow for the overlaying of the ET data, which were taken clockwise. The TOFD data vertical positions were adjusted to match the ET vertical positions.

The area highlighted in Figure 5.47 Region 1 (and 1a, a repeat of 1) has the low-voltage ET responses but has only one TOFD indication, and the VT results showed deep scratches but no crack-like indications.

Region 2 and 2a (repeat of 2) shows up on the VT as an area with a rougher texture and was heavily pitted. Also, some possible microcracks were detected. There were weak ET responses and one TOF-shaped response on the outer edge.

The ET indication at 140 mm (5.5 in.) rotation and 225 mm (8.9 in.) axial (indication 3) was determined via VT to be a round, rough patch on the interior of the penetration tube. The cause of this rough patch is not known.

The results show where the TOFD and the ET results find a common area of interest (Region 4 of Figure 5.47). This area is at 210 mm (8.25 in.) rotation and 225 to 260 mm (8.9 to 10.2 in.) axially into the tube. The VT results for this region show only scratches, however.

Region 5 contained a crack-like indication using VT, but this was not corroborated by the ET or the TOFD and is likely a scratch.

There were several areas in which NDE revealed the existence of indications, but these areas were not destructively examined because there was no confirmed cracking. Also, the penetration tube was considered to be a lower priority than the J-groove weld of Nozzle 31.

When the PNNL, ISI, and round-robin data are compared, some patterns emerge. The PNNL TOFD examination of the penetration tube found three distinct types of indications. The first is an apparent intrusion of the weld metal into the penetration tube caused during welding. These intrusions show up as time-of-flight–shaped indications close to the root of the weld/penetration tube and at a depth corresponding to the middle of the weld. The second type of indication are embedded reflectors that do not break either the inner or outer surfaces and are likely fabrication flaws in the penetration tube metal. The third type of indication was found by the zero-degree ultrasound. The PNNL zero-degree ultrasonic indications appear to be strings of defects in the weld metal close to the tube OD. These strings of defects appear to follow the line of the weld and are likely welding flaws.

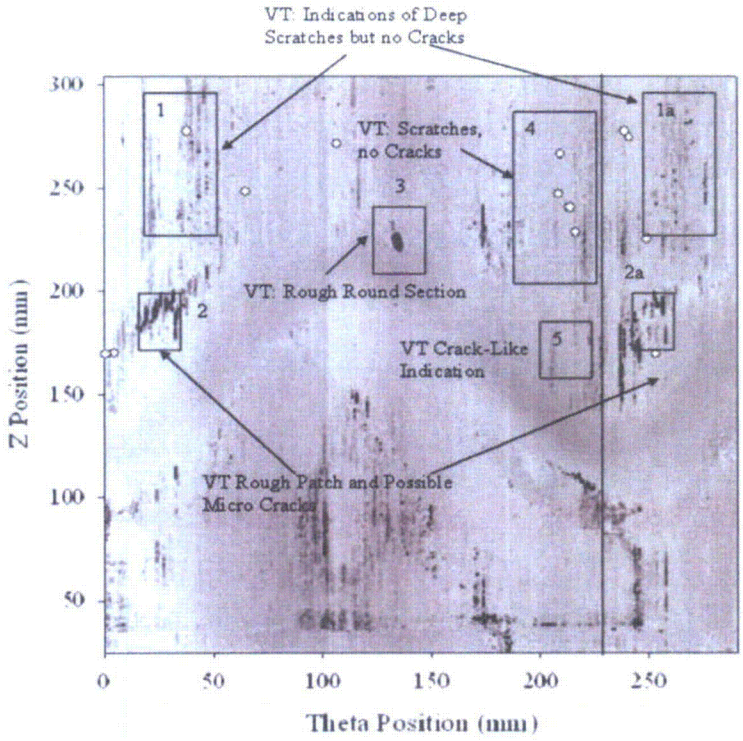

Figure 5.47 Combined Eddy Current Data with Overlaid Time-of-Flight Diffraction Indications and Visual Testing Characterization of the Results for the Penetration Tube of Nozzle 59

The compiled ultrasonic examinations of Nozzle 59 are shown in Figure 5.48, which summarizes the angular locations of reported indications from the round robin, the in-service inspections, and the PNNL inspections. For simplicity the indications are shown only by angle and not by the height of the indications in the penetration tube because nearly all of the ultrasonic indications are located at or near the J-groove weld. When the round-robin and in-service inspection data are examined, the two sets of indications correlate strongly with the weld intrusion indications found by PNNL. The embedded TOFD indications are not reflected in the round-robin or ISI results. The welding defects found using zero-degree ultrasound also were not reported by the round-robin or the ISI data.

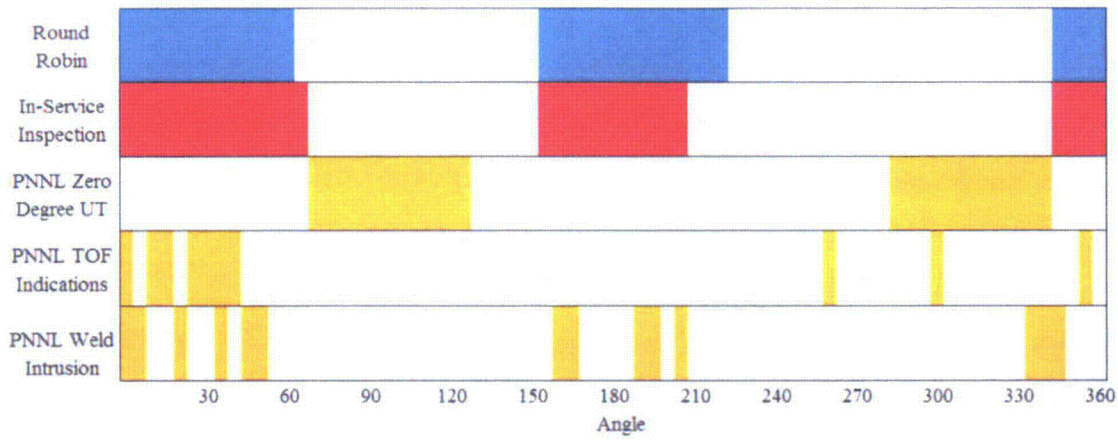

Figure 5.48 Compiled Ultrasonic Data for Nozzle 59

5.3.2 Nozzle 59 J-Groove Weld and Buttering

The J-groove weld and buttering were inspected volumetrically using ultrasound and the surface was examined using visual testing via replicant. No large crack-like indications were found in the J-groove weld using direct VT and VT using replicant, and the immersion UT indications appear to be embedded welding defects. The Microset replica and VT did reveal several small crack-like indications, but no indication was longer than 1 cm. The locations of these defects are given in Figure 5.49.

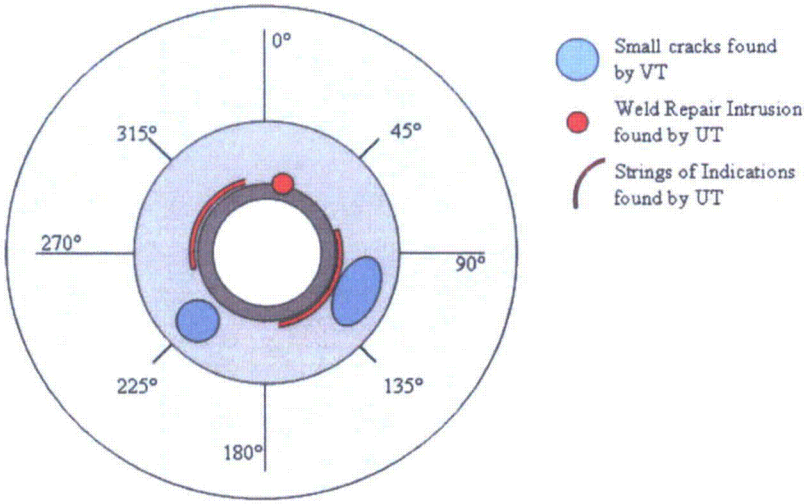

Figure 5.49 Nondestructive Examination Indications Found in Nozzle 59

Although a series of UT signals is coincident with the locations of the small crack-like indications at 90–135 degrees, the UT data in this area look a great deal like a string of fabrication flaws. Again, although NDE revealed that this area contained indications, the absence of confirmed cracking and confirmation that this was a leaker based on boric acid deposits meant that this weld was a lower priority than the weld on Nozzle 31.

Comparisons between the PNNL results and the ISI results for the J-groove weld surface are limited, as PNNL only performed a visual inspection via a replica. The in-service examination used eddy current and found a string of indications from 50–135 degrees and from 255–305 degrees. The PNNL visual examination of the replica made from the J-groove weld surface found crack-like indications at 112–135 degrees and at 225 degrees. The indications from 112–135 degrees are in agreement with the eddy current examinations but the indication at 225 degrees is not.

5.3.3 Nozzle 31 Penetration Tube

The TOFD and ET examination results for the Nozzle 31 penetration tube showed a good correlation, in that both techniques found the penetration tube to be free of significant surface-breaking defects. The penetration tube in Nozzle 31 contained no strong ET indications; only weak (<1 V) scratch-like indications were detectable. The only TOFD indications found were determined to be embedded in the tube and not surface-breaking, as no break in the lateral wave was seen.

Because TOFD and ET agreed that the penetration tube was the least likely component thus far to be cracked, the penetration tube of Nozzle 31 was considered the lowest priority for DE. This is interesting, as Nozzle 31 was considered to be leaking based on the presence of boric acid on the pressure vessel head. If Nozzle 31 had leaked, it would have had to leak through the J-groove weld (see Section 5.3.4).

A comparison of the PNNL, ISI, and round-robin tests of the penetration tube yields interesting results. The PNNL TOFD examination of the penetration tube of Nozzle 31 again found apparent weld intrusions and embedded indications in the penetration tube. The PNNL zero-degree ultrasound found a very large indication in the J-groove weld metal near zero degrees. The round-robin examinations of the penetration tube shows indications that are coincident with the apparent weld intrusion found by PNNL and possibly some of the large indication around zero degrees. The in-service inspection of the penetration tube was different from the PNNL and round-robin results, calling only one region near 300 degrees as having an indication described as "mid wall." PNNL called several embedded indications in the weld metal using TOFD near the 300-degree mark.

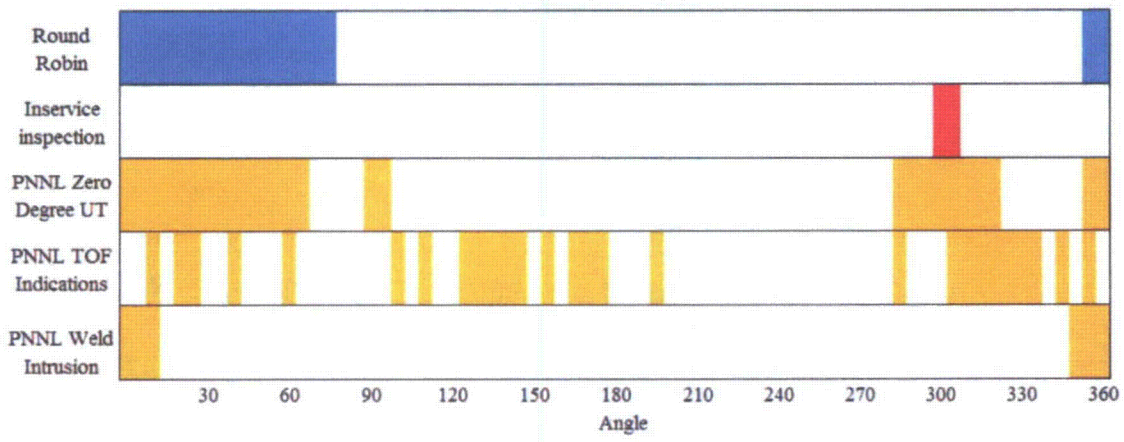

Figure 5.50 Compiled Ultrasonic Data for Nozzle 31

5.3.4 Nozzle 31 J-Groove Weld and Buttering

The J-groove weld of Nozzle 31 was found to have crack-like indications by bare metal VT, ET, and PT. The indications were not detectable using the volumetric UT inspection, but UT inspection did reveal what appeared to be areas with fabrication flaws. The locations of these indications are given in Figure 5.51.

Sixteen crack-like indications were found by ET in four distinct areas. Seven small crack-like indications were found clustered around 60 degrees, five were found clustered around 150 degrees, three were found clustered around 210 degrees (Figure 5.52), and one was found at 255 degrees. The ET indications at 200 and 225 degrees were confirmed as cracks using PT and bare-metal VT.

A crack-like indication was found using both PT and ET at 215 degrees. This indication is unusual for two reasons—the indication is circumferential, not axial like the other crack-like indications, and the ET response is relatively weak at 1.8 V at 15 dB. Because of this indication, all ET responses larger than 1.8 V were considered crack-like for this analysis.

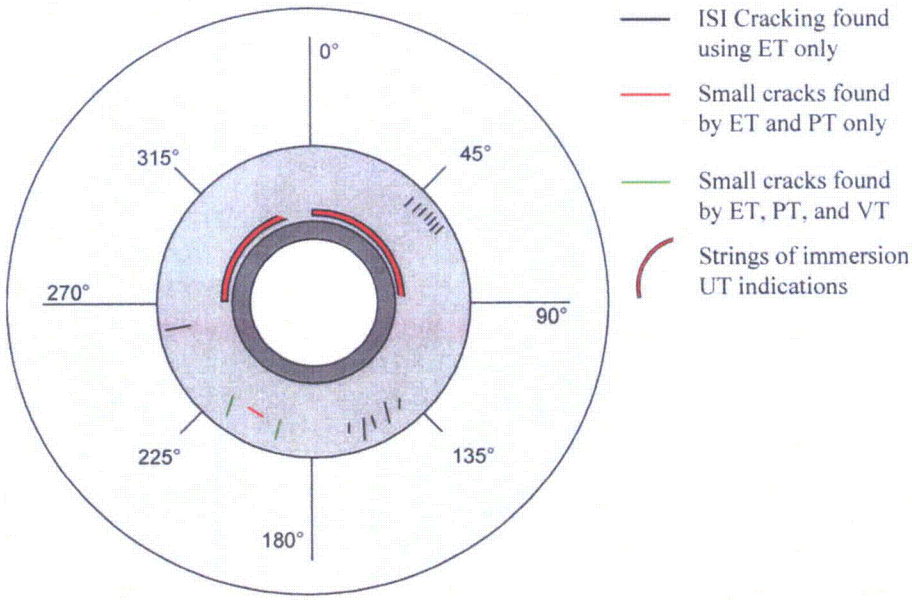

Figure 5.51 Nondestructive Examination Indications Found in Nozzle 31

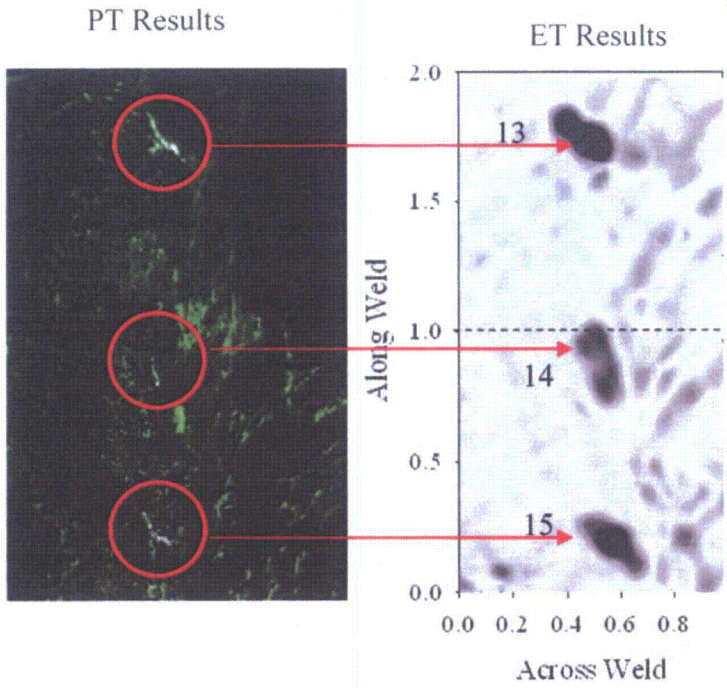

Figure 5.52 Correlated Penetrant Dye and Eddy Current Testing Results for the Weld/Butter Wetted Surface Interface in Nozzle 31 Centered at 210 Degrees

Results of the eddy current examinations of Nozzle 31 by PNNL and the ISI team are found in Table 5.6 and showed both consistencies and differences. The PNNL ET was performed under laboratory conditions and found many more indications than did the ISI examination. All indications called by the ISI team can be matched with PNNL indications, although the ISI team and PNNL appear to have a 10-degree shift in registration. All the ISI indications are associated with larger flaws (higher crack opening dimension (COD)) that are 30–45% of the EDM notch in amplitude and 7 mm or longer.

PNNL has acquired the ET results for the ISI examination of Nozzle 31. A review of the data shows that the ISI ET detected more indications than were called in the ISI report. When plotted side by side, it appears that the ISI ET examination found indications 9, 10, 11, and 12, and possibly 8. A side-by-side comparison of the PNNL and ISI ET results is shown in Figure 5.53.

The region around 210 degrees also was compared, showing that the PNNL and ISI results were similar. The ISI ET examination detected indications 13 and 15 but not 14. The comparison between the PNNL and ISI results centered around 210 degrees is shown in Figure 5.54.

Based on the NDE of Nozzle 31, the interesting regions for destructive testing using the visual and immersion inspections included the regions found using VT, from 80 to 120 degrees and from 220 to 260 degrees, as well as the regions from −10 to 60 degrees and from 260 to 320 degrees as determined using immersion UT. It is worth noting that the region from 260 to 320 degrees has significant overlap with both techniques. Because of the confirmed crack-like indications in the weld, the J-groove weld of Nozzle 31 was considered the highest priority for DE.

Table 5.6 Comparison of PNNL and ISI ET Results for Nozzle 31 J-Groove Weld Surface

Indication	PNNL Angle	ISI Angle	Length (PNNL)	% EDM Notch (PNNL)
1	45°	NA	2 mm (0.078 in.)	20%
2	50°	NA	5 mm (0.20 in.)	18%
3	55°	NA	4 mm (0.16 in.)	32%
4	65°	NA	2 mm (0.078 in.)	18%
5	70°	NA	4 mm (0.16 in.)	21%
6	75°	NA	3 mm (0.12 in.)	24%
7	80°	NA	3 mm (0.12 in.)	22%
8	130°	NA	4 mm (0.16 in.)	22%
9	145°	155°	10 mm (0.39 in.)	31%
10	155°	NA*	8 mm (0.31 in.)	32%
11	160°	NA*	14 mm (0.55 in.)	40%
12	170°	NA*	5 mm (0.20 in.)	25%
13	200°	210°	8 mm (0.31 in.)	45%
14	215°	NA	10 mm (0.39 in.)	18%
15	225°	235°	9 mm (0.35 in.)	45%
16	255°	265°	7 mm (0.28 in.)	41%

* Indications not called by ISI teams but detected in the ISI ET data.

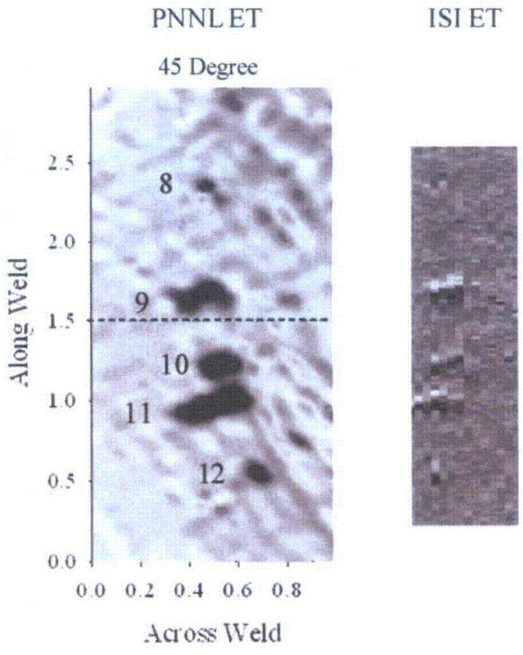

Figure 5.53 PNNL and ISI ET Results for the Weld-Buttering Interface Centered Around 150 Degrees

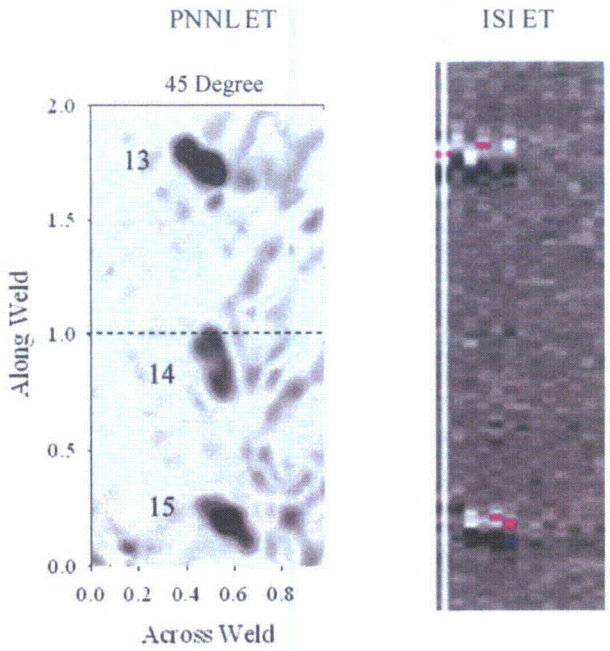

Figure 5.54 PNNL and ISI ET Results for the Weld-Buttering Interface Centered Around 210 Degrees

One result worth noting was the high false-call rate that PNNL staff obtained using VT via replicant. None of the indications found using VT or the replicas was confirmed using PT or ET, and one was shown to be a scratch by high-magnification photography.